

**SURFACE PROPERTIES AND CATALYTIC
ACTIVITY OF VANADIA SUPPORTED ON
RARE EARTH OXIDES**

**THESIS SUBMITTED TO THE
COCHIN UNIVERSITY OF SCIENCE AND TECHNOLOGY
IN PARTIAL FULFILMENT OF THE
REQUIREMENTS FOR THE DEGREE OF**

DOCTOR OF PHILOSOPHY

IN

CHEMISTRY

IN THE FACULTY OF SCIENCE

BY

RENUKA N.K.



**DEPARTMENT OF APPLIED CHEMISTRY
COCHIN UNIVERSITY OF SCIENCE AND TECHNOLOGY
KOCHI - 682 022**

NOVEMBER 2000

to my parents and brothers ...

CERTIFICATE

This is to certify that the thesis herewith is an authentic record of research work carried out by Renuka N. K. under my supervision, in partial fulfilment of the requirements for the degree of Doctor of Philosophy of Cochin University of Science and technology, and further that no part thereof has been presented before for any other degree.



Dr. S. Sugunan
(Supervising Teacher)
Professor in Physical Chemistry
Department of Applied Chemistry
Cochin University of Science and Technology
Kochi-22

Kochi-22
7th November 2000

DECLARATION

I hereby declare that the work presented in this thesis entitled, “**Surface properties and catalytic activity of vanadia supported on rare earth oxides**”, is entirely original and was carried out by me independently under the supervision of Dr. S. Sugunan, Professor in Physical Chemistry, Department of Applied Chemistry, Cochin University of Science and Technology, Kochi – 22, India, and has not been included in any other thesis submitted previously for the award of any degree.



Renuka N. K.

Kochi –22,

7th November 2000

ACKNOWLEDGEMENT

“A hundred times every day I remind myself that my inner and outer life are based on the labors of others.” - Einstein

With great pleasure I wish to express my deep sense of gratitude and obligation to my supervising guide, Prof. (Dr) S. Sugunan, for his valuable guidance, research training, constant encouragement and valuable suggestions throughout this work.

I am grateful to Dr. K. K. Mohammed Yusuff, Head of the Department of Applied Chemistry and Dr. P. Madhavan Pillai, Former head, Department of Applied Chemistry, for providing the necessary facilities. At this moment, it is my pleasure to acknowledge my sincere thanks to Dr. B. S. Rao, Catalysis Division, NCL, Pune, for allowing me to carry out some of the experiments in his laboratory.

I take this opportunity to thank all the teachers, non-teaching staff and research scholars of the Department of Applied Chemistry for their help during various occasions. I sincerely thank Dr. Jyothi T. M., Mrs. Rehna and Anas for their help throughout my work. The timely suggestions and help from C. G. R. is gratefully remembered at this context. Special regards to my dear juniors, Ms. Suja, Ms. Deepa, Ms. Nisha, Mrs. Sreejarani and Mrs. Manju and other friends for the warmth and cooperation they have shown towards me.

To my family I owe the moral support that they extended throughout my work. I wish to place on record my deep sense of indebtedness to my dear brother for his love, care and encouragement.

The financial support from the Council of Scientific and Industrial Research is gratefully acknowledged.

Renuka N. K.

PREFACE

Vanadia based catalysts have attracted much attention in industry which play a key role in oxidation catalysis. In fact almost all the heterogeneous oxidation catalysts used on industrial scale for production of fine chemicals contain vanadium as the main component of the active phase. By virtue of their selective oxidation activity, supported vanadia systems are superior to pure vanadia, which catalyse complete oxidation of the organics. The interaction with the support suitably modifies the property of the active species so as to tune the system in an economically and industrially attractive mode.

An investigation on the physical and chemical characterisation of rare earth oxide supported vanadia is attempted in the present study. La_2O_3 , Sm_2O_3 and Dy_2O_3 serve the purpose of supports. Supported catalysts were prepared and characterised using various physico chemical techniques. A detailed investigation of acid base properties is also carried out. The nature of interaction of vanadia with lanthanide oxide is discussed and the effect of vanadia loading on the activity of the systems towards reactions of industrial importance is explored.

The work has been arranged by sections spread out in five chapters. Chapter I is devoted for the general discussion on supported vanadia catalysts including review of literature. The instrumental methods adopted for the study and the theory of various techniques applied are discussed in Chapter II. Chapter III presents the physicochemical characterization of the samples including the structure obtained by various analytical procedures. The catalytic activity of the supported systems towards oxidation reactions and acid catalysed reaction is explored in Chapter IV. The conclusions derived from various observations regarding structural aspects and catalytic activity are summarized in Chapter V.

CONTENTS

		Page No.
CHAPTER 1	GENERAL INTRODUCTION	
1.1	Catalysis	1
1.2	Metal oxide catalysts	2
1.3	Methods of preparation of supported vanadia catalysts	4
1.3.1	Impregnation method	4
1.3.2	Ion exchange method	5
1.3.3	Chemical vapour deposition	5
1.3.4	Co precipitation method	5
1.4	Structure of supported catalysts; Metal support interaction	6
1.5	Structural models for surface vanadia species	9
1.6	Selective oxidation activity and acidity generation by vanadia loading	9
1.7	Reactions of supported vanadia catalysts	12
1.7.1	Oxidative dehydrogenation	12
1.7.2	Ammonoxidation	15
1.7.3	Oxidation of methanol	15
1.8	Rare earth oxides as catalysts	17
1.9	Acid base properties	19
1.9.1	Hammett indicator method	19
1.9.2	Electron donating property studies	21
1.9.3	Temperature programmed desorption studies	24
1.9.4	Cyclohexanol decomposition-A test reaction for acidity	25
1.10	Reactions selected for the present study	26
1.10.1	Oxidative dehydrogenation of ethyl benzene	27

1.10.2	Oxidative dehydrogenation of ethanol	29
1.10.3	Methylation of phenol	30
1.11	Present work	31
1.12	Objectives of the work	32
	References	33
CHAPTER II EXPERIMENTAL		
2.1	Materials	42
2.2	Preparation of the catalysts	42
2.2.1	Preparation of rare earth oxide supports	42
2.2.2	Preparation of supported catalysts	43
2.3	Characterisation of catalysts	43
2.3.1	Energy dispersive X-ray analysis	44
2.3.2	X-ray diffraction studies	45
2.3.3	FTIR spectral studies	46
2.3.4	Surface area analysis	47
2.3.5	Pore volume measurements - Mercury porosimeter	48
2.3.6	Thermal studies	49
2.4	Acid base property studies	50
2.4.1	Hammett indicator method	50
2.4.2	Electron donating property studies	51
2.4.3	Temperature programmed desorption (TPD) studies	53
2.5	Catalytic activity studies	53
2.5.1	Gas phase reactor	54
	References	56
CHAPTER III CHARACTERISATION AND SURFACE PROPERTIES		
3.1	EDX analysis	57
3.2	XRD studies	57
3.3	FTIR spectral studies	63

3.4	Thermogravimetric studies	68
3.5	Surface area and pore volume measurements	69
3.6	Acid base properties	72
3.6.1	Hammett indicator method	72
3.6.2	Electron donating property studies	74
3.6.3	Temperature programmed desorption studies	82
3.6.4	Cyclohexanol decomposition reaction	87
	References	94
CHAPTER IV	CATALYTIC ACTIVITY	
4.1	Oxidative dehydrogenation of ethyl benzene	96
4.1.1	Selective oxidation activity of the supported system	99
4.1.2	Reaction in absence of air	106
4.1.3	Effect of reaction temperature	109
4.1.4	Effect of flow rate	109
4.1.5	Deactivation study	110
4.2	Oxidative dehydrogenation of ethanol	116
4.2.1	Effect of vanadia	117
4.2.2	Effect of support	121
4.3	Methylation of phenol	124
4.3.1	Influence of acid base properties on selectivity	128
4.3.2	Ortho selectivity	129
	References	133
CHAPTER V	SUMMARY AND CONCLUSIONS	
5.1	Summary	136
5.2	Conclusions	138
	Further scope of the work	139

CHAPTER I

GENERAL INTRODUCTION

1.1 Catalysis

The history of catalysis began from 1796 with the studies by von Marum on the dehydrogenation of alcohols using metals. However, the term catalysis was first formulated by John Jacob Berzelius in 1836. Ostwald defined catalyst as a substance, which increases the rate of a chemical reaction. Today, in one form or another, catalytic science reaches across the entire field of reaction chemistry and catalytic technology is a keystone of much of modern industry which is used for the manufacture of value added fine chemicals. The field of catalysis is now so wide and detailed and its applications are numerous. The development of novel catalysts, making efficient use of energy and raw materials with minimal impact on the environment is an extremely challenging task.

The replacement of homogeneous catalysts by heterogeneous systems in chemical industry has brought about efficient catalytic processes that eliminate or minimise the use and possible release of environmentally hazardous materials. Heterogeneous catalysis facilitates the separation of catalyst from the products and offer new reaction pathways for higher product selectivity with costless disposal of the used catalyst in comparison with the homogeneous catalysts. Low energy synthesis, prevention of reactor corrosion etc. are other attractive features of heterogeneous catalysis.

Catalyst design, which is most crucial for the development of new catalytic processes, is an exclusively interdisciplinary endeavor, which is located at the interface of chemistry, chemical engineering and material science. It requires some understanding of the mechanism of the catalytic reaction, and the knowledge of vital structural parameters that determine the activity, selectivity and lifetime of the catalyst and their interdependence. Studies on the interrelation between structure and chemical properties of the solid materials and catalytic properties (structure - activity

relationships) are at the origin of catalyst design. Various concepts and techniques of solid state and surface chemistry are applied for synthesizing and modifying catalyst materials with the required structural and chemical properties. Another important aspect of catalyst design is the tailoring of textural properties, *ie.* geometrical shape, surface area and pore structure, which is essential for optimizing the mass transfer of the reactants and products in the process network of the catalyst.

Based on the physico chemical nature catalysts are generally classified as,

- metal oxides / mixed metal oxides
- zeolites
- natural clay minerals
- metal complexes
- enzyme catalyst
- cation exchanged resins

Apart from this, they can also be classified on the basis of their functions as,

- shape selective catalysts
- phase transfer catalysts
- redox catalysts
- acid base catalysts

Another mode of classification is based on their behaviour in a particular reaction; as structure sensitive and structure insensitive. Rates of structure sensitive catalytic reactions alter markedly when the crystallite size of the system is changed, whereas rate is independent of crystallite size for structure insensitive reactions.

1.2 Metal oxide catalysts

The developments in surface science techniques have provided important information about the surface structures, chemical compositions and electronic properties of the metal oxide surfaces. In metal oxides, coordinative unsaturation is principally responsible for the ability towards adsorption and catalysis of various reactions. Metal oxides are made of cations and anions. The ionicity of the lattice,

which is often less than that predicted by the formal oxidation states results in the presence of charged adsorbate species and the common heterolytic dissociation of the molecules. Exposed cations and anions form acidic and basic sites as well as acid base pairs. Besides this, the variable valency of the cation results in the ability of the oxides to undergo oxidation and reduction. These properties have determining effects on the interaction of molecules with oxide surface. In addition to being used as catalysts, metal oxides are also precursors for other important catalysts. For eg. in hydrodesulfurisation catalysts, cobalt molybdenum sulfide is the active phase in which Co-Mo mixed metal oxide is used as precursors.

The foremost use of metal oxides in catalysis is towards oxidation reactions, on which a large number of industrial processes are based. Generally these metal oxides are divided into four main categories; simple, mixed, modified and supported. The major advantage of multi component systems is that it is possible to tune oxygen sorption properties by meticulously choosing the required metal components so as to crystallize in a particular structural pattern. The reactivity of oxygen in this case is strongly dependent on the kind of neighbouring metal ions as well as M-O bonding distance and bond strength.

The present investigation is based on supported vanadia catalysts. This category of catalyst has innumerable applications in fine chemical industry, especially in the area of oxidation reactions of industrial importance. Vanadia has an age-old history in the vast area of heterogeneous catalysis as the catalyst used for contact process. It has an unusually large number of stoichiometries. Their structures are very similar and can be constructed from the same building blocks. This contributes to the easy conversion of one oxide to another of adjacent stoichiometry by oxidation or reduction. The easy oxidation and reduction and the existence of cations of different oxidation states in the intermediate oxides have been proved to be important factors for these oxides to possess a prominent role in redox catalysis. But for pure V_2O_5 , the selectivity to a desired product is too low, which often exhibits complete

oxidation activity. It is accepted that addition of other elements improves the selectivity. This is achieved by supporting vanadia on suitable supports. The fine dispersion of the active species on the support makes supported vanadia dominate over bulk vanadia. Supported vanadia catalysts are renowned for their activity towards various types of partial or selective oxidation reactions. A large number of research work have been devoted to provide insight into the nature and reactivity of supported vanadia catalysts.

1.3 Methods of preparation of supported vanadia catalysts

Crystallographic form of the supported oxide depends on the preparation method. The principal technique of supported catalyst preparation involves two stages. First stage is dispersion and is achieved by impregnation, adsorption from solution, co precipitation or deposition etc. while the second stage involves calcination. The loading as well as the details of drying and calcination conditions affects the dispersion of the final oxide on the support.

1.3.1 Impregnation method

In impregnation, a solution containing the desired cation is added to the support. If the volume of the solution is just enough to fill the pore volume of the support, the method is called impregnation by incipient method. Excess of the solution may be used and solvent is evaporated and the oxide is formed after calcination; the method is known as wet impregnation. The loading can be varied over a wide range by changing the concentration and the amount of solution used. The pH of the solution decides the final dispersion of the active oxide species. Different species will be generated in the solution with variation of the pH. For eg., at pH < 1, vanadyl cation, pH < 4 three dimensional decavanadate $[HV_{10}O_{28}]^{5-}$, pH < 7 two dimensional tetra and trivanadate, 9 - divanadate, 12 – monovanadate are the different species formed [1].

1.3.2 Ion exchange method

This process can be applied for oxides that have precursor compounds that dissolve in water and form ionic complexes that contain the desired metal ion. It involves ionization of the surface hydroxyl group of the support in aqueous medium. The desired ion is then attached to the surface by electrostatic force. Subsequent calcinations of the ion exchanged material produces the oxide. High dispersion can be attained through this method, since the electrostatic repulsion keeps the complexes apart.

Spraying in vacuo a solution of the precursor on the oxide is another method reported in the case of $\text{Fe}_2\text{O}_3\text{-MoO}_3$ [2]. Precursors can also be introduced in gas phase. This method is adopted for the preparation of $\text{V}_2\text{O}_5/\text{Al}_2\text{O}_3$, by treating Al_2O_3 with a stream of nitrogen containing VOCl_3 . VOCl_3 is then hydrolysed with steam diluted with nitrogen. The process can be repeated to increase the vanadium loading.

1.3.3 Chemical vapour deposition

Active component is deposited from a volatile inorganic or organometallic compound on the surface of the support by reaction with the OH groups. For eg. TiO_2 supported on alumina can be prepared using a heptane solution of TiCl_4 or $\text{Ti}(\text{OC}_3\text{H}_7)_4$ [3].

1.3.4 Co-precipitation Method

In this method, the active and supporting oxides or their precursors may be co precipitated from a solution containing compounds of each element. Here the active component is dispersed throughout the bulk as well as on the surface. This method was adopted by Cavani *et al.* in the preparation of V/Ti systems by adding NH_4OH to a mixed V(IV) and Ti (IV) solution [4].

Another method is heating a mixture of the oxides. This leads to the spreading of the active oxide over the support. Repeated impregnation or a combination of ion exchange and impregnation can increase the final loading.

1.4 Structure of supported catalysts; metal-support interaction

Vanadia species get stabilised on the surface of the metal oxide support. The interaction, which results in the stabilisation can be viewed either in terms of minimization of surface free energy or in terms of formation of new chemical compounds. The actual structure present will depend amongst other things on the chemical nature and crystal structure of the support, the vanadium loading, and on the presence of adventitious impurities. Metal - support interaction leads to several physical and morphological changes of the support as well as the active oxide species. Often oxides are prepared by calcinations at relatively high temperature that reduces the surface area. A support effectively reduces sintering and thereby enhances the effective surface area. Support also serves as a heat conduction medium. This is particularly applicable for oxidation reactions, which have large heat of reaction. A support of high thermal conductivity helps to remove heat from the reaction site and reduces hot spots, which usually degrade selectivity. Apart from this, supports are used to improve mechanical strength, thermal stability and lifetime of the active metal species. In some other cases, support provides a certain desirable morphology for the oxides, like exposure of a particular plane, which will be active for specific reactions.

Results reported in bibliography indicate that the dispersion of vanadium oxide as well as the structure can be understood on the basis of the acid base character of the supports used; the basic and amphoteric oxides favour the bidimensional dispersion (often with the formation of compounds), whereas acidic supports favour three-dimensional micro units of V_2O_5 . The formation of new compounds is thermodynamically favourable, but kinetically limited. High temperature calcination enhances the formation of compounds. The tendency of the vanadia species to get dispersed is related to its basicity and decreases as basicity decreases. The

agglomeration of vanadia species to form crystalline vanadia is favoured with the acid character of the support. Accordingly, V_2O_5 crystals supported on SiO_2 is reported by Lopez Nieto et al [5]. Metal vanadates are observed on basic metal oxide supports [6].

The formation of these different types of vanadia species can be accounted as follows; since vanadia is comparatively acidic, it reacts easily with basic oxides with preferential formation of vanadates, whereas a weaker interaction with the acidic supports favor the aggregation of VO_x leading to the formation of crystalline V_2O_5 . Earlier works in this regard are briefly discussed below.

Dispersion of vanadia on ZrO_2 system is reported by Scharf *et al.* [7] and Sohn *et al.* [8]. A rapid formation of a multilayered structure has also been observed on ZrO_2/V_2O_5 , as a consequence of weak interaction between the support and the dispersed vanadium oxide. If vanadium loading exceeds theoretical monolayer, $Zr_2V_2O_7$ is formed [9]. Dependence of surface species formation on the acid base behaviour of the support has been further proved by various studies [7, 10].

On the most basic support, MgO , isolated VO_4 tetrahedra without bridging V-O-V oxygen ions forming $Mg_3V_2O_8$ like structure appeared within a larger range of vanadium loading. Dimeric VO_4 tetrahedra of the type $Mg_3V_2O_7$ and the mixed ortho and pyro magnesium vanadates have also been observed depending on the catalyst preparation procedure or vanadium loading [11-14]. Formation of the dispersed species at lower coverages and formation of crystalline vanadates at higher vanadia loadings are observed in the case of basic metal oxides like La_2O_3 , Sm_2O_3 and Bi_2O_3 [6].

Vanadium oxide formation intermediate between those on MgO and Al_2O_3 or SiO_2 has been observed on catalysts supported on hydrotalcites. The results obtained for vanadia supported on mixed oxides suggest that it is possible to control the

structure and reactivity of vanadia monolayers by modifying the local structure of the support. Martralis *et al.* observed an important influence of Ti/Al ratio on the type of vanadium species in vanadia supported on TiO₂/Al₂O₃ supports [15]. Thus for a given vanadium loading, the higher the alumina content, (within the range of 10-82 wt %) the higher is the surface area and the dispersion of vanadia. Modification of support TiO₂ lead to the formation of surface species on V/Ti-Al while crystalline V₂O₅ was seen on V/Ti catalyst.

Characterisation studies on V-SiO₂ systems have shown the existence of isolated VO₄ tetrahedra of the type (SiO)₃-V=O in dehydrated catalysts[16]. Isolated tetrahedral species are also observed on catalysts supported on Al₂O₃, TiO₂ and ZrO₂ at very low vanadium loadings. At higher vanadia percentage, VO₄ tetrahedral units form aggregates leading to chains or bidimensional arrays. At higher surface coverages the V⁵⁺ become six coordinated similar to that of metavanadate or decavanates. On metals oxides like Al₂O₃ and TiO₂, tetrahedral species are favoured together with other species upon dehydration. V₂O₅ crystallites appeared only above 60 % of monolayer coverage by vanadia for Al₂O₃. For TiO₂, crystalline vanadia appeared above 100% of the theoretical monolayer coverage [5].

In addition to acid base properties, the final vanadium content depends on the possible modification of the support during impregnation / or calcination steps. The structure of TiO₂ [17] and ZrO₂ [18] can be transformed during calcination and these modifications are enhanced in the presence of vanadia. Modification of the support during calcination step is also observed in natural sepiolite [19, 20] or Mg-Al hydrotalcite like materials [21] used as supports. In the former case, the initial Mg₈Si₁₂O₃(OH)₄ crystalline phase is transformed into MgSiO₃ in a degree which depend on vanadia loading and calcination temperature. In the latter case, Al₂O₃ is greatly dispersed on amorphous MgO material. In the case of zirconia – vanadia system, transition from amorphous to tetragonal phase is delayed in proportion to vanadia content [8].

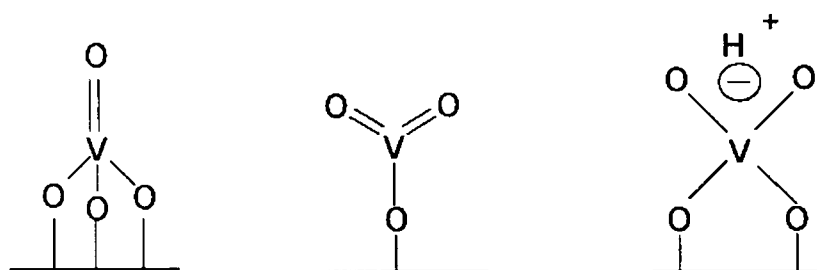
In the case of MgO, it is transformed to Mg(OH)₂ when the impregnation is carried out in the presence of water. In this circumstance, vanadia is partially occluded in the bulk of the catalyst and results in a lower surface vanadium concentration after calcinations. This has been concluded from the difference in values of the bulk and surface V/Mg atomic ratios [22]. Phase transformation of the support may be enhanced by the adding vanadium oxide as seen in the case of TiO₂ (anatase to rutile).

1.5 Structural models for surface vanadia species

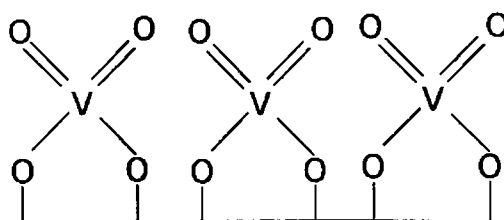
Various structural models proposed for the surface vanadia are given in Figure .1

1.6 Selective oxidation activity and acidity generation by vanadia loading

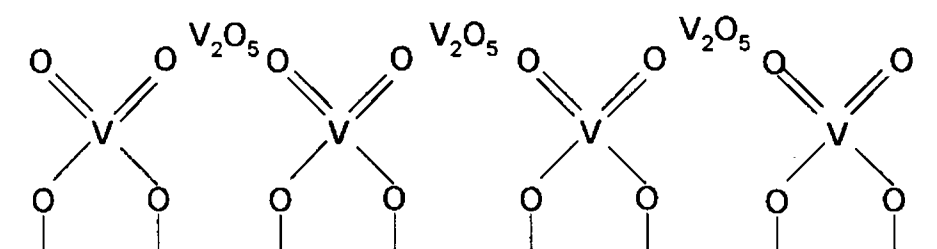
The most important aspect of supported vanadia systems is the selective oxidation activity towards partial oxidation products. The complete oxidation of the organics is minimised in the case of supported vanadia systems and thereby enhances selective oxidation products, which are industrially important. The selective oxidation activity is attributed to the lattice oxygen mobility. Isotopic oxygen exchange reaction conducted on supported vanadia call attention to the significance of lattice oxygen mobility of the systems in oxidation reactions [23]. Two vacancies are required for the exchange and it is available on the catalyst surface of pure V₂O₅ indicating high oxygen mobility. All layers in the crystals can participate because diffusion of oxygen is much faster. This will result in over oxidation. In the case of supported system, either one or two exchange may take place due to low diffusion rate since no bulk oxygen is available in supported V₂O₅, where the vanadia species are bound to support.



Monomeric units



Below mono layer



Above monolayer

Figure 1.1. Structural models of surface vanadia species

This inference can be applied to the activity of the catalysts for partial oxidation reactions. Deo *et al.* determined the reactivity of several supported systems in the partial oxidation of methanol [24]. The selectivity towards acetaldehyde followed the same trend in oxygen exchange reaction. The above-mentioned order

for supported system was also observed for the partial oxidation of butane to maleic anhydride [25].

Oxidation reactions over supported vanadia catalysts are known to take place through Mars and van Krevelen mechanism. In this mechanism, the reactant is first oxidized by lattice oxygen. The catalyst in turn is oxidized by gaseous oxygen to regenerate the system. On supported metal oxides, there is no large reservoir of bulk oxygen, which is able to abstract large number of hydrogen atoms. According to Sachtler *et al.*, the selectivity in the Mars and Van Krevlen oxidation reactions is determined by the intrinsic activity of oxygen species and their availability, *ie.* the first one or two oxygen atoms must be active, but the other lattice oxygen must be inactive. Only then the oxidation stops at the desired level of a partially oxidized product [26, 27]. Abstraction of many hydrogen atoms from the hydrocarbon will lead to a breaking of C-C bonds and consequently to complete oxidation. Thus, the locally limited amount of reactive oxygen atoms might be responsible for the high selectivity of the supported metal oxides.

Vanadia addition increases both Lewis and Bronsted type acidity. It has been proposed that surface Bronsted acid sites are also there in supported catalysts, which are located at bridging V-O-support bond. At lower percentage of vanadia, Bronsted acidity was found to increase. At higher vanadia composition, number of both Lewis and Bronsted acid sites sites are enhanced [28]. Studies by Hatayama *et al.* are also in agreement with this result. Bronsted acid sites were found to increase with vanadia composition [29]. Vanadium ion acts as the center for Lewis acidity. This view is in agreement with the work reported by Miyata *et al.* [30]. Both the types of acidities are remarkably increased by vanadia loading in the case of ZrO_2/V_2O_5 .

1.7 Reactions of supported vanadia catalysts

1.7.1 Oxidative dehydrogenation

Oxidative dehydrogenation (ODH) reactions constitute a major portion among the reactions catalysed by supported vanadia catalysts. In the case of ODH reactions, it is the selective oxidation activity that makes the system superior to pure vanadia. Bulk vanadia is known to possess a vast reservoir of oxygen, which becomes highly mobile when the oxide is in a partially reduced state, leading to over oxidation [31]. When incorporated on suitable supports, the selective oxidation activity is increased to a large extent. The different catalytic behaviour of bulk and supported vanadia catalysts are usually related to the modifications and environment of V-species, which can modify its redox properties. Some of the selective oxidative dehydrogenation reactions catalysed by supported vanadia catalysts are discussed below.

Active and selective catalysts for the oxidation of alkanes are obtained by mixing vanadium and magnesium oxides. Magnesium vanadates, *ie.* $\text{Mg}_3\text{V}_2\text{O}_8$, and/or $\text{Mg}_2\text{V}_2\text{O}_7$, are observed in the most effective catalysts suggesting that these constitute the active phases in the ODH of butane [31]. However, while V-Mg-O catalysts seem to be the most active and selective catalysts in the ODH of propane and n-butane, they show a low selectivity to ethane during the ODH of ethane [32, 33]. In an opposite trend, V/Al catalysts are found to be very much active for ethane [34] and propane oxidative dehydrogenation [35]. But selectivity to C_4 olefins is low in the case of n-butane ODH [36]. The role of 'Mo' in molybdenum doped V-Mg-O catalysed butane ODH has been reported by Dejoz *et al.* [37]. The incorporation of Mo modifies the number of V^{5+} species on the catalyst surface, reducibility of selective sites and catalytic performance. Here the selectivity and yield of ODH products were very low.

Different activity of these vanadates can be explained by their redox properties. If the vanadate is composed of a more reducible cation, it would be able to form oxygen anion vacancies more easily and migration of oxygen in the lattice is also more rapid. These will replenish the oxygen more easily and so, selectivity towards dehydrogenation will be lower. When ODH of butane was investigated over vanadates of Mg, Sm, Nd, Zn, Cr, Eu, Ni, Cu and Fe, there was a general correlation between selectivity for dehydrogenation with the reduction potential of the cation; the more easily reducible the cations are, the less selective the catalysts is. The only notable exception was Cr, which may be due to the presence of Cr^{6+} on the surface [38].

Corma *et al.* studied the catalytic properties of the supported vanadium oxide catalysts in the ODH of propane [6]. The most selective catalysts were obtained when vanadia was supported on basic metal oxide supports, *ie.*, MgO , Bi_2O_3 , La_2O_3 and Sm_2O_3 , while acidic oxide supports exhibited very low activity suggesting a parallelism between the appearance of metal vanadates (and absence of V_2O_5) and selectivity to ODH products. Efforts aimed at relating the structure of the dispersed vanadia to its activity and selectivity suggested that both isolated and oligomeric tetrahedral species can provide active and selective sites for ODH.

Comparison of the most effective supported vanadium oxide catalysts in the ODH of propane shows that except in the case of V/ Ti catalysts, a higher selectivity is obtained at vanadium loading below that of the theoretical monolayer [31]. In addition, for most of these catalysts, tetrahedral V^{5+} species are proposed to be the selective site in ODH reaction, as they are the main species present at sub monolayer coverages.

Propane ODH over V-Zr catalysts indicates high C-oxide selectivity on bulk ZrV_2O_7 and at low surface densities and appear to be associated with exposed unselective V-O-Zr and Zr-O-Zr sites. At low surface coverages, rate increases due

to the increase of polyvanadate species and decreases further with vanadia addition. This is due to the formation of V_2O_5 , which decreases the concentration of VO_x species exposed at cluster surface. At a given surface vanadia density, rate increases with increase in calcination temperature. This was explained by the formation of polyvanadate species at higher temperature. So the oxygen in the poly vanadate species is more active than in isolated surface vanadyl species [39].

An attempt to relate the catalytic performance and redox properties of the catalysts was done by Lopez Nieto *et al.* [40]. They pointed out that, the reducibility of vanadium atom will influence the selectivity to oxidative dehydrogenation products. This dependence is explained by its effect on the rate of selective redox processes involving vanadium species on the catalyst surface.

More recently, V- containing molecular sieves have been found to be highly active for the formation of oxyhydrogenation products during oxidation of ethane [41, 42] and propane [43- 45]. Other studies include selective oxidation of *n*- butane to maleic anhydride on V-P-O catalysts, selective oxidation of paraffins [46-49], ODH of ethane on V-Mo-Nb-O catalysts [50, 51].

Blasco *et al.* studied and summarized the general factors, which affect the ODH activity of supported systems [31]. He pointed out that apart from vanadia loading there are some other factors which control the activity and selectivity in ODH reactions. The selectivity was found to depend on the nature of alkane fed. Depending on the size of the reactant, the distance between the active sites also has a deciding role. Aggregate forms of vanadium and its coordination number are the other factors, which influence the activity and selectivity of supported vanadia catalysts. Both isolated and dimeric tetrahedral V^{5+} species were found to be active and selective towards partial oxidation products. The reducibility plays a major role in selectivity in the sense that the more reducible the catalyst, the less selective the

supported system. A good correlation was obtained for the catalytic activity and selectivity with the reducibility for ODH reactions on supported vanadia systems.

1.7.2 Ammoxidation

Ammoxidation is the reaction in which the CH_3 group in a side chain of an aromatic system or heterocyclic ring is converted into $-\text{CN}$ (nitriles) in presence of ammonia and oxygen. Vanadium oxide based catalysts are frequently used for catalyzing this reaction [52-54]. Propane ammoxidation was investigated by J. Nilsson *et al.* using Al-Sb-V catalysts [55]. The active phase identified for the system was $\text{Al}_{1-x}\text{Sb}_x\text{V}_x\text{O}_4$. Acrylonitrile selectivity was determined by the presence of isolated vanadium centers which are surrounded by Al and/ or Sb.

In the ammoxidation of 3-picoline over V_2O_5 [56], the nitrile formation was reported at (010) plane. The plane exposes equal number of $\text{V}=\text{O}$ groups and naked V^{5+} ions [57]. The amount of toluene adsorbed was correlated to $\text{V}=\text{O}$ frequency and each molecule adsorbed covers eight $\text{V}=\text{O}$ groups having eight neighbouring naked vanadium ions [58]. The active site used in the description of the mechanism is chosen to be an ensemble of four $\text{V}=\text{O}$ groups having neighbouring V ions exposed.

1.7.3 Oxidation of methanol

The selective oxidation of methanol to formaldehyde is extensively studied on vanadia-based catalysts. Pure V_2O_5 and a number of supported VO_x monolayer catalysts at low temperature dehydrates methanol to dimethyl ether. Selectivity to formaldehyde is usually increased, while activity is decreased with decreasing reducibility of the catalysts. High selectivity to formaldehyde (< 90 %) has been found with VO_x/SiO_2 [59] and VO_x/SnO_2 catalysts [60]. Recently it has been reported methyl formate could be directly produced with high selectivity and yield by catalytic methanol oxidation on V-Ti oxide [61, 62].

Structure sensitivity of methanol oxidation reaction on single crystals of V_2O_5 and MoO_3 was reported by Tatibouet [63]. Product selectivity is found to change with the crystal planes of the single crystals of V_2O_5 and the percentage of vanadia. Formaldehyde selectivity increased with increase in area of (001) crystal face of vanadia. Improved selectivity are obtained in the catalytic oxidation of methanol to formaldehyde using hexagonal orthovanadates of the type $Sr_{3-x}La_{2x/3}(VO_4)_2$ in comparison with those using the strontium and lanthanum orthovanadates reported separately by P. Salagre and J. E. Sueiras [64].

Selective catalytic reduction of nitrogen oxides is an important reaction in connection with the abatement atmospheric pollution. Selective catalytic reduction using ammonia is an effective method for treating flue gases from stationary combustion sources. Vanadia based systems were found to be very effective for the reduction of nitrogen oxides [65-67]. Highest activity reported for V_2O_5/TiO_2 system was found to be associated with two-dimensional VO_x clusters at intermediate loadings as reported by Nickll *et al.* [68].

Partial oxidation of methane is another reaction catalysed by supported vanadia systems efficiently [69-72]. Oxidation of toluene to benzaldehyde over V_2O_5/TiO_2 samples was reported by H. Miyata *et al.* A π complex formation of toluene was reported with the vanadium ion and CH_3 groups of the π complex are in turn dehydrogenated by $V=O$ species to form benzyl species. The formation of an aldehyde type intermediate before the oxidation of the benzyl species to benzoate on the system was also confirmed. Aniline alkylation was also attempted with supported vanadia catalysts [73].

Only a limited number of reports are seen in literature on rare earth oxide supported vanadia systems. They include oxidative dehydrogenation of propane reported by Corma and co workers and [6] and oxidative dehydrogenation of butane over $LnVO_4$ [74]. They proposed that redox properties of the cation 'M' in the

support having M — O — V bridging unit would affect the reactivity and selectivity of the catalyst.

1.8 Rare earth oxides as catalysts

Rare earth oxides are widely accepted basic catalysts. The activity is very much independent of electronic and magnetic properties of the oxides and is believed to depend on the relative basicity or surface structure. Paramagnetic nature, lattice oxygen mobility and / or variable valency of lanthanide ions have deciding role in the activity towards various reactions.

Oxygen exchange reactions conducted on these catalysts with the aim to establish correlation between the rate of exchange of oxygen ions in the various oxides and their behaviour as heterogeneous catalysts point to the high mobility of lattice oxygen. The slow step was the dissociative adsorption of molecular oxygen, the rate being dependent on the 4f electronic configuration of the metal cation. Winter has proposed that the kinetic features of lattice oxygen exchange in the rare earth oxides are dependent primarily on the unit cell volume of the Ln^{3+} ion and ascribes the rate-limiting step to desorption of molecular oxygen.

Activities of rare earth oxides have been explored for a wide variety of oxidation reactions, which depend on the lattice oxygen mobility and potential cation variable valency. Oxidation of molecular hydrogen is an important reaction in this category. Activation energy determined for the reaction was the same as that corresponding to $^{18}\text{O}_2$ exchange reaction indicating lattice oxygen participation for oxidation. As expected, nonstoichiometric oxides of Pr and Tb are found to possess maximum activity in which $\text{Ln}^{3+} \longrightarrow \text{Ln}^{4+}$ inter conversion occurs more rapidly. CO oxidation carried out over rare earth oxides confirms this conclusion. The rate of CO oxidation increased with mobility of lattice oxygen [75]. But the acidic CO_2 gets adsorbed on comparatively basic rare earth oxides forming carbonate species, causing self inhibition [75, 76]. So the overall reaction was expected to depend on the rate

of CO₂ desorption. Studies conducted on CeO₂ also agreed well with the participation of lattice oxygen in oxidation process [77, 78].

Other rare earth catalysed reactions include hydrogenation and dehydrogenation reactions. Hydrogenation studies of ethylene reported over these systems indicate that neither lattice oxygen mobility nor cation variable valency are important factors in governing the activity. Activity of these systems towards dehydrogenation of a variety of hydrocarbons is reported [79, 80]. Overall dehydrogenation activity for most reactions increased regularly with increase in atomic number of rare earth metal in the oxide.

Double bond migration causing isomerisation of cyclic olefins, 1-hexene and 1,5-hexadiene are reported over rare earth oxides, which were pre-calcined in air. Catalysts that were vacuum calcined showed much higher activity for the above reaction, revealing that anion vacancies and other surface defects are the leading factors [81].

Winter has done a detailed study of the decomposition of nitrogen oxides (N₂O) over rare earth oxides and a mechanism was also put forward by him [82-85]. Lattice oxygen participation was obvious from the activation energy of the reaction. A close inverse correspondence exists between decomposition activity and oxide lattice parameters, such as molecular volume and nearest Ln-O or O-O bond distance. But no correlation was seen between catalytic activity and magnetic properties of Ln³⁺ ions which do not vary regularly with lattice parameters. The general features of NO decomposition also closely parallel to those observed for the conversion of N₂O [82].

Catalytic cracking of butane was reported by Minachev *et al.* [86]. Activities were quite low compared to conventional cracking agents like Al₂O₃. Another set of reaction studied over earth oxides include ketonization of acids and alcohol. Oxide

basicity was found to be an important factor contributing to catalytic activity since ketone yield from a given reactant has generally been observed to decrease with decrease in the radius of rare earth cation.

Exchange type reactions constitute another interesting category that utilized the activity of rare earth oxides. These catalysts are found to be efficient for the interconversion of ortho and para hydrogen. The reaction proceeds by a physical paramagnetic mechanism where the 4f electronic configuration of the cation was found to be the deciding factor at low temperature, whereas 5s and 5p electrons control the activity by a chemical mechanism at higher reaction temperature [87, 88]. Minachev *et al.* studied the deuterium exchange on cyclohexane over CeO₂, Nd₂O₃ and Gd₂O₃ and found more or less equal activity with Al₂O₃ under similar reaction conditions.

1.9 Acid base properties

Surface acidity and basicity investigation have received considerable attention in recent years, since they provide significant information in determining the behaviour of the catalyst surface. A systematic investigation of the activity and selectivity of a catalyst and acid base property (strength, amount and type) enabled the identification of an optimum catalyst with desired acid base properties for a specific reaction. Development in this area has given rise to numerous methods for exploring these properties. They include visual colour change method using indicators, spectrophotometric method, gaseous adsorption studies etc. Discrimination between Lewis and Bronsted type acidities is also feasible by the above-mentioned techniques.

1.9.1 Hammett indicator method

Hammett indicator method proposed by Walling using adsorption of electrically neutral indicators is a simple method to determine and compare the acid base property of solid catalysts [89]. The solid is titrated against an organic base /

acid using Hammett indicators in nonaqueous solvents such as benzene. Non-aqueous condition ensures practically no interaction with the catalyst surface. Here the acid/base strength is expressed by the Hammett acidity function, H_0 . If the colour of the indicator adsorbed on the solid is acidic, the H_0 of the solid surface will be lower than the pK_a of the indicator. If colour is basic, H_0 value will be greater than the pK_a of the indicator applied.

Acid strength of a solid catalyst is described as the ability of the solid to convert an adsorbed neutral base into its conjugate acid. The amount of acid or acidity is the number in mmols of the acid sites per unit weight of the oxide. This is measured as the amount of base, which reacts with the solid acid. If the reaction proceeds by proton transfer from surface to indicator [a neutral base, B] acid strength is expressed by Hammett acidity function,

$$H_0 = pK_a + \log [B / BH^+]$$

where BH^+ is the concentration of the conjugate acid.

In the case of a Lewis acid site,

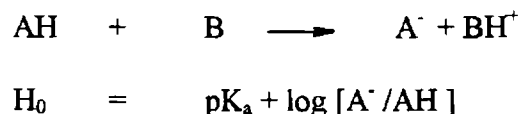
$$H_0 = pK_a + \log [B / AB]$$

where A is a Lewis acid or electron pair acceptor.

The lower the pK_a of the colour changing indicator, the greater the acid strength of the system.

Similarly, it is possible to determine the base strength, which is defined as the ability of the solid surface to donate electron pair to an adsorbed acid indicator by observing colour change of an acid indicator. At the end point, the colour due to the conjugate acid form of the indicator appears.

For the reaction of indicator AH with solid base \bar{B} ,



Approximate value of the basic strength on the surface is the pK_a value of the indicator at which the intermediate colour appears.

Indicators with different pK_a values enable the determination of the amount of acid of various strengths. According to Tanabe, the total amount, *ie.* both Lewis and Bronsted type of acidity/ basicity can be measured by Hammett indicator method [90]. But some contradictory reports are there that only Bronsted acidity can be evaluated through this procedure since this method is limited to solids where exchange of protons occurs [91]. Hammett indicator is mainly useful to determine the acid-base property of white samples. In the case of coloured samples, a standard white sample is added during the experiment [90]. However, it should be emphasised that the reference used should exhibit a wider range of acidity than the sample.

Yamanaka and Tanabe have described a common scale for the determination of the distribution of surface acid/base strength taking into account the bifunctional character of the surface [92, 93]. The curves for acidic and basic strength distribution intersects at the point where both acidity and basicity is equal to zero. This point is defined as the $H_{0, \max}$ parameter by the authors. This value was found to be better than the zero point charge determined for water solutions since it expresses actual acid/base property taking into account all parameters like structure of the surface, moisture content and the intrinsic nature of the solid [94].

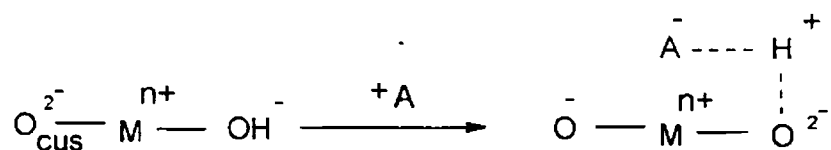
1.9.2 Electron donating property studies

Metal oxides are well known for their basicity due to the presence of electron transfer sites, which make them suitable for catalyzing a wide variety of reactions. The adsorption of electron acceptors has been investigated to study and characterize

the electron donating property of the metal oxides [95, 96]. Flockhart and coworkers associated the donor sites on the metal oxide with unsolvated hydroxyl ions and defect centers involving oxide ions [97]. As a result of electron transfer, radical anion formation occurs on the surface of the solid. The surface shows remarkable colouration by the adsorption of the electron acceptor. The generation of radical anions is further confirmed by ESR spectral studies. The spectra obtained was unresolved indicating that the anisotropy of the hyperfine structure arises from the hindered rotational freedom of the adsorbed species. This has been confirmed from literature [95, 98]. A g value of 2.003 was obtained for ESR spectra of TCNQ adsorbed oxides, which was identified to be that of TCNQ anion radical.

Electron donor strength of a metal oxide surface is defined as the conversion power of an adsorbed electron acceptor to its anion radical. If the electron acceptor used is a strong one, *ie.*, with high electron affinity value, anion radical formation takes place both at strong and weak donor sites, whereas a weak acceptor get adsorbed only on strong donor sites. The electron donating capacity can be expressed as the limiting electron affinity value at which free radical anion formation is not observed at the metal surface.

Studies carried out on TiO_2 by Che *et al.* inferred that surface hydroxyl ions are the sources of basicity at low activation temperature; weakly coordinated oxide ions having major contribution at higher activation temperature [99]. A detailed investigation of electron donating sites on oxide surfaces has been carried out by D. Cordischi and co workers [100]. A correlation between electron donating capacity and Lewis basicity was suggested and the donor sites were proposed to be a coordinatively unsaturated oxygen ion, ($\text{O}^{2-}_{\text{cus}}$) associated with a nearby OH group, whose proton interacts with the radical anion formed giving stability. Adsorbed radical interact with the protons. So Bronsted acidity stabilizes the radical ion formed. The active site can be considered as acid base pair as shown in figure.



Meguro et al. reported adsorption of electron acceptors on alumina and they proposed that surface hydroxyl groups are responsible for electron donating property of the oxides [98]. A plausible mechanism was suggested by them for the adsorption of electron acceptors on alumina surface activated at 500°C, due to surface hydroxyl ions. The ionization potential of hydroxyl ion being small (~ 2.6 eV in gas phase), [101], an oxidation reduction process was put forward.



Electron donating property of ZrO₂ studied by Esumi *et al.* revealed the effect of calcination temperature on adsorption of electron acceptors [102]. An increase of calcination temperature reduces the amount of adsorbed electron acceptor indicating reduction of OH⁻ on the surface. Above 900° C, amount adsorbed again increased due to the formation of surface oxide ions.

Solvent effects on the acid base interaction of the electron acceptor with the metal oxide was studied on alumina and TiO₂ [103]. The amount of TCNQ adsorbed and the concentration of anion radicals formed decreased with an increase in acid base interaction between TCNQ and basic solvent for both the oxides. The effect of solvent on adsorption of chloranil was further reported by Esumi and co workers [104]. The amount of chloranil adsorbed decreased with an increase of acid base interaction between the basic solvent and chloranil and also decreased with an increase of acid base interaction between the acidic solvent and electron donor sites. Drago equation was applied to understand the nature of interaction of different solvents with TCNQ. Acid base enthalpy is high for acetonitrile and the order was acetonitrile > ethyl acetate > 1,4-dioxane. So adsorption is depressed by the interaction between TCNQ and acetonitrile. The concentration of radical anions

formed decreased with increase of acid base interaction between electron acceptor and organic solvent.

Sugunan *et al.* carried out a detailed study of electron donating capacity of rare earth oxides and their mixed analogues as a function of temperature and composition [105-107]. Electron donating capacity of lanthanum oxide and the influence of addition of strontium oxide was studied and found that electron donating capacity was improved by doping strontium [108]. Magnetic and electron donating properties of samaria at different activation temperatures were also reported by the same authors [109]. It was found that the number of both strong and weak donor sites are increased with increase in activation temperature. During adsorption, magnetic moment decreased and reached a limiting value at the same concentration at which limiting amount of EA was adsorbed. Reports on electron donating capacity of mixed oxides of La and Al showed the limit of electron transfer to be between 1.77 and 2.40. La_2O_3 promoted surface properties of alumina without altering the limit of electron transfer [110]. The increase of electron donating capacity was attributed to increase of Al-O-La bonds. The same group also reported investigation of electron donating property of manganese ferrosinels and the limit of electron transfer was found between 1.77 and 2.40 in terms of electron affinity of the electron acceptor [111].

1.9.3 Temperature Programmed Desorption Studies

Chemisorption of molecules such as ammonia, pyridine, CO_2 etc. is often used as a probe for the surface properties of metal oxides. By probing the interaction of the molecules with the surface, information can be obtained on the oxidation state of the metal ion, coordination symmetry, degree of coordinative unsaturation of the surface OH and presence and nature of Lewis and Bronsted acid sites. Among these categories, TPD of ammonia is one of the most promising technique, facilitating the direct determination of the strength and distribution of acid sites. Interaction with the surface will be quite strong since ammonia is a fairly hard base. Ammonia being a strong Lewis base and smaller than pyridine, can detect most of the acid sites and

the distribution of sites according to the acid strength can be obtained. However, a quantitative distinction between the Lewis and Bronsted acid sites cannot be achieved by this method. This can be attained by *in situ* IR measurement of adsorption of pyridine on the solid surface.

When chemisorbed on a surface possessing acid properties, NH_3 can interact with acidic protons, electron acceptor sites and hydrogen from neutral or weakly acidic hydroxyls [112]. NH_3 when adsorbed on a surface can be retained in different modes, [113]. a) hydrogen bonding via one of its hydrogen atoms to a surface oxygen atom or oxygen of the hydroxyl group (weakest interaction) b) transfer of protons from surface OH to ammonia (Bronsted acidity). These two interactions will involve neighbouring anions or OH groups. Another mode of interaction, which is the strongest interaction, is the coordination to an electron deficient atom (Lewis acidity). The fourth one involves dissociative adsorption in the form of surface NH_2 or NH and OH. A complete transfer of H^+ to ammonia from Bronsted sites to produce NH_4^+ ions also occurs.

The advantage of the TPD method over other techniques is that it allows the study of the catalyst under conditions more or less similar to that of reaction. A minimum temperature of about 100°C is necessary to eliminate physical adsorption. Both Lewis and Bronsted type of activities are obtained by temperature programmed desorption studies using ammonia.

1.9.4 Cyclohexanol decomposition – a test reaction for acidity

The utility of alcohol decomposition as a test reaction for acid base property studies of metal oxides is well established. Since alcohols are amphoteric, they interact easily with both acid and base sites. It was observed that metal oxides are catalysing both dehydration and dehydrogenation of alcohols. Alkene formation associated with dehydration was proposed to be due to the participation of Bronsted acid sites. Acidic OH groups catalyses dehydration reaction.

Davis suggested alcohol conversion selectivity as a measure of basicity of metal oxides [114]. 1-alkene formation accompanied by water elimination was observed to depend on the base strength of the oxide. Alcohol decomposition was carried out over various systems by Mamoru Ai while studying acid base properties of various metal oxides. Dehydration rate was found to be proportional to acidity whereas dehydrogenation, which proceeds by a concerted mechanism was found to be proportional to both acidity and basicity [115].

Bezouhanava *et al.* have proposed cyclohexanol decomposition as a simple and fast method to determine the functionality of metal oxide catalysts [116]. They interpreted the dehydrogenation activity as related to the existence of basic sites originating from the lattice oxygen. Dehydrogenation of the ring was observed in this case and was related to the influence of transition metal. Stronger acid sites are needed for dehydration to take place compared to other secondary and tertiary alcohols, like isopropyl alcohol or tertiary butyl alcohol.

Catalytic decomposition of cyclohexanol over $Mg_{1-x}Zn_xAl_2O_4$ reported by Joshi and co workers gave idea about the surface properties, structure and catalytic activity correlation. Correlation was established between transport properties, surface acidity and catalytic behaviour [117]. Results on alumina published by Pines *et al.* point out to the formation of methyl cyclopentene on stronger acidic sites which is formed by the isomerisation of cyclohexene [118].

1. 10 Reactions selected for the present study

Oxidative dehydrogenation reactions are an attractive alternative to classical dehydrogenations. Dehydrogenation of the alkanes to corresponding alkenes is a highly endothermic process that has to be carried out at temperature above 600°C. At this high temperature, other unwanted reactions leading to coke formation also occur, and catalyst needs frequent regeneration. Since this process is equilibrium limited and energy intensive, there is strong incentive for the development of ODH process.

In ODH reactions, abstracted hydrogen is oxidized, releasing heat of reaction and the conversion becomes significant at a much lower reaction temperature which is not equilibrium limited. For the present investigation, oxidative dehydrogenation of ethyl benzene and ethanol are selected.

1.10.1 Oxidative dehydrogenation of ethyl benzene

Vanadium based catalysts are extensively used for oxidative dehydrogenation of ethyl benzene. The main product of commercial importance is styrene along with ethylene, traces of benzene, toluene etc. Commercial processes use high reaction temperatures and low ethyl benzene pressures in the feed to achieve favourable ethyl benzene conversions. Super heated steam is used to provide the energy needed by the reaction, to dilute the reactant and to reduce catalyst coking.

The catalysts reported in the literature for the ODH of ethyl benzene to styrene include metal oxides [119-126], and phosphates [127-129] and organic polymers [130, 131]. Two possible types of catalysis have been proposed for the ODH of ethyl benzene. First one involves redox operation of transition metal oxide and the other involves catalytically active coke.

Of the transition metal oxides, V-Mg-O system is the most active and selective for ethyl benzene to styrene conversion. Chang *et al.* reported the reaction over V(V) and V(IV) magnesium vanadates [132]. It was observed that the activity and selectivity of ODH of ethyl benzene do not correlate with the oxidation state of vanadium and show a constant styrene selectivity with little dependence on reaction temperature and ethyl benzene conversion. The active species responsible for the formation of styrene was concluded to be $Mg_3V_2O_8$. Explanation for this behaviour was achieved by quoting studies done by Kung *et al.* [133,33]. The V-O-V bond in MgV_2O_6 and $Mg_2V_2O_7$ permits easy oxygen removal from the lattice and thereby preferring complete oxidation of hydrocarbon. But in case of magnesium orthovanadate, all the oxygen atoms are bonded on V-O-Mg. Thus oxygen removal

will be difficult and the activity for total oxidation will be low yielding selective oxidation product.

Murakami and co workers studied this reaction over SnO₂-P₂O₅ system. [134]. α -'H' abstraction leading to π allyl mechanism was suggested for the reaction pathway. The active component was recognized to be a type of Sn-P compound. A reduction – oxidation mechanism was suggested by them for the reaction, where tin, the basic component activates oxygen and 'P' the acidic component activates ethyl benzene.

Deuterium exchange studies carried out on Si- Al catalysts have shown that the adsorbed intermediate of ethyl benzene are dissociated in the α -position [135]. The active oxygen on the surface was found to be the O⁻ species. The lattice oxygen in turn supplies O⁻. The acid site of Ho between 1.5 and -5.6 is proposed to adsorb ethyl benzene reversibly abstracting the α H at the basic OH site adjacent to the acid site, and the base sites of pK_a between 17.2 and 26.2 activates gaseous oxygen to form O⁻ which abstract the β hydrogen.

A number of studies have been devoted to the active oxygen species that is responsible for ODH reactions. An improved activity for lattice oxygen was observed on 'Mo' containing oxides [136]. In some other cases, active species were also supposed to be M = O groups [124,137,138]. In the case of spinel ferrites, adsorbed oxygen species (O⁻) were the active species [137-139]. Their studies concluded that acid sites withdraw electron of the aromatic ring to enhance the acidic property of the α hydrogen and is interacting with OH near to surface.

An investigation about the mechanism of the reaction suggested active participation of lattice oxygen. Lattice oxygen abstracts H and oxidation of the catalyst occurs by gas phase oxygen [122]. Lattice oxygen appears from the surface

layer, whereas bulk oxygen was reported to be inactive [140]. The participation of the lattice oxygen is further supported by the work done by Haber *et al.* [136].

Kim *et al.* studied and reported oxidation of ethyl benzene over lanthanide promoted catalysts [141]. They found that pure lanthanide oxide catalyses almost complete oxidation of the organics. Praseodymia was found to be the best promoter among the various oxides used (La, Ce, Pr and Nd). They attributed this enhanced activity to the low activation energy for electronic conduction compared to other three systems.

1.10.2 Oxidative dehydrogenation of Ethanol

Recently, oxidative dehydrogenation of ethanol to value added fine chemicals have reserved an interesting technological importance in connection with the utilization of biomass as a chemical source [142]. Commercially used catalysts are silver based ones. Nowadays metal oxides are explored for their substitution. Among the oxides screened, molybdenum and vanadium based catalysts are the promising candidates for the above reaction [143]. Oyama *et al.* reported structure insensitivity of ethanol decomposition over $\text{SiO}_2\text{-V}_2\text{O}_5$ system [144]. At low temperature, acetaldehyde was the main product while at high temperature it was ethylene. Acetic acid formation was also observed at intermediate temperatures. At low conversion, vanadia species was found to be responsible for the activity. Quaranta and co workers extended this work by using TiO_2 coated SiO_2 as support. An enhancement in activity towards acetaldehyde was observed due to the interaction of TiO_2 and molecular dispersion. An improved selectivity for acetaldehyde, on the basis of greater heat dissipation and isothermicity was observed on $\alpha\text{-Al}_2\text{O}_3/\text{V}_2\text{O}_5$ as reported by Quaranta *et al.* [145].

$\text{MgO-V}_2\text{O}_5$ system was selected as catalyst for the above-mentioned reaction and the selectivity towards acetaldehyde was found to depend on the nature of compound formation between MgO and V_2O_5 . The $\text{Mg}_3\text{V}_2\text{O}_8$ was found to be the

most active and selective catalyst than MgV_2O_6 that exhibited very low selectivity and activity. The high activity of $\text{Mg}_3\text{V}_2\text{O}_8$ was correlated with creation of holes and the position of the Fermi potential [146].

Decomposition of ethanol over vanadium silicate molecular sieves have been reported [147]. It was presumed that acetaldehyde formation was facilitated by the V=O species while simultaneous interaction of both V=O and V-O-Si linkages is responsible for ethylene formation. Nakagawa *et al.* studied the promoting effect of V_2O_5 on V/Ti system in the oxidation of ethanol and the promoting effect is attributed to the formation of amorphous or two dimensional vanadium oxide [148]. Oxygen in the V=O species act as strong basic site, playing significant role in hydrogen abstraction from alcohol. Generally the total oxidation activity of V_2O_5 based catalysts is attributed to the high activity of oxygen sites. Samples with higher V^{4+} species were found to favour partial oxidation products and the reactivity was influenced by the acidity of the systems.

1.10. 3 Methylation of phenol

In recent years, alkyl phenol synthesis has become interesting, since the products are of high commercial value. Both O- and C- alkylated compounds are formed and the selectivity of the products was found to depend upon the acid base property of the catalysts employed [149, 150]. The demand for these chemicals has increased in recent years owing to the growing use of their derivatives. Products include o-cresol, 2,6-xylenol, anisole etc. Generally attempted catalysts include $\gamma\text{-Al}_2\text{O}_3$, silica alumina, SAPOs, zeolites, ALPOs, metallic sulfates, phosphates etc. It has been found that strong acidic sites favour O-alkylation, while strong basic sites favour C-alkylation [151]. A contradictory claim was put forward that it is the acidic sites that favour C-alkylation [152, 153]. This was in agreement with Balsama *et al.* who confirmed the enhancement of C-alkylated products by strong acidic sites [154].

Methylation of phenol was studied by S. Velu and co workers on Mg-Al hydrotalcites[155]. Activity of the reaction was compared with pure MgO and Al₂O₃ and physically mixed MgO-Al₂O₃. Of these, calcined hydrotalcites with Mg-Al ratio of 4 : 1 was the most active. They suggested a participation of combined acidic and basic sites for the reaction.

An IR study of phenol adsorbed on SiO₂-Al₂O₃ and MgO revealed that ortho selectivity is strongly controlled by the adsorbed states of phenol [156]. Since in the case of SiO₂/Al₂O₃, the plane of benzene ring of phenolate ion is close to the catalyst surface, any of ortho, meta and para position can be attacked by a methyl cation formed from methanol. On the other hand, only the ortho position can be methylated in the case of MgO, because ortho position is near to the surface. The difference in adsorption depends on the acid strength of the catalyst. Since the acid strength if Si/Al is very high, the acid sites interact with the π electron of the benzene ring of the phenolate ion bending the molecule slightly towards the surface.

1. 11 Present work

The need for novel oxidation catalysts prompted us to use La₂O₃, Sm₂O₃ and Dy₂O₃ as the supports for the present investigation. Rare earth oxides are excellent supports for oxidation reactions since they are highly non reducible. Besides, their binding energy is very low which makes the replenishment of consumed oxygen very easy. Reports on catalysis by vanadia supported on these oxides are very rare. Different vanadia loadings are attempted to modify the properties of rare earth oxides and to get an understanding of the active species of vanadia on the support. Since the supports are basic in nature, impregnation of vanadia is expected to bring about vanadates, which are excellent catalysts for oxidative dehydrogenation reactions. Vanadia impregnation also leads to acidity generation so that acid catalysed reactions would be feasible over these systems.

1. 12. Objectives of the work

Main objectives of the present work are

- ↳ To prepare rare earth oxide supported vanadia with different vanadium loadings and to examine the surface properties employing different instrumental techniques like EDX, XRD, FTIR, BET surface area, pore volume measurements etc.
- ↳ To understand surface species of vanadia on basic lanthanide oxides.
- ↳ A thorough understanding of the acid base properties of V-Ln catalysts using techniques like TPD, adsorption studies, cyclohexanol decomposition and conventional Hammett indicator method.
- ↳ To test the activity of supported systems in the oxidative dehydrogenation of ethyl benzene and to understand the active vanadia species.
- ↳ To evaluate the catalytic activity of these systems in the oxidative dehydrogenation of ethanol.
- ↳ To test the catalytic activity of these systems in the alkylation of phenol with methanol and to attempt the correlation of acid base properties of the catalysts and the product selectivity.

References

1. M. Pope and B. Dale, *Quart. Rev. (London)*, 22 (1968) 527
2. M. Carbucicchio and F. Trifiro, *J. Catal.*, 62 (1980) 13.
3. G. B. Mc Vicker and J. J. Ziemiak, *J. Catal.*, 95 (1985) 473.
4. F. Cavani, G. Centi, E. Foresti and F. Trifiro, *J. Chem. Soc. Farady Trans. 1* (1987) 83.
5. J. M. Lopez Nieto, G. Kremenik and J. L. G. Fiero, *Appl. Catal.*, 61 (1990) 235
6. A. Corma, J. M. Lopez Nieto, N. Paredes, M. Perez, Y. Shen, H. Cao and S. L. Suib, *Stud. Surf. Sci. Catal.*, 72 (1992) 213.
7. U. Schart, M. Schrami-Marth, A. Wokaun and A. Baiker, *J. Chem. Soc. Faraday Trans.*, 87 (1991) 3299.
8. J. R. Shon, S. G. Cho, Y. I. Pae and S. Hayashi, *J. Catal.*, 159 (1996) 170.
9. M. Santai, A. Andersson, L. R. Wallenberg and B. Rebenstorf, *Appl. Catal. A*, 106 (1993) 51
10. G. Deo & I. E. Wachs, *J. Phys. Chem.*, 95 (1991) 5889
11. M. Chaar, D. Patel, M. Kung and H. H. Kung, *J. Catal.*, 105 (1987) 483
12. M. Chaar, D. Patel, M. Kung and H. H. Kung, *J. Catal.*, 109 (1988) 463
13. T. Blasco, J. Lopez Nieto, A. Dejoz and M. I. Vazquez, *J. Catal.*, 157 (1995) 271
14. D. Siew Hew Sam, V. Soenen and J. C. Volta, *J. Catal.*, 123 (1990) 417.
15. K. H. Martralis, M. Ciardelli, M. Ruwet and P. Grange, *J. Catal.*, 157 (1995) 368
16. N. Das, H. Eckert, H. Hu, I. E. Wachs, J. Walcer and F. Feher, *J. Phys. Chem.*, 97 (1993) 8240.
17. Busca, G. Centi, L. Marchetti and F. Trifiro, *Langmuir*, 2 (1986) 568

18. P. D. L. Mercera, J. G. van Ommen, E. B. M. Doesburg, A. J. Burggraat and J. R. H. Ross, *Appl. Catal.*, 57 (1990) 127
19. A. Corma, J. Lopez Nieto, N. Paredes and M. Perez, *Appl. Catal. A*, 97 (1993) 159
20. M. L. Ocelli, in : M. L. Ocelli (Ed.) , *Fluid and Catalytic cracking role in Modern refining*, ACS Symp. Ser., 375 (1988) 162
21. F. Rey, V. Fornes and J. M. Rojo, *J. Chem. Soc., Faraday Trans.*, 88 (1992) 2233
22. Corma, J. M. Lopez Nieto and N. Paredes, *Appl. Catal. A:*, 104 (1993) 161
23. C Doornkamp, M. Clement, X. Gao, G. Deo, I. E. Wachs and V. Ponec, *J. Catal.*, 185 (1999) 415.
24. G. Deo and I. E. Wachs, *J. Catal.*, 146 (1994) 323
25. I. E. Wachs, J. Jehng, G. Deo, B. M. Weckuyson, V. V. Guliants, J. B. Benziger and S. Sundaresan, *J. Catal.*, 170 (1997) 75.
26. W. M. H. Sachtler and N. H. De Boer, "Proceedings 3rd International Congress on Catalysis, Amsterdam, 1964", p. 240, Wiley, New York, 1965;
27. W. M. H. Sachtler, G. J. H. Dorgelo, J. Fahrenfort and R. J. H. Voorhoev, "Proceedings 4th International Congress on Catalysis, Moscow, 1968" (B. A. Kazansky, Ed.), p. 454, Adler, New York, 1968)
28. J. Le. Bars, J. C. Vedrine, A. Aurox, S. Trautmann, M. Baerns, *Appl. Catal. A : Gen.*, 119 (1994) 341
29. F. Hatayama, T. Ohno, T. Maruoka, T. Ono and H. Miyata, *J. Chem. Soc. Faraday Trans.*, 87 (16) (1991) 2629.
30. H. Miyata, K. Fujii and T. Ono, *J. Chem. Soc. Faraday Trans. 1*, 84 (1988) 3121
31. T. Blasco, J. M. Lopez Nieto, *Appl. Catal. A: Gen.*, 157 (1997) 117.
32. P. Concepcion, A. Galli, J. M. Lopez Nieto, A. Dejoz and M. I. Vazquez, *Top. Catal.*, 3 (1996) 451
33. P. M. Michalatos, M. C. Kung, I. Jahan and H. H. Kung, *J. Catal.*, 140 (1993) 226.

34. J. Le Bars, A. Auroux, M. Forisier, J. Vadrine, *J. Catal.*, 162 (1996) 250
35. J. G. Eon, R. Olier and J. Volta, *J. Catal.*, 145 (1994) 318.
36. A. Galli, J. M. Lopez Nieto, A. Dejoz and M. I. Vazquez, *Catal. Lett.*, 34 (1995) 51.
37. A. Dejoz, J. M. Lopez Nieto, F. Marquez and M. I. Vazquez, *Appl. Catal. A: Gen.*, 180 (1999) 83
38. H. H. Kung, M. C. Kung, *Appl. Catal. A: Gen.*, 157 (1997) 105
39. A. Khodakov, J. Yang, S. Su, E. Iglesia and A. T. Bell., *J. Catal.*, 177 (1998) 343
40. J. M. Lopez Nieto, J. Soler, P. Concepcion, J. Herguido, M. Menendez and J. Santamaria, *J. Catal.*, 185 (1999) 324
41. P. Concepcion, J. M. Lopez Nieto and J. Perez-Pariente, *Catal. Lett.*, 28 (1994) 9
42. P. Concepcion, J. M. Lopez Nieto and J. Perez-Pariente, *Stud. Surf. Sci. Catal.*, 94 (1995) 681
43. L. W. Zatorski, G. Centi, J. M. Lopez Nieto, F. Trifiro, G. Bellusi and V. Fattore, *Stud. Surf. Sci. Catal.*, 49 (1989) 1243
44. G. Bellusi, G. Centi, S. Perathoner, F. Trifiro, in *Catalytic Selective Oxidation*, ACS Symp. Ser., 523 (1993) 281
45. T. Blasco, P. Concepcion, J. M. Lopez Nieto and J. Perez-Pariente, *J. Catal.*, 152 (1995) 1.
46. G. Centi, F. Trifiro, J. Ebner and V. Franchetti, *Chem. Rev.*, 88 (1988) 55
47. B. K. Hodnett, *Catal. Rev. Sci. Eng.*, 27 (1985) 373.
48. G. Centi (Ed.), *Catal. Today*, 16 (1993) 1.
49. F. Cavani, F. Trifiro in *Catalysis- A specialist Periodical Report*, vol. 11. Royal Society of Chemistry, London, 1994, p. 246
50. E. M. Thorsteinson, T. P. Wilson, F. G. Young and P. H. Kasai, *J. Catal.*, 52 (1978)116.

51. R. Burch and R. Swarnakas , *Appl. Catal.*, 70 (1991) 129.
52. Y. Murakami, M. Niwa, T. Hattori, S. Osawa, I. Igushi and H. Ando, *J. Catal.*, 49 (1977) 83
53. A. Andersson and S. T. Lundin, *J. Catal.*, 58 (1979) 383
54. M. Niwa, H. Ando and Y. Murakami, *J. Catal.*, 70 (1981) 1.
55. Jerker Nilsson, Angel R. Landa Canovas, Staffan Hansen and Arne Andersson, *J. Catal.*, 160 (1996) 244
56. A. Andersson, J. O. Bovin and P. Walter, *J. Catal.*, 98 (1986) 204
57. A. Andersson, *J. Solid State Chem.*, 42 (1982) 263
58. A. Andersson, in M. Che and G. C. Bond (Eds.), *Stud. Surf. Sci. Catal.*, Elsevier, Amsterdam, 1985, vol. 21, pp. 381-402.
59. K. Kijenski, A. Baiker, M. Glinski, P. Dollenmeier and A. Wokaun, *J. Catal.*, 101 (1986) 1
60. B. M. Reddy, K.K. Narasimha, Ch. Sivaraj and P. Kanta Rao, *Appl. Catal.*, 55 (1989) L1
61. G. Busca, P. Tittarelli, E. Tronconi and P. Forzatti, *J. Solid State Chem.*, 67 (1987) 91
62. G. Busca, A. S. Elmi and P. Forzatti, *J. Phys. Chem.*, 91 (1987) 5263
63. J. M. Tatibouet, *Appl. Catal. A.*, 148 (1997) 213.
64. P. Salagre and J. E. Sueiras, *J. Chem. Soc. Chem. Comm.*, (1998) 1084
65. H. Schneider, S. Tschudin, M. Schneider, A. Wokaun, A. Baiker, *J. Catal.*, 147 (1994) 5
66. M. Schneider, M.M. Maciejewski, S. Tschudin, A. Wokaun, A. Baiker, *J. Catal.*, 149 (1994) 326.
67. M. Schneider, U. Scharf, A. Wokaun, A. Baiker, *J. Catal.*, 150(1994) 284.
68. J. Nickl, G. Dutoit, A. Baiker, U. Scharf and A. Wokaun, *Appl. Catal. A*: 98 (1993) 173.

69. Q. Sun, J. Jehng, H. Hu, R. G. Hermann, I. E. Wachs and K. Kiler, *J. Catal.*, 165 (1997) 91
70. H. F. Liu, R. S. Liu, K. Y. Liew, R. E. Johnson and J. H. Lunsford, *J. Am. Chem. Soc.*, 106 (1984) 4117
71. N. D. Spencer, *J. Catal.*, 109 (1987) 187
72. N. D. Spencer and C. J. Pereira, *J. Catal.*, 116 (1989) 399
73. S. Narayanan, S. Prabhu Prasad, *J. Mol. Catal. A: Chem.*, 96 (1995) 57.
74. D. Patel, P. J. Anderson and H. H. Kung, *J. Catal.*, 125 (1990) 132.
75. L. A. Sazanov, E.V. Artmonov and G.N. Mitrofanova, *Kinet. Katal.*, 12(1971)378.
76. E. V. Artamonov, and L. A. Sazanov, *Kinet. Katal.*, 12 (1971) 961.
77. M. Breysse, M. Guenin, B. Claudel, H. Latrielle and J. Veron, *J. Catal.*, 27 (1972) 275
78. M. Breysse, M. Guenin, B. Claudel and J. Veron, *J. Catal.*, 28 (1973) 54
79. R. A. Briggs and H. S. Taylor, *J. Am. Chem. Soc.*, 63 (1941) 2500
80. C. B. Mc. Gough and G. Houghton, *J. Phys. Chem.*, 65 (1961) 1887.
81. V. D. Sokolovski, L. A. Sazonov, G. K. Boreskov and Z. V. Moskvina, *Kinet. Katal.*, 9 (1968) 130.
82. E. R. S. Winter, *J. Catal.*, 22 (1971) 158
83. E. R. S. Winter, *J. Catal.*, 15 (1969) 144
84. E. R. S. Winter, *J. Catal.*, 34 (1974) 431
85. E. R. S. Winter, *J. Catal.*, 19 (1970) 32
86. Kh. M. Minachev and Yu. S. Khodakov, *Kinet. Katal.*, 6 (1965) 89
87. D. R. Ashmead, D. D. Eley and R. Rudham, *Trans. Faraday Soc.*, 59 (1963) 207.

88. D. D. Eley, H. Forrest and R. Rudham, *J. Catal.*, 34 (1974) 35.
89. C. Walling, *J. Am. Chem. Soc.*, 72 (1950) 1164
90. K. Tanabe, "Solid acids and bases" Academic Press, New York, 1970
91. J. Kijenski, A. Baiker, *Catal. Today*, 5 (1989) 1.
92. T. Yamanaka, K. Tanabe, *J. Phys. Chem.*, 79 (1975) 2409.
93. T. Yamanaka, K. Tanabe, *J. Phys. Chem.*, 80 (1976) 1723.
94. G. A. Parks, *Chem. Rev.*, 65 (1965) 177
95. H. Hosaka, T. Fujiwara, K. Meguro, *Bull. Chem. Soc. Jpn.*, 44 (1971) 2616
96. B. D. Flockhart, I. R. Leith and R. C. Pink, *Trans. Faraday Soc.*, 66 (1970) 469.
97. B. D. Flockhart, I. R. Leith and R. C. Pink, *Trans. Faraday Soc.*, 65 (1969) 542.
98. K. Meguro and K. Esumi, *J. Colloid and Interface Science*, 59 (1977) 93.
99. M. Che, C. Naccahe and B. Imelik, *J. Catal.*, 24 (1972) 328.
100. D. Cordischi, V. Indovina and A. Cimino, *J. C. S. Faraday I*, 70 (1974) 2189.
101. V. M. Vedeneev, L. V. Gurvich *et al.*, "Cleavage energies of Chemical bond. Ionisation potential and electron affinity Hand book" (in Russian). Izd. An SSSR, 1960.
102. K. Esumi and K. Meguro, *Bull. Chem. Soc. Jpn.*, 55 (1982) 315.
103. K. Esumi, K. Miyata and K. Meguro, *Chem Soc. Jpn.*, 58 (1985) 3524
104. K. Esumi, K. Miyata, Fumio Waki and Kenjiro Meguro, *Bull. Chem. Soc. Jpn.*, 59 (1986) 3363
105. S. Sugunan, G. Devika Rani and P. A. Unni Krishnan, *J. Mater. Sci. Technol.*, 10 (1994) 425;
106. S. Sugunan and J. M. Jalaja, *Collect. Czech. Commun.*, 59 (1994) 2605 ;

107. S.Sugunan, K.B.Sherly and G.Devika Rani, *React. Kinet. and Catal. Lett.*, 51 (2) (1993) 525.
108. S. Sugunan, B. Varghese, *React. Kinet. Catal. Lett.*, 57 (1) (1996) 87.
109. S. Sugunan and J. J. Malayan, *J. Adhesion Sci. Technol.* 9 (1) (1995) 73.
110. S. Sugunan and K. B. Sherly, *Indian J. Chem.*, 32 A (1993) 689.
111. S. Sugunan, D. John, N. K. Renuka, M. Varghese, K. Sreekumar and C. G. Ramankutty, *React. Kinet. and Catal. Lett.*, 66 (1) (1999) 39.
112. J. Kijenski, A. Baiker, *Catal. Today*, 5 (1989) 1.
113. Aline Auroux and Antonella Gervasini, *J. Phys. Chem.*, 94 (1990) 6371
114. B. H. Davis, in: *Adsorption and catalysis on Oxide surfaces*, eds. M. Che and G. C. Bond, *Stud. Surf. Sci. Catal.*, vol. 21 (Elsevier, Amsterdam, 1985) p. 309.
115. Mamoru Ai, *Bull. Chem. Soc. Jpn.*, 50 (10) (1997) 2579.
116. C. Bezouhanava, M. A. Al – Zihari, *Catal. Lett.*, 11 (1991) 245.
117. M. V. Joshi, S. G. Oak and V. S. Darshane, *Catalysis- Modern trends*, (Eds.) N. M. Gupta and D. K. Chakrabarty.
118. H. Pines and C.N. Pillai, *J. Am. Chem. Soc.*, 82 (1960) 2401.
119. A.Cortes and J. L. Seoane, *J. Catal.*, 34 (1974) 7.
120. A.Joseph, R. L. Mednick, M. L. Shorr, S. W. Weller and P. Rona, *Israel J. Chem.*, 12 (1974) 739.
121. W. Kania and K. Jurczyk, *Appl. Catal*, 61 (1990) 35.
122. J. Hanuza, B. Jezouska-Trzebiatowska and W. Oganowski, *J. Mol. Catal.*, 4 (1978) 271.
123. Z. Dziewiecki and A. Makowski, *React. Kinet. Catal. Lett.*, 13 (1980) 51.
124. R. J. Rennard Jr., R. A. Innes and H. E. Swift, *J. Catal.*, 30 (1973) 128.
125. G. V. Shakhnovich, I. P. Belomestnykh, N. V. Nekrasov, M. M. Kostyukovsky and S. L. Kiperman, *Appl. Catal*, 12 (1984) 23.

126. J. Hanuza, B. Jezowska-Trzebiatowska and W. Oganowski, *J. Mol. Catal.*, 29 (1985) 109.
127. Y. Murakami, K. Iwayama, H. Uchida, T. Hattori and T. Tagawa, *Appl. Catal.*, 2 (1982) 67.
128. G. Emig and H. Hoffmann, *J. Catal.*, 84 (1983) 15.
129. G. E. Vrieland and P. G. Menon, *Appl. Catal.*, 77 (1991) 1.
130. J. Iwasawa, H. Nobe and S. Ogasawara, *J. Catal.*, 31 (1973) 444.
131. G. C. Grunewald and R. S. Drago, *J. Mol. Catal.*, 58 (1990) 227..
132. W. S. Chang, Y. Z. Chen, B. L. Yang, *Appl. Catal A: Gen.*, 124 (1995) 221.
133. M. C. Kung and H. H. Kung, *J. Catal.*, 134 (1992) 668
134. Y. Murakami, K. Iwayama, H. Uchida, T. Hattori and T. Tagawa, *J. Catal.*, 71 (1981) 257.
135. T. Tagawa, T. Hattori and Y. Murakami, *J. Catal.*, 75 (1982) 66.
136. J. Haber and B. Grzybowska, *J. Catal.*, 28 (1973) 489.
137. W. R. Cares and J. W. Hightower, *J. Catal.*, 23 (1971) 193.
138. R. J. Rennard and W. L. Khel, *J. Catal.*, 21 (1971) 282.
139. K. M. Sancier, P. R. Wentrcek and H. Wise, *J. Catal.*, 39 (1995) 141
140. I. Aso, M. Nakao, M. Egashira, N. Yamazoe and T. Seiyama, *Shokubai*, 18 (1976) 106..
141. J. J. Kim and S. W. Weller, *Appl. Catal.*, 33 (1987) 15.
142. B. O. Palsson, S. Fathi-Ashar, D. F. Rudd and E. N. Lightfoot, *Science*, 213 (1981) 513.
143. Kung H. H. " Transition metal oxide surface chemistry and Catalysis" *Stud. Surf. Sci. Catal.*, Elsevier, Amsterdam, 45 (1989) 200.

144. S. T. Oyama, K. B. Lewis, A. M. Carr and G. A. Somarjai in "Proceedings, 9th International Congress on Catalysis, Calgary, 1988" (Eds. M. J. Philips and M. Ternan), vol. 3, p. 1489, Chemical Institute of Canada, Ottawa, 1988. .
145. N. E. Quaranta, R. Martino, L. Gambaro and H. Thomas, in "New developments in selective oxidation II", Stud. Surf. Sci. Catal., vol. 82, p. 811, Elsevier, Amsterdam, 1994.
146. Said, Abd El – Aziz, Abd El – Wahab, M. M. Mohammed , J. Chem. Technol. Biotechnol., 63 (1) (1995) 78.
147. S. Kannan, T. Sen and Sivasankar, J. Catal., 170 (1997) 304.
148. Y. Nakagawa, T. Ono, H. Miyata and Y. Kubokawa, J. Chem. Soc. Faraday Trans., 79 (1) (1983) 2929.
149. Z. H. Fu and Y. Ono, Catal. Lett., 21 (1993) 43.;
150. V. Durgakumari, and S. Narayanan and L. Gukzi, Catal Lett, 5 (1990) 377.
151. C. Benzouhanava and M. A. Al Zihari, Appl Catal , 8 (1992) 45.
152. R. T. Tliemat- Manzalji, D. B. Bianchi and G. M. Pajonk, Appl. Catal., 101 (1993) 339
153. M. Marizewski, J. P. Bodibo, G. Perof and M. Guisnel, J. Mol. Catal., 50 (1989) 211.
154. S. Balsama, P. Beltrame, P. L. Beltrame, L. Borni and J. Zuretti, Appl Catal., 13 ,161(1984).
155. S. Velu, C. S. Swami, Appl. Catal. A: Gen., 119 (1994) 241
156. K. Tanabe and T. Nishizaki, Proc. 6th Intern. Congr. Catalysis, 2 (1977) 863.

CHAPTER II

EXPERIMENTAL

Introduction

The performance of a catalyst depends on the method of preparation and catalyst pretreatment conditions apart from the reaction parameters. Variation in the preparation conditions very much alters the catalytic behaviour and hence the preparation method of the catalyst is very crucial to get the optimum catalyst for a specific reaction. So utmost care should be taken during the preparation of the systems. The materials used and the methodologies are described in this chapter.

2.1 Materials

$\text{La}(\text{NO}_3)_3$, $\text{Sm}(\text{NO}_3)_3$ and $\text{Dy}(\text{NO}_3)_3$ were obtained from Indian Rare earth Ltd., Udyogamandal, Kerala (purity 99.9 %) NH_4VO_3 (purity 99.5%) was provided from S. D. Fine Chem. Ltd., Boisar.

2.2 Preparation of the catalysts

2.2.1 Preparation of rare earth oxide supports

Rare earth oxides used as supports were prepared from the corresponding nitrates via hydroxide method as reported earlier [1]. A dilute solution of lanthanide nitrate was boiled and precipitated as hydroxides by the dropwise addition of 1:1 NH_3 until the precipitation was complete. It was then allowed to digest on a steam bath until the precipitate was flocculated and settled. Boiling was continued for five minutes and allowed to settle overnight. The precipitate was washed several times with deionised water by decantation and made free from nitrate ions. It was then dried overnight at 100°C and calcined at 400°C for 3 h. to form the respective oxides. These were then sieved to get particles of the required mesh size (< 100 microns).

2.2. 2 Preparation of supported catalysts

Supported vanadia catalysts were prepared by the conventional wet impregnation method (excess solvent technique) as reported by Kanta Rao and co workers [2]. Required quantity of NH_4VO_3 was dissolved in aqueous oxalic acid solution and stirred for 3 h. with the support. Excess solvent was then evaporated to dryness on a water bath, dried in an air oven overnight, calcined at 450°C for 6 h. and sieved to obtain particles of mesh size <100 microns. The catalyst systems selected for the present investigation are shown in Table 2. 1.

Table 2. 1. Percentage of vanadia in rare earth oxide supports.

% of vanadia	Supports		
	La_2O_3	Sm_2O_3	Dy_2O_3
0	L	S	D
3	L3	S3	D3
7	L7	S7	D7
11	L11	S11	D11
15	L15	S15	D15

2.3 Characterisation of catalysts

For catalytic study, a thorough knowledge of surface structure is inevitable. Catalyst characterisation is an integral step in catalyst design and is performed with the aim to find a link between catalyst performance and structural and electronic properties of the catalyst. Two sets of parameters are defined to assess the performance of a catalyst, i) physical properties (mechanical structure and texture and macro distribution of metal phase) which influences the life time, mass and heat transfer phenomena and accessibility of active sites and ii) active site parameter which links the reaction behaviour with the number and nature of active site. In this

regard, it is essential that the nature and molecular structure of the surface species should be systematically investigated and active sites should be thoroughly probed.

The materials prepared were subjected to the following analytical procedures; EDX analysis, X-Ray diffraction studies, FTIR spectral studies, measurement of specific surface area and pore size distribution, thermal studies and acid base property studies.

2.3.1 Energy dispersive X-ray analysis

EDX is an analytical technique that qualitatively and quantitatively identifies the elemental composition of materials. When electrons of appropriate energy impinge on a sample, they cause emission of X-rays whose energies and relative abundance depend upon the composition of the sample. This method is sensitive to very low concentrations; minimum detection limit is below 0.1 % in the best case. Furthermore, the technique is practically nondestructive in most cases and the requirements for sample preparation are minimal.

The principle of EDX can be summarised as follows. An electron beam from a scanning electron micrograph ejects an electron from an inner shell of the sample atom. An electron from a higher energy shell in the atom fills the resulting vacancy. While falling to a state of lower energy, this vacancy-filling electron must give up some of its energy, which appears in the form of electromagnetic radiation. The energy of the emitted radiation is exactly equal to the energy difference between the two electronic levels involved. Since this energy difference is fairly large for inner shells, the radiation appears as X-rays. As all elements have a unique configuration of electron energy levels, the X-ray pattern spectrum will be a unique characteristic of that particular element. Furthermore, under given analysis conditions, the number of X-rays emitted by each element bears a more or less direct relationship to the concentration of element in the sample.

The X ray peak positions along the energy scale identify the element present in the sample, while the integrated peak areas, after application of appropriate correction factors, can give us the percentage concentration of each of these elements.

2.3.2 X- Ray Diffraction studies

X-ray diffraction is one of the most important tools of solid state chemistry, since it constitutes a powerful and readily available method for determining atomic arrangements in solids. The method is based on the scattering of X rays by matter, with accompanying variation in intensity in different directions due to interference effects. A fixed wavelength is chosen for the incident radiation and diffraction pattern is obtained by observing the intensity of the scattered radiation as a function of scattering angle 2θ . Values of d spacings are obtained using Bragg's equation. From Bragg's expression, which relates the d spacing and scattering angle with the wavelength (λ) of the incident radiation, d spacing can be calculated.

Bragg's equation can be stated as,

$$n\lambda = 2d \sin\theta, \quad \text{where } n \text{ is the order of diffraction.}$$

XRD is used for a qualitative and quantitative identification of the crystalline compounds present in the samples. The lattice type, unit cell dimensions, space group and ultimately the motif configuration of crystals can be obtained along with electron distribution within atoms, measurement of limits of solid solubility, randomness and imperfections in the lattice etc. The mean crystallite size of a material can also be determined from the broadening of an X-ray diffraction peak, which is inversely proportional to crystallite size and this is achieved by following the Scherrer method using the formula,

$$d = 0.9 \lambda / \beta \cos \theta$$

which is derived from Bragg's equation. 'd' is the thickness of the crystal, and β = FWHM (half the width of the peak with maximum intensity).

XRD pattern is obtained by Rigaku D-Max C X-Ray Diffractometer. A stationary Ni filtered Cu K α radiation ($\lambda = 1.5404 \text{ \AA}$) and a movable detector, which measure the intensity of the diffracted radiation as a function of angle 2θ are the main parts of the instrument.

2.3.3 FTIR Spectral Studies

Vibrational spectroscopy is widely used in the field of characterisation of heterogeneous catalysts. Dispersion of the metal species and its structure, support-metal interaction, metal-metal interactions etc. are some of the valuable information obtained from IR spectral studies. It provides information on the bulk catalyst structure as well as the structure of surface sites that are either directly observable (eg. surface OH and surface M-O bonds) or that is made observable by pre-adsorption of probe molecules. The frequencies and intensities of the IR bands of the adsorbed probe molecules provide abundant evidence on the state of the supported metal (dispersion, structure, metal-support interaction, metal-metal interaction etc.)

The intensities of the IR adsorption band depend upon the change of dipole moment brought by the variations in the molecular geometry for the vibration concerned. Bonds possessing ionic character tend to give strong IR bands. This characterisation technique has a prominent role in identifying the surface species in the case of supported vanadia catalysts.

FTIR spectra of the powder samples were measured by the KBr disk method over the range $4000 - 400 \text{ cm}^{-1}$. Shimadzu DR 8001 instrument was used for the purpose. The entire frequency range of electromagnetic waves transmitted through the sample was recorded simultaneously and the output of the detector was fed to a computer, which reinforces the spectrum using Fourier Transform.

2.3. 4 Surface area analysis

BET method introduced by Brauner, Emmett and Teller was adopted for surface area analysis. By the introduction of a number of simplifying assumptions, the BET theory extends Langmuir model to multilayer adsorption. The adsorption in the first layer is assumed to take place on an array of surface sites of uniform energy. Molecules in the first layer act as sites for multilayer adsorption. It is further assumed that the evaporation–condensation characteristics and heats of adsorption are identical for all layers except the first and is equal to the heat of liquefaction of the adsorbate. BET equation can be represented as,

$$\frac{P}{V(P_0 - P)} = \frac{1}{CV_m} + \frac{(C - 1)P}{CV_m P_0}$$

which demands a linear relation between

$$\frac{P}{V(P_0 - P)} \quad \text{and} \quad \frac{P}{P_0} \quad \text{where}$$

$$\text{Slope} = \frac{C - 1}{CV_m} \quad \text{and intercept} = \frac{1}{CV_m}$$

Here,

- P = adsorption equilibrium pressure;
- P₀ = saturated vapour pressure;
- V = volume of nitrogen adsorbed at pressure P
- V_m = volume of nitrogen used for monolayer

coverage

C is measure of adsorbent- adsorbate interaction energy , $= e^{\frac{(E_q - E)}{RT}}$

Combining slope and intercept equations, V_m can be calculated.

Specific surface area is related to V_m by the equation

$$\text{Surface area, (in m}^2 \text{ g}^{-1}\text{)} = \frac{V_m N_A A_M}{22414 \times \text{weight of the catalyst}}$$

N_A is the Avagadro number.

A_M is mean cross sectional area of nitrogen molecule (16.2 Å²)

Micromeritics Flowprep -060 instrument was used to determine the surface area with nitrogen gas as adsorbate. Previously activated samples were degassed at 200°C under nitrogen flow for 2 h. and then brought to 77 K using liquid nitrogen.

2.3.5 Pore volume measurements – Mercury porosimeter

Pore size distribution is of interest primarily for the prediction of the effective diffusion in a porous catalyst in conjunction with calculation of the ease of access of reactant molecules to the interior of a catalyst pellet by diffusion.

This method is based on the behaviour of non-wetting liquids (contact angle at liquid/solid $> 90^\circ$) like mercury in capillaries, usually assuming pores to be cylindrical. Interfacial tension opposes the entrance of the liquid into the pores. An external pressure must be applied to make the liquid enter the pores. For a cylindrical pore, the force opposing entrance to the pore act along the circumference and equals $2\pi r \gamma \cos \phi$, where γ is the surface tension and ϕ is the contact angle (for mercury, $\phi = 140^\circ$). External pressure, which opposes this force, acts along the entire pore cross sectional area and is equal to $\pi r^2 P$

At equilibrium,

$$\begin{aligned} \pi r^2 P &= 2\pi r \gamma \cos \phi. \\ \text{ie., } P &= \frac{2\gamma \cos \phi}{r} \end{aligned}$$

When the volume of mercury pressed into the solid is measured simultaneously, the integral volume of the capillaries as a function of their radius is obtained and by differentiation of the curve, the pore size distribution can be calculated.

Measurement of pore volume and pore size distribution of the catalysts was carried out using Quantachrome, Auto scan-92 porosimetry (USA). In this

instrument, the solid sample is immersed in a reservoir of mercury, the upper part of which ends in a narrow capillary. The upper part of mercury was in contact with a conducting wire, just touching the mercury surface. Pressure application detaches the contact with wire cutting electrical circuit. Through a micrometer arrangement, contact was reestablished and the difference in volume of the mercury gives the volume of the pore occupied by mercury under pressure.

2.3.6 Thermal studies

In thermal analysis the physical parameters are determined as a function of temperature. Thermogravimetric analysis was used as an important tool in the characterisation procedure of a catalyst which provide valuable information about drying ranges, hydration, phase transformations, decomposition temperature, stability limits etc. In thermogravimetry, the weight of a sample was recorded over a period of time under controlled heating. A plot of weight against temperature was made, which is denoted as the thermogram. The temperature was plotted on abscissa and weight on ordinate. From the thermogram, information can be obtained about the various forms or products at various temperatures with the knowledge of the molecular weight of the parent system. DTG is the first derivative plot of the TG curve from which a better understanding of the weight loss can be obtained from the dip in the curve.

Shimadzu TGA-50 instrument was used for carrying out thermogravimetric studies. Recording analytical balance with provision of controlled heating (thermal balance) is the main part of this instrument. Heating rate was 10°C / minute in nitrogen atmosphere. 20 mg sample was used. The TG data were computer processed to get thermograms. The horizontal portion of the curve indicates the regions where there is no weight loss or the sample is thermally stable. Curved regions indicate weight loss.

DTA is used to get idea about phase transition or chemical reactions in a particular temperature and is followed through observation of heat adsorbed or liberated. This technique is suitable to study the structural changes within a solid at elevated temperature. Here the temperature difference of the sample and a reference material was monitored while both are subjected to a linearly increasing environmental temperature. Within a constant heating rate, any transition or thermally induced chemical reaction in the sample will be recorded as a peak or dip in an otherwise straight graph [3]

2.4 Acid base property studies

Acid base properties are decisive parameters in the field of heterogeneous catalysis, which pedals the activity and selectivity of the catalysts to a large extent. Four independent methods are adopted here for a thorough understanding of these properties; Hammett indicator method, electron donating property study, temperature programmed desorption of ammonia and decomposition of cyclohexanol. Experimental procedures for these methods are described as follows.

2.4.1 Hammett indicator method

Benzene used for acidity and basicity measurement was purified by a method reported earlier [4]. Trichloroacetic acid (SQ Grade) obtained from Qualigens Fine Chemicals was used without further purification.

A sample of the solid as powder (0.1 g) was suspended in an inert nonaqueous solvent (benzene) adding two drops of indicator (0.1 N) and was allowed to stand for 10 minutes to attain equilibrium. This was titrated against the titrant (acid / base) until a permanent colour change was obtained. The titrant must be stronger in acid / base than the adsorbed indicator. It was kept for 12 h to check the end point. Indicators used for the titration method are given in Table.2 along with pK_a values and colour changes in acidic and basic media.

2.4.2 Electron donating property studies

Adsorption of electron acceptors has been investigated to study and characterise the electron donating property of the system. Reagents used and purification methods are as follows.

7,7,8,8-tetracyanoquinodimethane (TCNQ) [Merk-Schuchardt] was purified by repeated crystallization from acetonitrile [5]; chloranil (2,3,5,6-tetrachloro benzoquinone)[Sisco Research Laboratories Pvt. Ltd.] was crystallized from benzene before use [4]. Chloroform was used as the solvent for the recrystallization of *p*-dinitrobenzene [6]. SQ grade acetonitrile [Qualigens Fine Chemicals] was purified by passing through silica gel for drying followed by distillation with P₂O₅ and fraction between 79 – 82°C is collected [7].

The following procedure was adopted for adsorption studies. The oxides were activated at 500°C for 2 h prior to each experiment. The sample (0.5 g) was placed in a 25 ml test tube fitted with mercury sealed stirrer and out gassed at 10⁻⁵ Torr for 1 h. 10 ml of the solution of the electron acceptor in acetonitrile was added. The solution was stirred for about 4 h. at 25°C in a thermostatic water bath. The amount of electron acceptor adsorbed on the catalyst surface was estimated by measuring the absorbance at the λ_{\max} of the electron acceptor (EA) by means of Shimadzu 160-A spectrometer before and after adsorption.

The electron affinity values of the different electron acceptors and their λ_{\max} in acetonitrile are given in Table 2. 3.

Langmuir type adsorption isotherms were obtained by plotting equilibrium concentration of electron acceptors against amount of electron acceptors adsorbed. From the Langmuir adsorption isotherms, limiting amount of electron acceptor adsorbed was calculated.

Table 2.2. Hammett indicators used and their pK_a values

Indicator	pK_a	Colour	
		Base form	Acid form
Crystal violet (Romali)	+ 0.8,	Blue	Yellow
Dimethyl yellow (Loba Chemie Industrial Company)	+ 3.3,	Yellow	Red
Methyl red (E. Merck India Pvt. Ltd.)	+ 4.8	Yellow	Red
Bromothymol blue (Qualigen Fine Chemicals)	+7.2	Blue	Yellow
2,4-dinitroaniline (E. Merck India Pvt. Ltd.)	+15	Violet	Yellow

Table 2.3. Electron acceptors used and their electron affinity values

Electron acceptors (EA)	Electron affinity (eV)	λ_{max} (nm)
7,7,8,8-tetracyanoquinodimethane (TCNQ)	2.84	393.5
2,3,5,6-tetrachloro benzoquinone (Chloranil)	2.40	288
p-dinitrobenzene (PDNB)	1.77	262

2.4.3 Temperature Programmed Desorption (TPD) studies

TPD of ammonia is a simple technique to find out the acidity and acid strength distribution. Total acidity (both Bronsted and Lewis) measurement is achieved through this procedure.

A definite amount of pelletised catalyst sample was placed in the stainless steel reactor of 1 cm I.D. and 15 cm length kept in a cylindrical furnace. The sample was degassed at 300°C for 2 h under nitrogen flow. It was then cooled to room temperature and a definite amount of ammonia was injected in to the reactor and allowed to adsorb for half an hour. Under controlled temperature programme, amount of ammonia leached out was trapped into H₂SO₄ solution (0.025 N) and ammonia desorbed was determined by back titration with NaOH (0.025 N).

$$\text{Amount of ammonia desorbed} = \frac{\Delta V \times N_{\text{NaOH}} \times 5 \times 17}{\text{Weight of the sample}}$$

ΔV = difference in titre values of NaOH between blank H₂SO₄ and the ammonia scrubbed H₂SO₄ at each temperature. The acid strength distribution was obtained from a plot of the amount of ammonia desorbed against temperature.

2.5 Catalytic activity studies

All the reactions were done in vapour phase. Vapour phase reactor has several advantages over liquid phase reactor. First and foremost is that the reaction can be performed at much higher temperature than the boiling point of a low boiling reactant. Other advantages are effortless regeneration of the catalyst, variation of contact time etc. Instrumental method is described below.

2.5.1 Gas phase reactor

The vapour phase reactions were carried out at atmospheric pressure in a fixed bed, vertical, down flow, quartz reactor consisting of 2.2 cm I.D and 30 cm length kept in a cylindrical furnace mounted vertically. The catalyst (3 grams as pellets) was loaded in the middle of the reactor and packed with silica beads. A thermocouple was placed in the middle of the reactor to measure the temperature at the reaction zone. The catalyst was activated in a current of dry air prior to each experiment at 773 K for 6 hours and then brought to the reaction temperature in presence of nitrogen flow. The reactant feed was introduced at the top of the reactor by means of an infusion pump (SAGE Instruments, Model 352, USA). The gas products obtained were cooled by circulating chilled water outside the tube and were collected, analysed in a gas chromatograph (Shimadzu, Model 15-A) fitted with FID and TCD. The reactor set up is shown in figure 2.1.

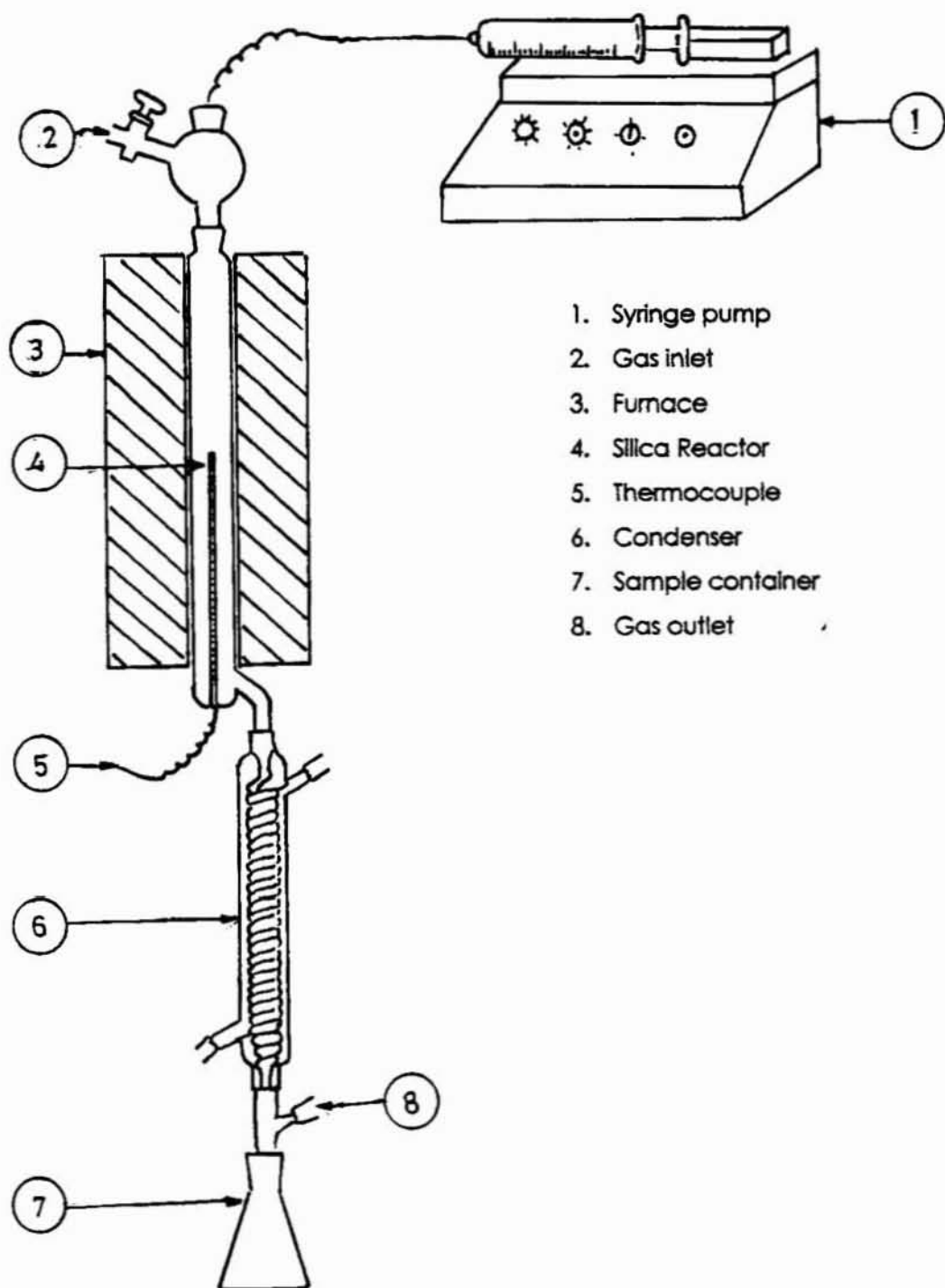


Fig. 2.1 Reactor set up for reactions carried out in vapor phase

References

1. Encyclopaedia of Industrial Chemical analysis, (Ed.) F. D. Snell and L. S. Ettre, Vol. 17, p. 475 (Interscience, New York, 1973).
2. K. V. Narayana, A. Venugopal, K. S. Rama Rao, V. Venkat Rao, S. Khaja Masthan and P. Kanta Rao, Appl. Catal. A, 150 (1977) 269.
3. D. A. Skoog, D. M. West and F. J. Holler, "Analytical Chemistry-An Introduction" Sanders College Publishing, p. 108
4. L. F. Fiesser and M. Fieser, " Reagents for Organic synthesis" John Wiley, New York, p. 125 (1967)
5. D. S. Acker and W. R. Hertler, J. Am. Chem. Soc., 84 (1962) 3370
6. B. S. Furness, A. J. Hannaford, V. Roger, P. W. G. Smith and A. R. Tatchel, "Vogel's Text Book of Practical Organic Chemistry" 4th edn., ELBS, London, (1978) p. 708.
7. A. I. Vogel, A Text Book of Practical Organic Chemistry" 3rd edn., ELBS, London, (1973) p. 407

CHAPTER III

**CHARACTERISATION
AND SURFACE PROPERTIES**

Introduction

Physicochemical characterisation of the supported systems is done to ensure the purity of the prepared samples and to get an insight to the nature of active sites on the catalysts. EDX, XRD, BET surface area analysis, pore volume measurements, thermal studies, acid base property studies etc. are carried out. Results of the various analysis are discussed in this chapter.

Pure rare earth oxides prepared by hydroxide method were colorless. Preparation of the supported catalysts via wet impregnation method imparted a pale yellow colour to the catalyst systems. The colour of the samples deepened as the concentration of vanadia is increased in the supported system.

3.1 EDX analysis

Percentage composition of lanthanide element and vanadium in supported systems determined by using Energy Dispersive X-ray analysis are given in Table 1. The chemical composition of the supported system is obtained from these results.

3.2 XRD studies

X-ray diffraction enables the identification of various crystalline materials in the catalyst samples. XRD patterns for the supported system obtained using Cu K α radiation are given in Figures 3.1 to 3.3. Samples were calcined at 500°C. For comparison, diffraction patterns of the supports and pure V₂O₅ are also included. The addition of vanadia reduces the crystalline nature of the support, as is evident from the figures. i.e., the transformation of lanthanide oxides from amorphous to hexagonal / body centered cubic is delayed by the presence of vanadia. This is assumed to be due to the dispersion of vanadia species.

Table 3.1 Elemental composition of rare earth oxide supported vanadia system

Catalyst	Percentage composition	
	V	Ln
Sm ₂ O ₃	0	100
S3	3.37	96.63
S7	6.85	93.15
S11	11.27	88.73
S15	14.59	85.41
La ₂ O ₃	0	100
L3	2.82	97.18
L7	6.33	93.67
L11	9.32	90.69
L15	14.09	85.91
Dy ₂ O ₃	0	100
D3	2.98	97.02
D7	7.94	92.06
D11	11.51	88.49
D15	14.81	85.41

Fig. 3.1 depicts the X-ray diffraction pattern of Sm / V catalysts. Prominent peaks due to crystalline samaria appeared at 2θ values 28.0, 32.5, 48.0, 55.5. After vanadia incorporation additional peaks appeared at 2θ values 18.6, 24.6 (very intense), 31.0, 33.2 and 49.0. These peaks are identified to be due to samarium orthovanadate formed by supporting vanadia. This is in agreement with Corma *et al* that basic oxides preferably form compounds with V₂O₅, who reported lanthanide orthovanadates on La₂O₃ and Sm₂O₃ supported vanadia [1]. Peaks due to crystalline vanadia are found to be absent in the supported catalysts even at higher percentage of vanadia. X-ray diffraction patterns of other systems also indicate the presence of orthovanadate and absence of V₂O₅ crystallites. LaVO₄ exhibited peak at 2θ value of

29.4 due to orthovanadate, whereas for DyVO_4 the intense peak corresponding to orthovanadate is seen at 2θ value of 25.0. From the relative intensity of the peaks, it was observed that the percentage of rare earth orthovanadate is increasing with vanadia loading.

From the XRD data, crystallite size is calculated using Scherrer's equation. The mean crystallite size obtained for rare earth supports and supported vanadia analogues are presented in Table 3.2. No remarkable conclusion can be attained from the crystallite size with reference to vanadia loading.

Table 3. 2. Crystallite size of supported vanadia catalyst on lanthana

Catalyst	Crystallite size (nm)
Sm_2O_3	19.94
S3	9.39
S7	54.63
S11	8.61
S15	6.51
La_2O_3	14.51
L3	60.66
L7	39.69
L11	18.56
L15	0.21
Dy_2O_3	23.25
D3	15.26
D7	19.32
D11	26.32
D15	31.52
V_2O_5	30.33

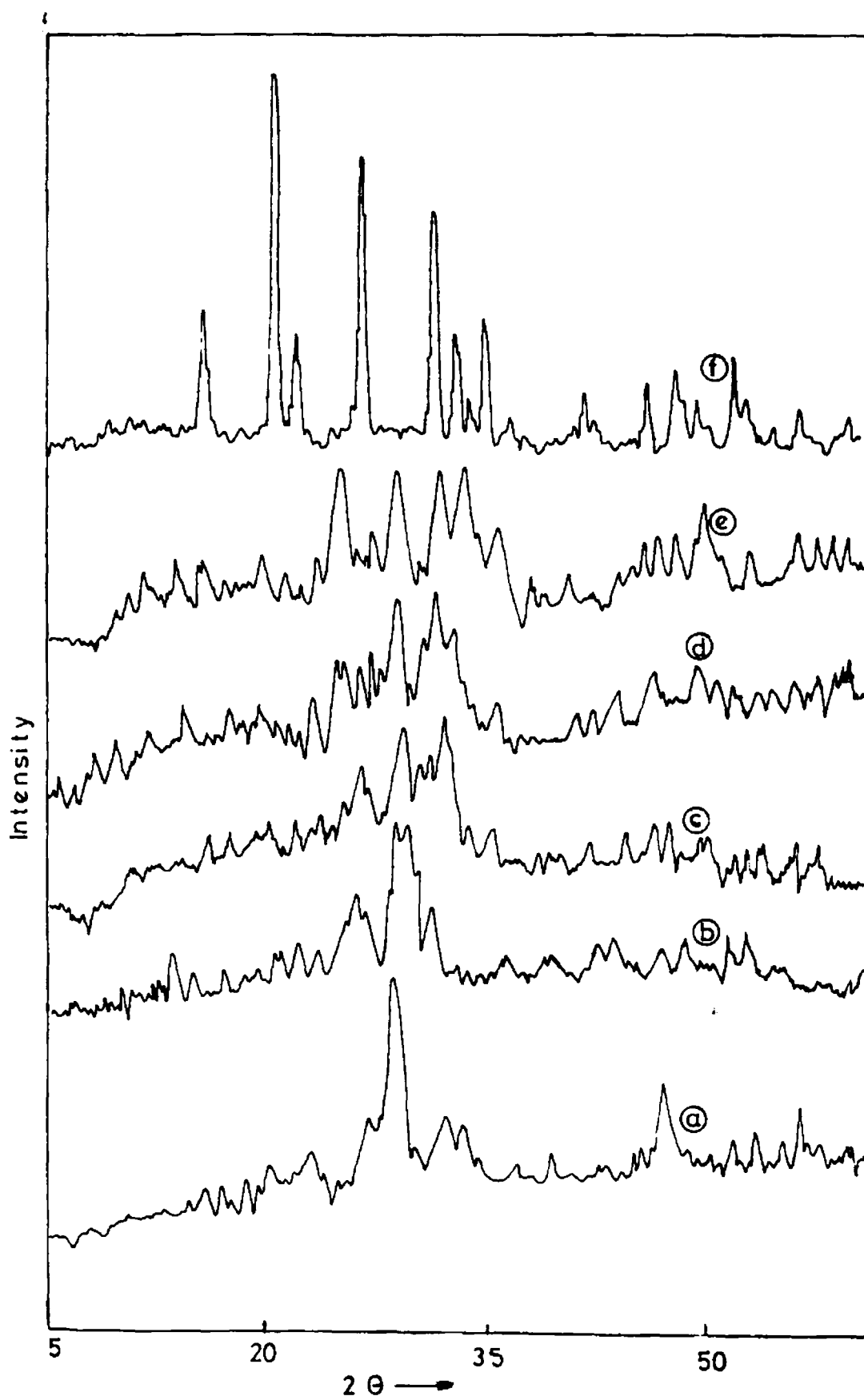


Fig. 3.1 X-ray diffraction patterns of Sm / V system. a) Sm_2O_3 ; b) S3; c) S7
d) S11; e) S15; f) V_2O_5

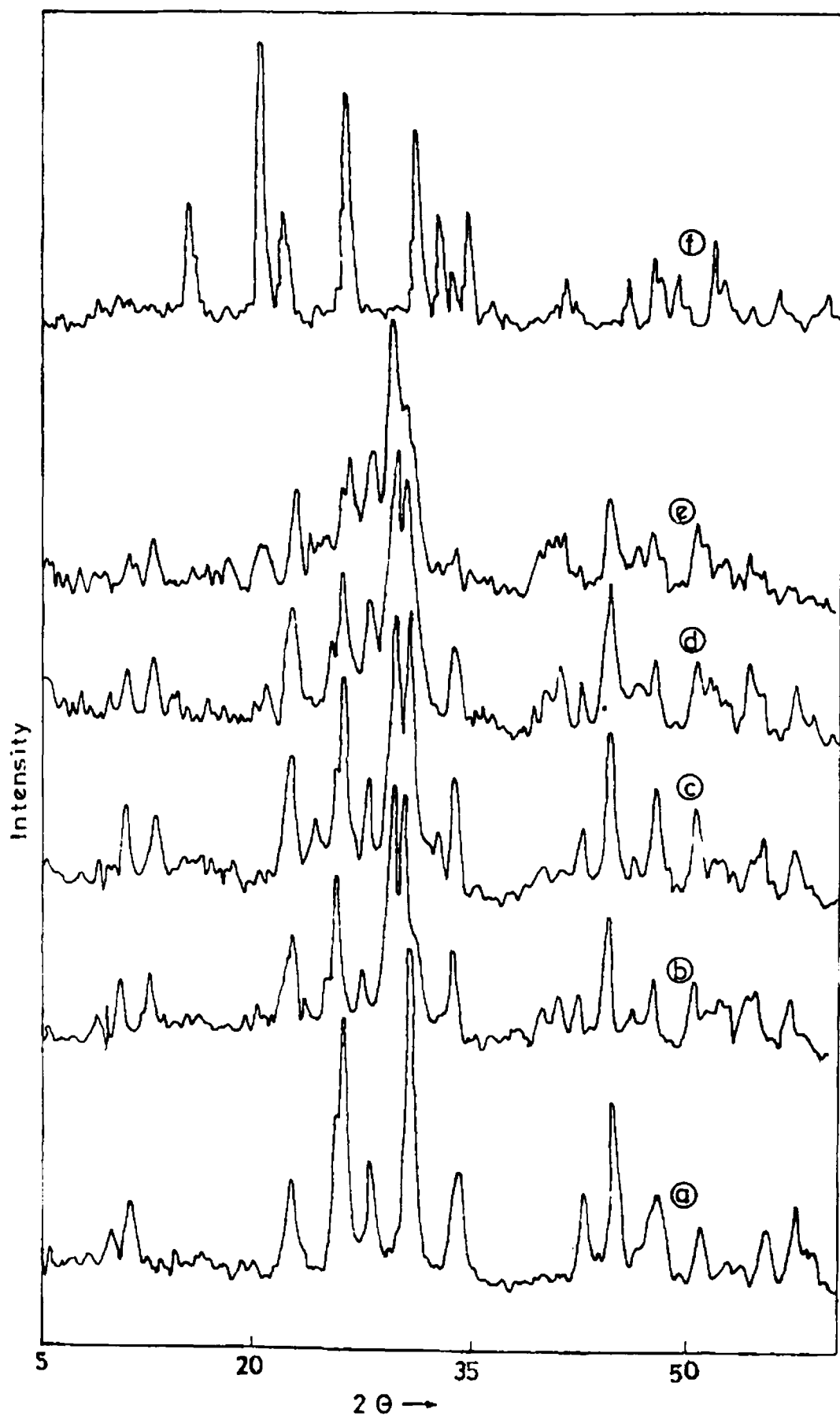


Fig. 3.2 X-ray diffraction patterns of La / V system. a) La_2O_3 ; b) L3; c) L7
d) L11; e) L15; f) V_2O_5

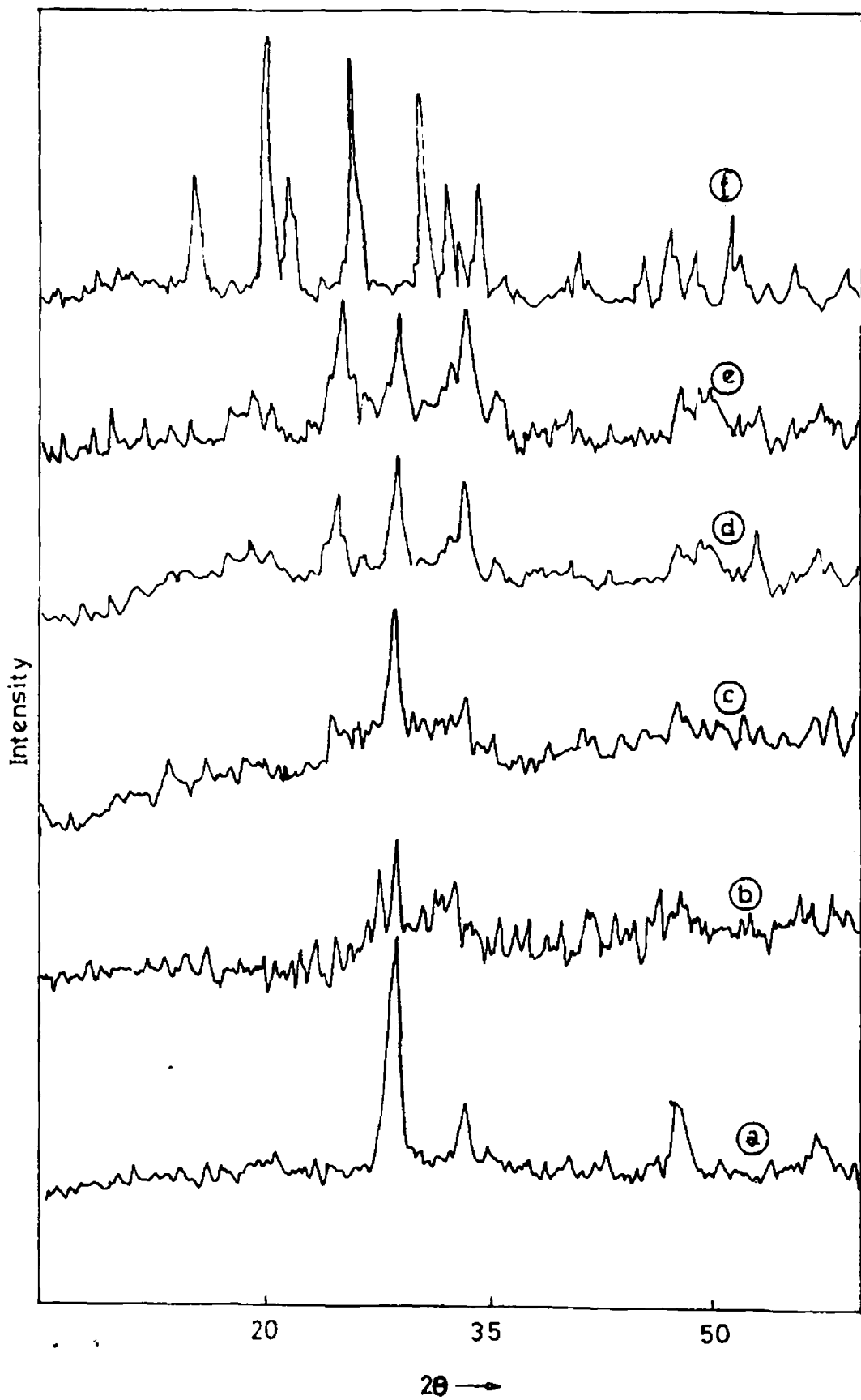


Fig. 3.3 X-ray diffraction patterns of Dy / V system. a) Dy_2O_3 ; b) D3; c) D7
d) D11; e) D15; f) V_2O_5

3. 3 FTIR spectral studies

Fourier Transform IR spectrum is identified as a very useful tool for analyzing the structure of the supported catalysts. FTIR spectra of the systems calcined at 500°C are obtained by KBr disk method (Figs. 3.4-3.7). It is obvious that additional bands arise in the spectra after vanadia loading.

Fig. 3. 5 describes the spectra of La / V series. IR data also prove the absence of crystalline vanadia, which was evident from the XRD pattern. The characteristic band of V_2O_5 is not observed in the spectrum at 1020 cm^{-1} even at higher vanadia loadings. Spectra of pure V_2O_5 is given in figure 3.4. The weak band at 1060.7 cm^{-1} is attributed to V=O stretching mode that arises from the surface vanadyl species for samaria system. Intensified bands are obtained by DRIFT spectral studies. The DRIFT spectra of La_2O_3 and La/V are given in Figs.3.8 and 3.9 respectively. The position of the band due to surface vanadia is shifted according to the support selected due to the interaction between vanadia and support. DRIFT spectra of vanadia supported on samaria is shown in Fig. 3.10. In the case of S series, this band appeared at 1062.8 cm^{-1} . For D series this band was observed at 1065 cm^{-1} . This slight shift can be explained by the decrease in bond length or in terms of strength of M – O – V bond, where 'M' is the metal ion in the support. Among the three lanthanide systems, Dy is more electronegative and hence the V=O stretching region is seen in the higher wave number region. The surface species of vanadium is identified as monooxo species, because, a dioxo species is expected to give rise to several combination bands [2]. This observation indicates the absence of O=V=O fragments on the surface species. High value of V=O stretching frequency indicates the absence of polyvanadyl surface species which exhibit V=O stretching frequencies in the $1000 - 950\text{ cm}^{-1}$ region [3]. Thus isolated species on the surface of the support is apparent. One broad band is observed in the range $700-900\text{ cm}^{-1}$ which account for the VO_4^{3-} entity that results from ortho vanadate [4]. This confirms the formation of lanthanide orthovanadates on Ln / V systems which is in agreement with the XRD pattern. Region at $3600-3000\text{ cm}^{-1}$ exhibits broad band due to hydrogen bonded hydroxy groups.

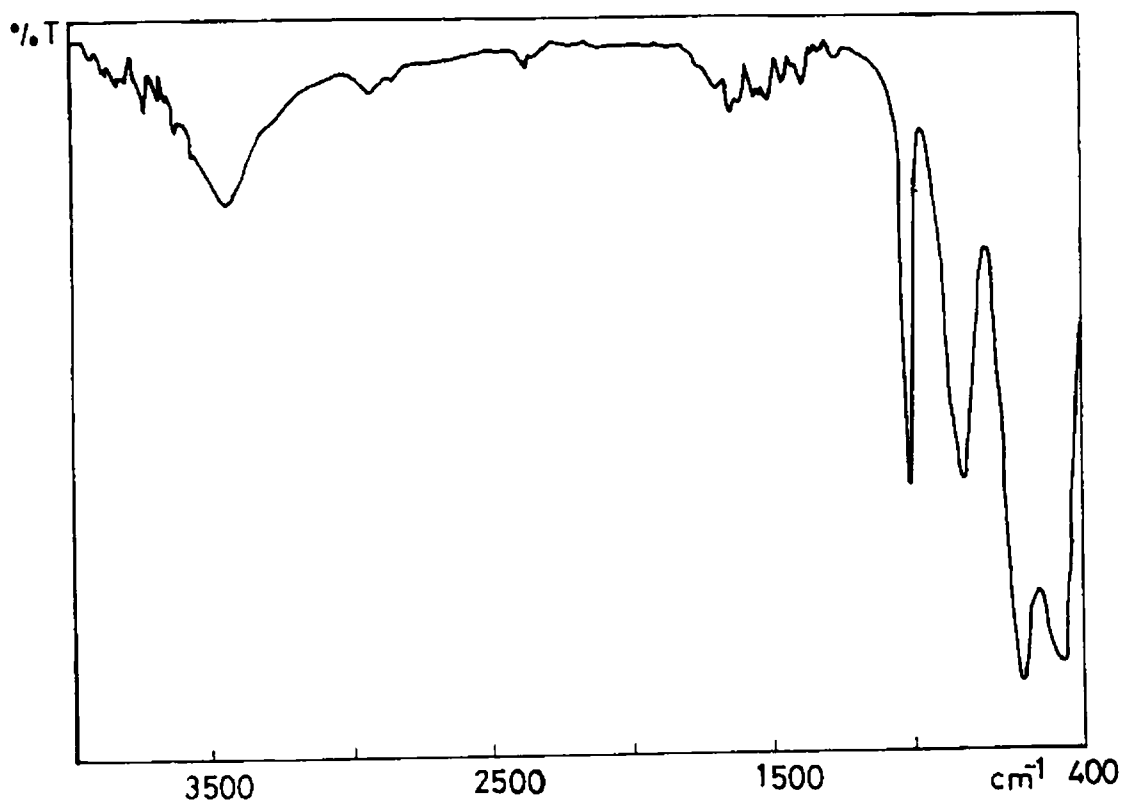


Fig. 3.4 FTIR spectrum of V_2O_5

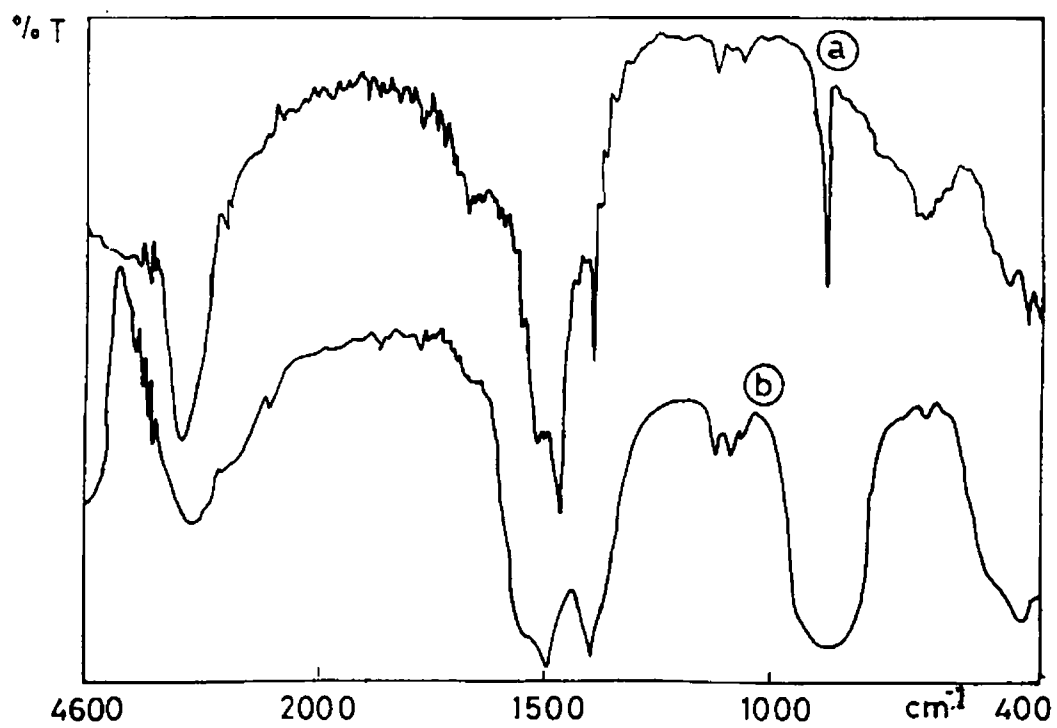


Fig. 3.5 FTIR spectra of (a) La_2O_3 (b) La / V system

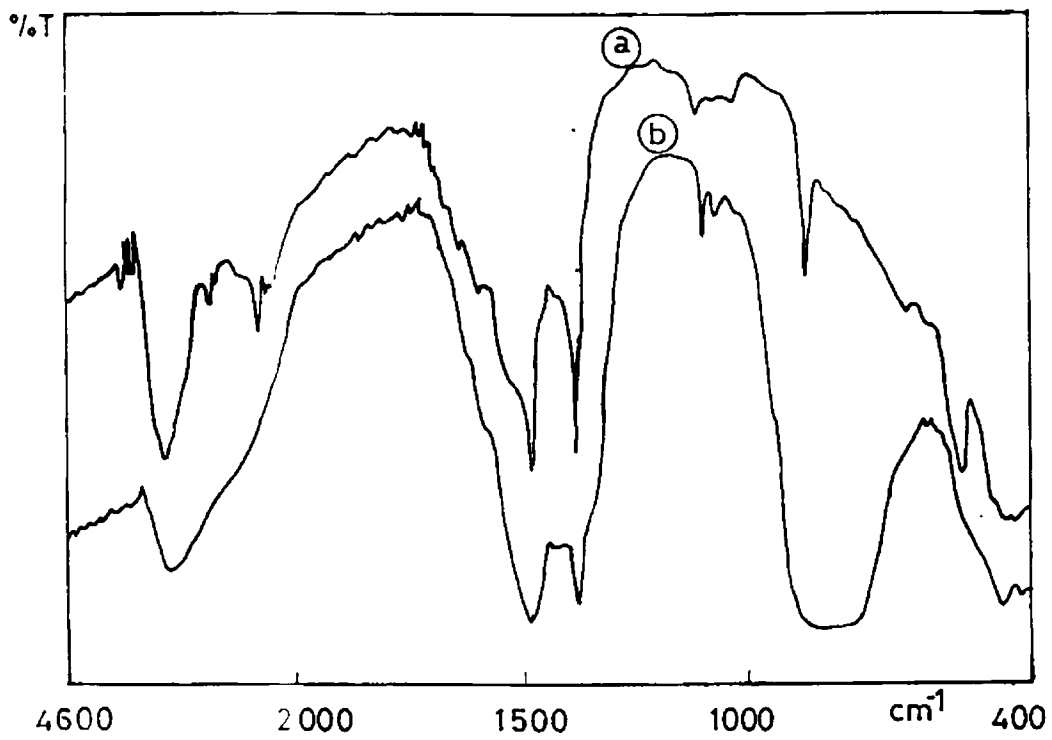


Fig. 3. 6. FTIR spectra of (a) Sm₂O₃ (b) Sm / V system

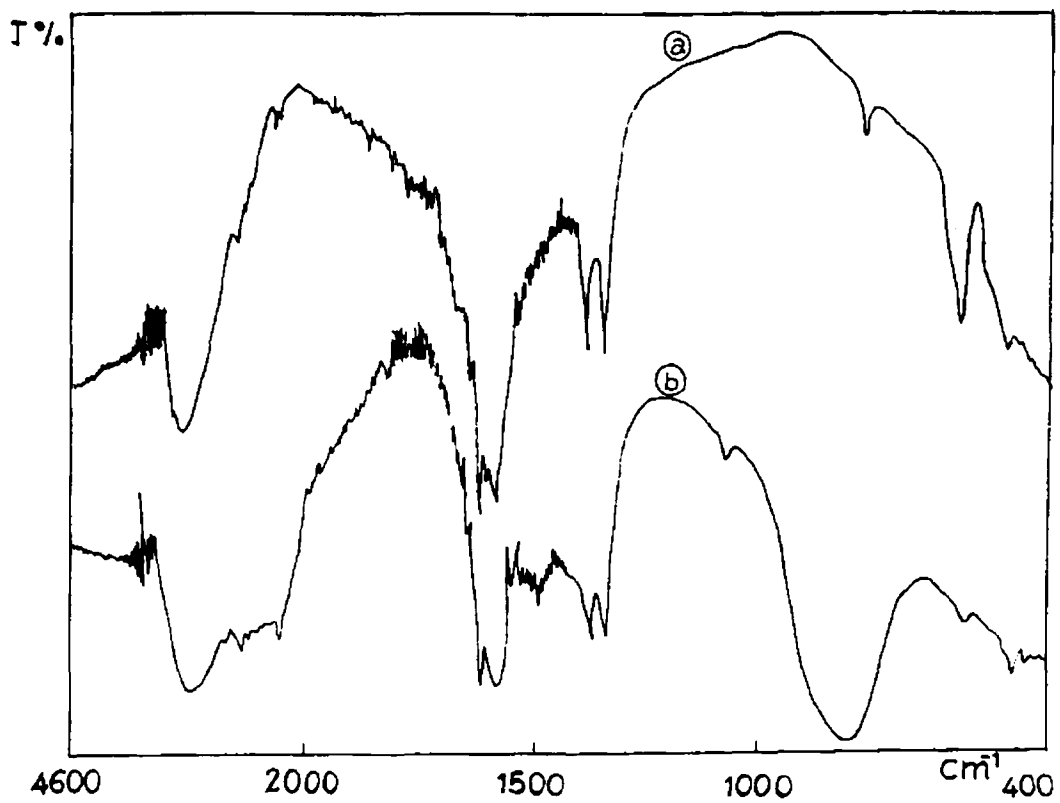


Fig. 3. 7. FTIR spectra of (a) Dy₂O₃ (b) Dy / V system

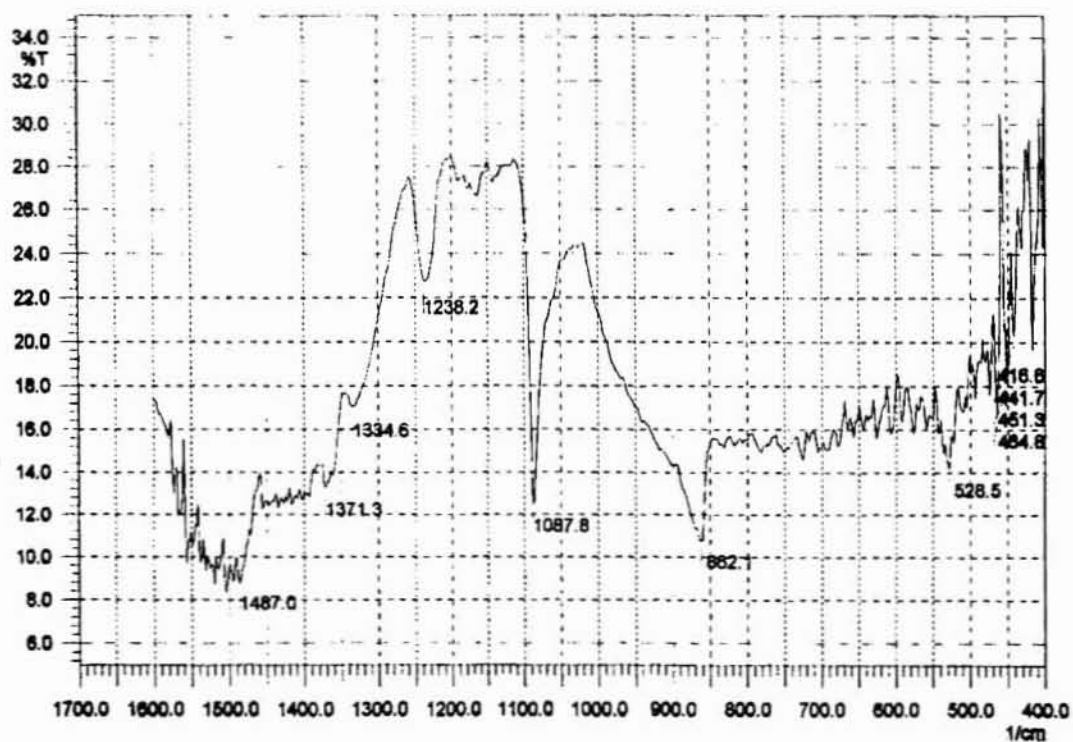


Fig. 3.8. Diffuse reflectance infrared (DR-IR) spectrum of La_2O_3

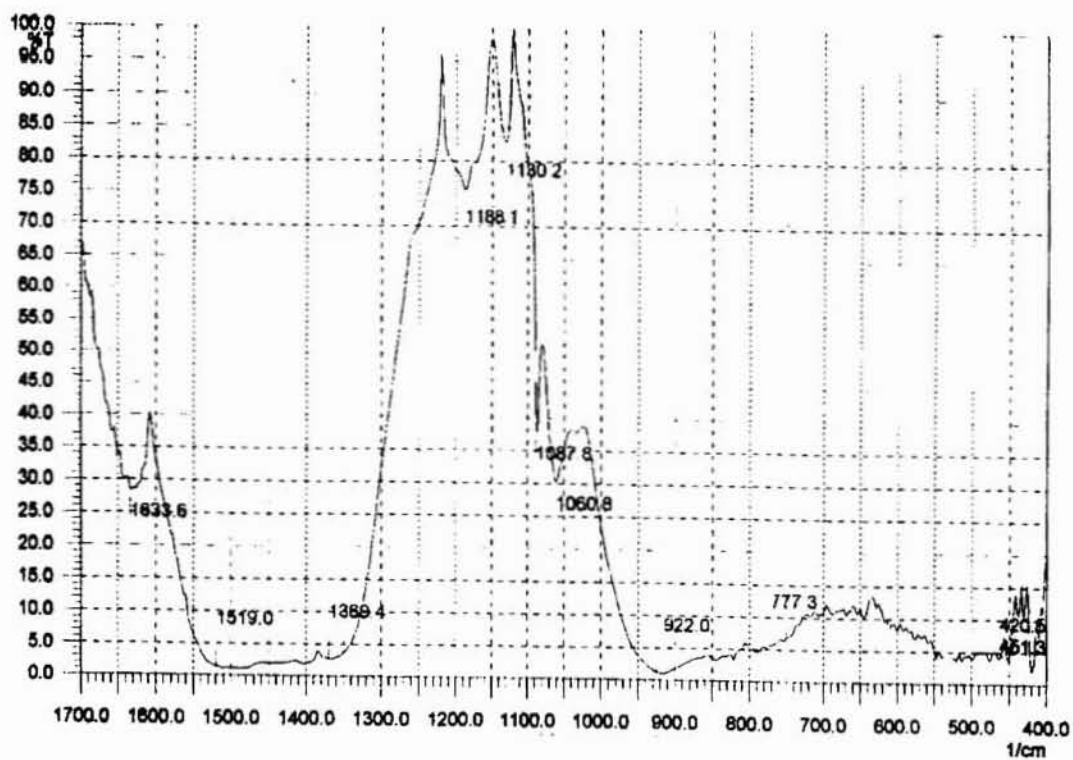


Fig. 3.9. Diffuse reflectance infrared (DR-IR) spectra of La/V system

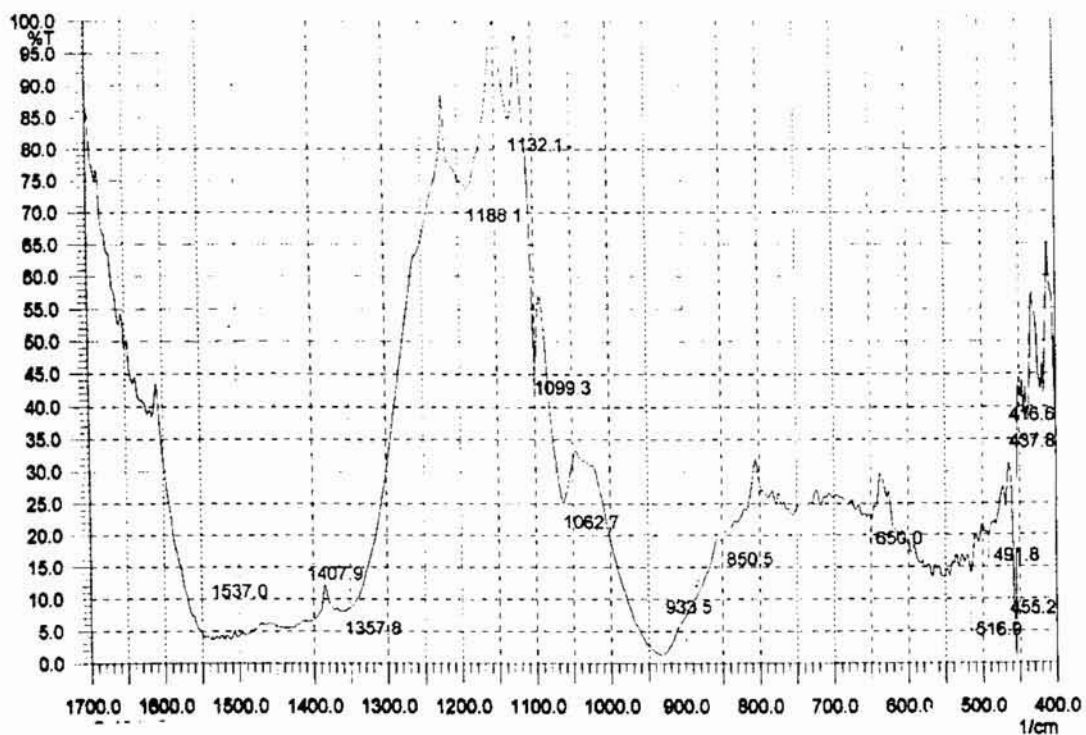


Fig. 3.10. Diffuse reflectance infrared (DR-IR) spectra of Sm/V system

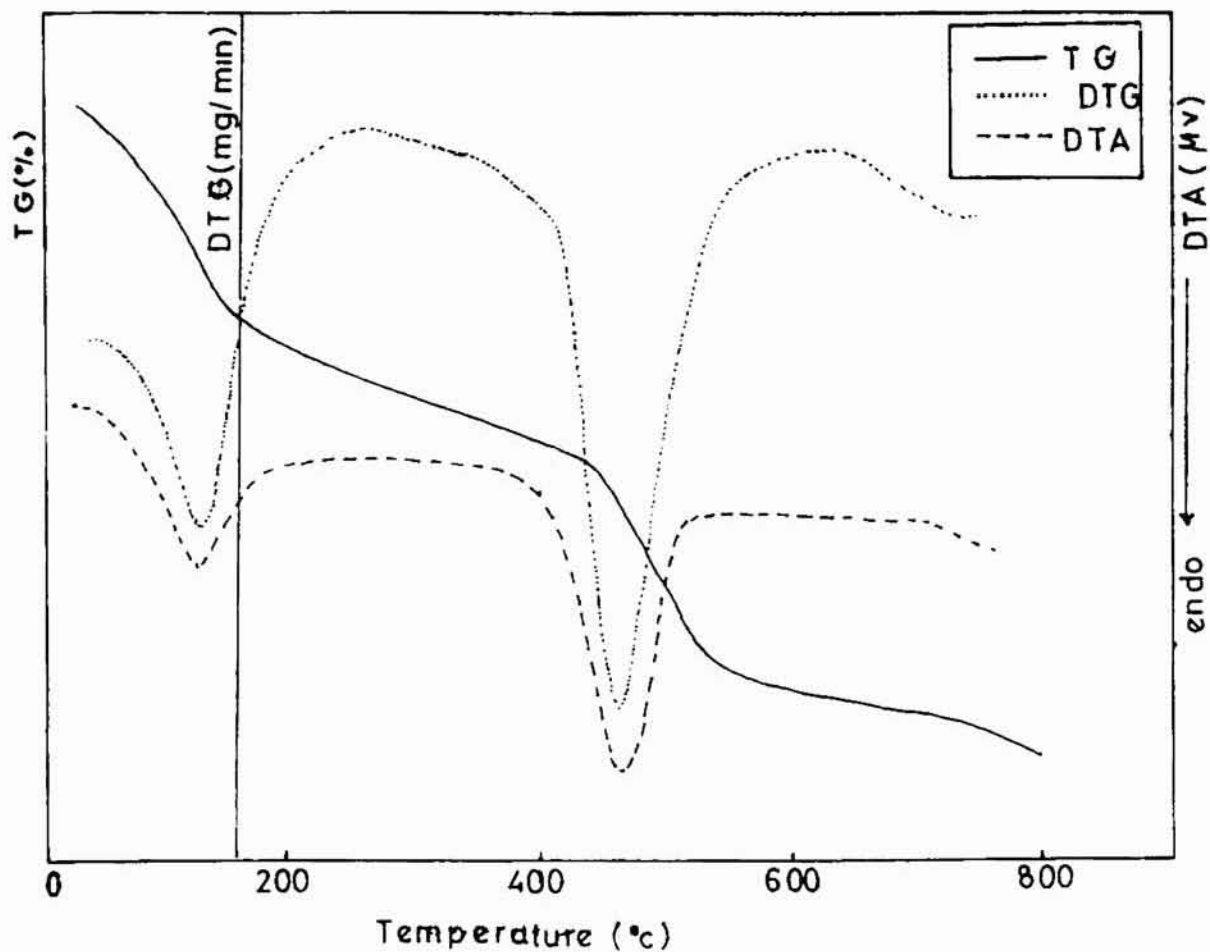
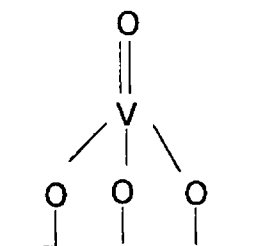


Fig. 3.11. TG-DTA curves of La_2O_3 supported vanadia

There is a shift in the region of the band to lower frequency for the supported system. The IR band at higher frequency has been assigned to the most basic hydroxyl group and the decrease in frequency of the surface hydroxyl group has been associated with increasing acidity of the corresponding surface hydroxyl groups [5]. This ensures that basic OH groups on the surface are participating in bond formation.

Based on the information perceived from the FTIR spectra, the structure of amorphous vanadia can be drawn. The surface metal oxide species coordinate to the oxide support by titrating the basic surface hydroxyls of the support. It has been well established that isolated tetrahedral units are present on the surface of vanadia supported systems with $O=V(O-S)_3$ units [6-8]. So the monooxo structure of the dispersed vanadia can be tentatively assigned the following structure.



3. 4 Thermogravimetric studies

TG analysis provides information about the stability of the catalyst upon thermal treatment. The various entities formed by heating upto a specific temperature are apparent from the thermal studies. Thermal analysis curve for La / V system is given in Fig.311 . All the three supported systems exhibited a more or less same trend. For pure lanthanide oxides, an initial weight loss is observed in 100-200°C region which corresponds to loss of adsorbed water and / or water of crystallization. In the 250-350°C range there is the formation of well defined hexagonal LaOOH intermediate. This oxy hydroxides get dehydrated further up to 400°C to form the sesquioxides of the lanthanides. Further heating leads to removal of adsorbed surface carbonates, which is formed as an effect of strong interaction of basic lanthanide oxides with atmospheric CO₂ during preparation [9-11]. In the case of

supported systems, two distinct weight losses are observed in the thermogram (Fig. 3.11). DTG pattern also supports this conclusion. There is an initial weight loss in the 100-200°C region due to loss of physisorbed water. Further weight loss, which occurs in the 350-450°C range, corresponds to excessive dehydration or loss of surface hydroxyls since the percentage of rare earth oxide is high in supported samples. Besides, formation of orthovanadate is also taking place in this region. Tetragonal orthovanadate formation by heating above 400°C is reported by Oliveira and coworkers [12]. Vanadia loss takes place only after 800 °C, indicating that the supported systems are found to be stable up to 800°C.

DTA profile for the supported system shows two endothermic peaks. The peak around 150 °C represents the loss of water from the substance. Transformation of $\text{La}(\text{OH})_3$ to La_2O_3 gives rise the second peak located at 400-450°C region. The endothermic peak of orthovanadate formation at ~ 400°C is merged with the peak of La_2O_3 formation due to higher % of La_2O_3 in the system.

3. 5 Surface area and Pore volume measurements

Surface area measurement by BET method gave the following results (Table 3.3). It is apparent that there are no marked variations in surface area, indicating that the impregnation procedure didn't appreciably affect the morphology of lanthanide oxides. Still there is an initial loss in surface area in the case of Sm and La series. Pore volume also shows a similar trend. This may be due to filling of small pores and due to a decrease of pore radii of bigger pores as a result of deposition of vanadia on the surface. Further vanadia addition prevents the agglomeration of the particles, which leads to an enhancement in the surface area. In the case of D series, the initial surface area decrease is not observed. There is an increase in the surface area and pore volume, which can be attributed to dispersion of vanadia species on the surface.

Pore size distribution of the catalysts is given in Fig. 3.12. Dubinin has classified pores into micropores ($< 20 \text{ \AA}$), mesopores ($20\text{-}200 \text{ \AA}$) and macropores ($> 200 \text{ \AA}$), based on their diameter [13]. According to this, a major portion of the pores was distributed in the macropore range. A few were observed in mesoporous region also. Micropores were found to be absent. From Figure 3.12, it can be inferred that vanadia addition reduced the number of the pores in the macroporous region and a shift to mesoporous region is observed. The decrease of surface area at low vanadia loading is due to this filling of pores.

Table.3. 3 BET surface area and pore volume of the samples calcined at 500°C

Catalyst	Surface area (m^2/g)	Pore volume (cm^3/g)
Sm_2O_3	20.78	1.41
S3	17.19	0.89
S7	21.91	0.64
S11	25.54	0.67
S15	23.48	0.59
La_2O_3	45.23	1.06
L3	35.13	1.11
L7	32.13	1.01
L11	40.53	1.40
L15	48.16	0.86
Dy_2O_3	21.99	0.83
D3	26.09	0.90
D7	23.29	0.78
D11	18.71	0.68
D15	18.01	0.65
V_2O_5	2.56	0.02

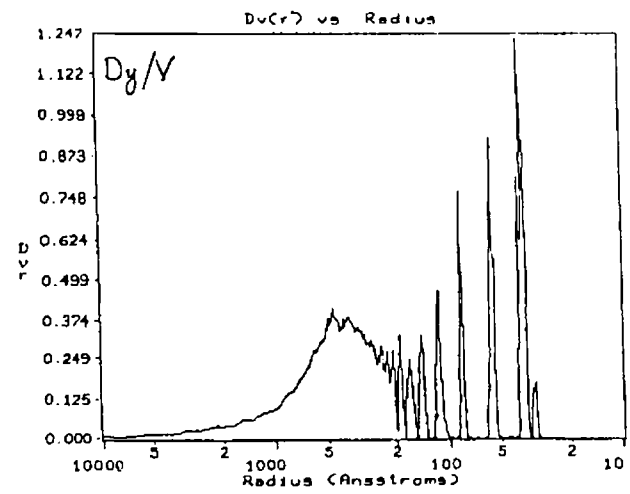
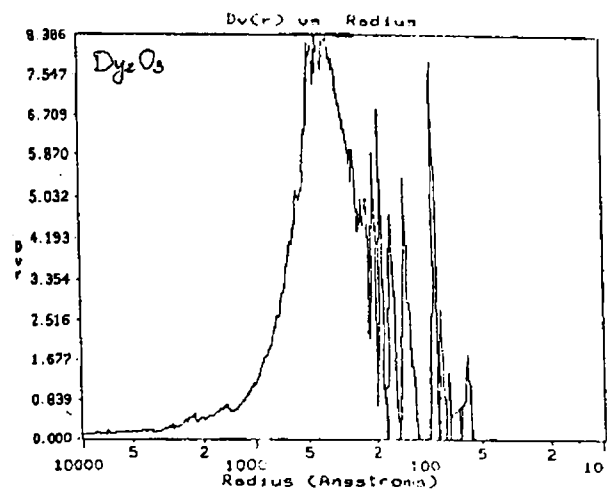
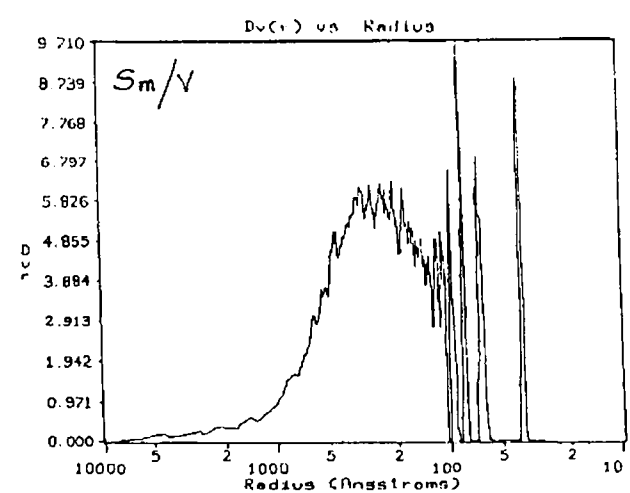
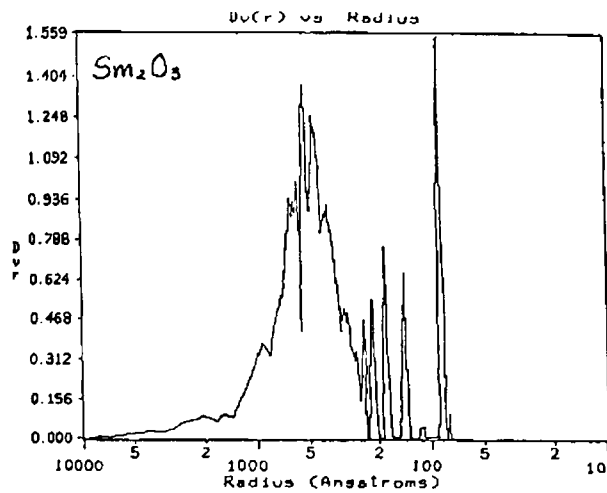
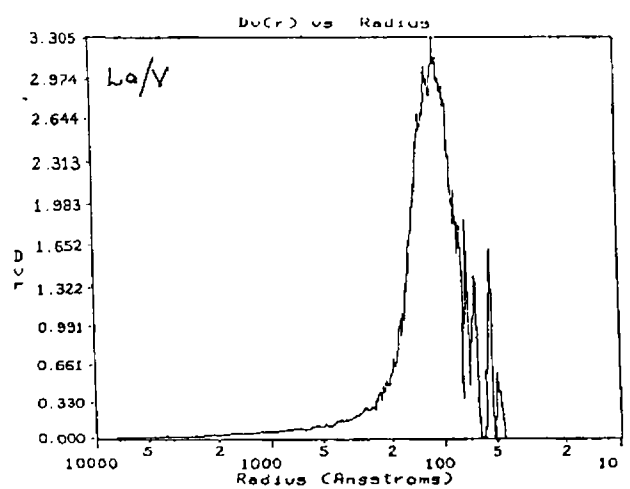
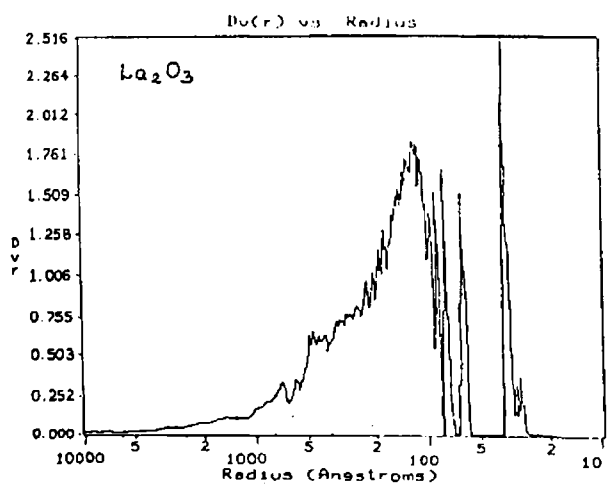


Fig.3.12 Pore volume distribution curves of rare earth oxides and supported vanadia.

3.6 Acid base properties

The acidic and basic properties of the oxides are very significant for the development of scientific criteria in catalyst application. Determination of strength of sites exposed on the solid surface as well as their distribution is a necessary requirement to understand the catalytic properties. To a major extent, the catalytic activity of metal oxides is decided by acid base properties. The conversion and selectivity of a reaction are influenced not only by the nature of active sites, but also by their number and strength.

The effect of vanadia incorporation on acid base properties of rare earth oxide supports is analysed by four independent methods, viz, indicator method, adsorption studies, temperature programmed desorption of ammonia and vapour phase decomposition of a secondary alcohol. Various conclusions derived by these investigations are presented in coming sections. Basicity studies are conducted by indicator method and adsorption of electron acceptors. Temperature programmed desorption and cyclohexanol decomposition are adopted for tracing the strength and distribution of acidic sites.

3.6.1 Hammett indicator method

Results of basicity studies using Hammett indicator method are summarized in Tables 3.4 to 3.6. None of the catalysts exhibited acidity at activation temperature of 500 ° C. Out of the six indicators tried, the present system responded only to dimethyl yellow, methyl red and bromothymol blue, showing that catalyst surface has basic sites with strengths $3.3 \leq H_0 \leq 7.2$. Very strong basic sites are found to be absent on the surface. Strong basic sites should impart basic colour to indicators of high pKa values.

Table 3. 4. Basicity data of Sm / V system

Catalyst	Basicity (mmol/g)		
	pKa \geq 3.3	pKa \geq 4.8	pKa \geq 7.2
Sm ₂ O ₃	0.346	0.084	0.059
S3	0.279	0.072	0.047
S7	0.180	0.065	0.051
S11	0.147	0.063	0.048
S15	0.116	0.055	0.042

Flockhart *et al.* have assigned the surface basicity to unsolvated hydroxyl ions and defect centers involving oxide ions[14]. For Sm/V and Dy/V series of catalysts, basicity is decreased as the composition of vanadia increased from 3 to 15 wt% (Tables 3.4 & 3.6). The decrease in basicity may be due to removal of basic surface OH groups during impregnation by the bond formation with vanadia salt, which agrees with the IR data.

Table 3.5. Basicity data of La / V system.

Catalyst	Basicity (mmol/g)		
	pKa \geq 3.3	pKa \geq 4.8	pKa \geq 7.2
La ₂ O ₃	0.530	0.170	0.097
L3	0.384	0.110	0.063
L7	0.220	0.101	0.048
L11	0.448	0.138	0.067
L15	0.570	0.181	0.099

Participation of surface hydroxyl groups in the formation of surface vanadia is confirmed from this observation. La/V systems show a deviation from other supported analogues. Addition of small amount of vanadia (< 7 wt%) reduces the

Table 3. 4. Basicity data of Sm / V system

Catalyst	Basicity (mmol/g)		
	pKa \geq 3.3	pKa \geq 4.8	pKa \geq 7.2
Sm ₂ O ₃	0.346	0.084	0.059
S3	0.279	0.072	0.047
S7	0.180	0.065	0.051
S11	0.147	0.063	0.048
S15	0.116	0.055	0.042

Flockhart *et al.* have assigned the surface basicity to unsolvated hydroxyl ions and defect centers involving oxide ions[14]. For Sm/V and Dy/V series of catalysts, basicity is decreased as the composition of vanadia increased from 3 to 15 wt% (Tables 3.4 & 3.6). The decrease in basicity may be due to removal of basic surface OH groups during impregnation by the bond formation with vanadia salt, which agrees with the IR data.

Table 3.5. Basicity data of La / V system.

Catalyst	Basicity (mmol/g)		
	pKa \geq 3.3	pKa \geq 4.8	pKa \geq 7.2
La ₂ O ₃	0.530	0.170	0.097
L3	0.384	0.110	0.063
L7	0.220	0.101	0.048
L11	0.448	0.138	0.067
L15	0.570	0.181	0.099

Participation of surface hydroxyl groups in the formation of surface vanadia is confirmed from this observation. La/V systems show a deviation from other supported analogues. Addition of small amount of vanadia (< 7 wt%) reduces the

basicity. Further addition increases basicity. This leads to the conclusion that basic sites are generated at higher vanadia loadings on La / V system.

More information regarding basicity is obtained from the adsorption studies using electron acceptors.

Table 3.6. Basicity data of Dy / V system.

Catalyst	Basicity (mmol/g)		
	pKa \geq 3.3	pKa \geq 4.8	pKa \geq 7.2
Dy ₂ O ₃	0.311	0.081	0.043
D3	0.139	0.078	0.019
D7	0.129	0.066	0.018
D11	0.103	0.041	0.014
D15	0.070	0.036	0.012

3.6.2 *Electron donating property studies*

Electron donating capacity is the measure of Lewis basicity, since the adsorption involves transfer of electrons to the adsorbate from the catalyst surface. The strength and distribution of basic sites are followed by the adsorption of electron acceptors (EA). Electron donor strength of a surface, which is defined as the conversion power of an adsorbed electron acceptor to its anion radical, can be expressed as the limiting electron affinity value, at which free radical anion formation is not observed. Electron donating capacity depends on the nature of donor sites and the electron affinity of the electron acceptors used. The extent of electron transfer decreases with decrease in electron affinity value of the electron acceptor. If the electron acceptor is having high electron affinity, anion radical formation occurs both at strong and weak donor sites. But if it is weak, adsorption occurs only at stronger sites. Here electron acceptors selected for the study were tetracyanoquinodimethane (TCNQ), chloranil and p-dinitrobenzene (PDNB); their electron affinity being 2.84, 2.40 and 1.77 eV respectively.

For the supported systems, PDNB adsorption was too negligible which is an evidence for the absence of very strong basic sites. Electron donor adsorption imparted characteristic colouration to the catalyst surface suggesting the formation of radical anions of TCNQ and chloranil. On support oxides, TCNQ adsorption developed a bluish green colour and chloranil developed a pale pink colour. In the case of supported catalysts, which were pale yellow coloured, the colours generated were pale green and pale grey respectively. The plot of equilibrium concentration of electron acceptor against amount of EA adsorbed on the surface was found to be of Langmuir type, which is confirmed by the linear Langmuir plot (Fig. 3.13). From the langmuir curves obtained, limiting amount of EA adsorbed on each system was determined (Figs 3.14-3.19). Limiting amount of electron acceptors for the three Ln / V systems is presented in Table 3.7. Since TCNQ is a stronger EA, leading to adsorption on both weak and strong donor sites, limiting amount adsorbed is higher in the case of TCNQ adsorption. Chloranil forms radical anions only on comparatively

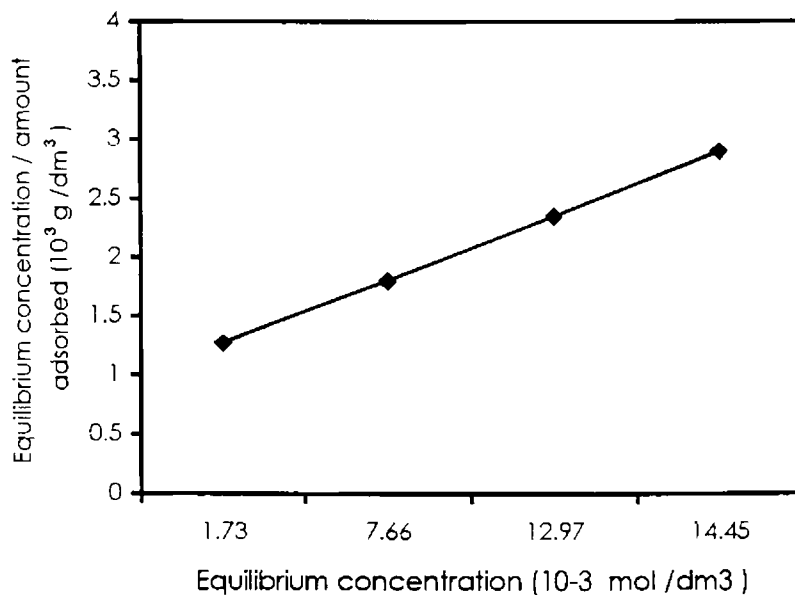


Fig. 3.13 Linear form of Langmuir isotherm obtained for the adsorption of TCNQ over Sm_2O_3 in acetonitrile.

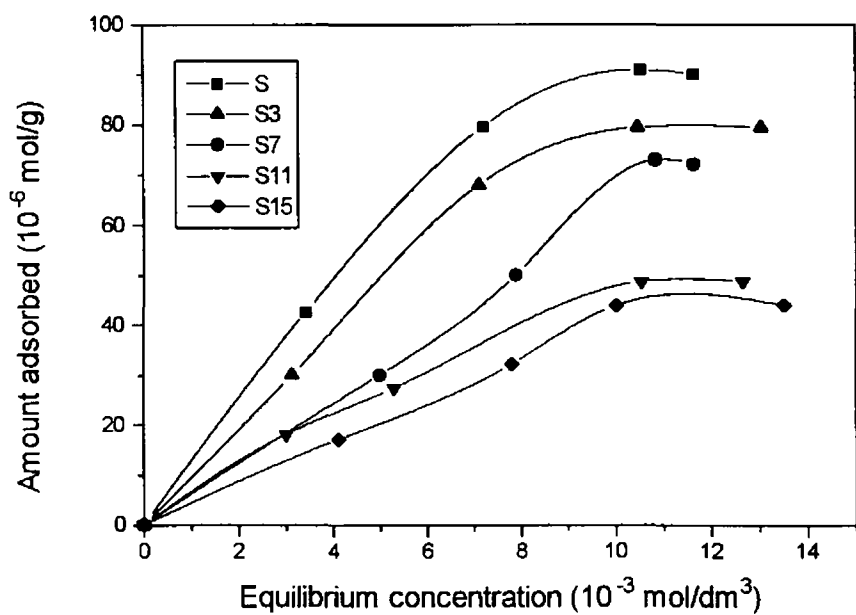


Fig. 3. 14 Adsorption isotherms of chloranil in acetonitrile over Sm / V systems

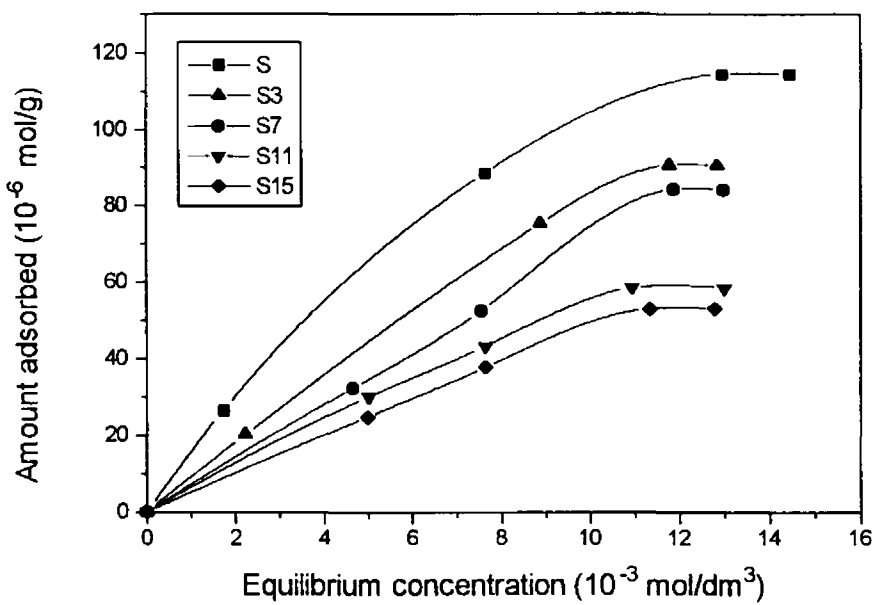


Fig. 3. 15 Adsorption isotherms of TCNQ in acetonitrile over Sm / V system

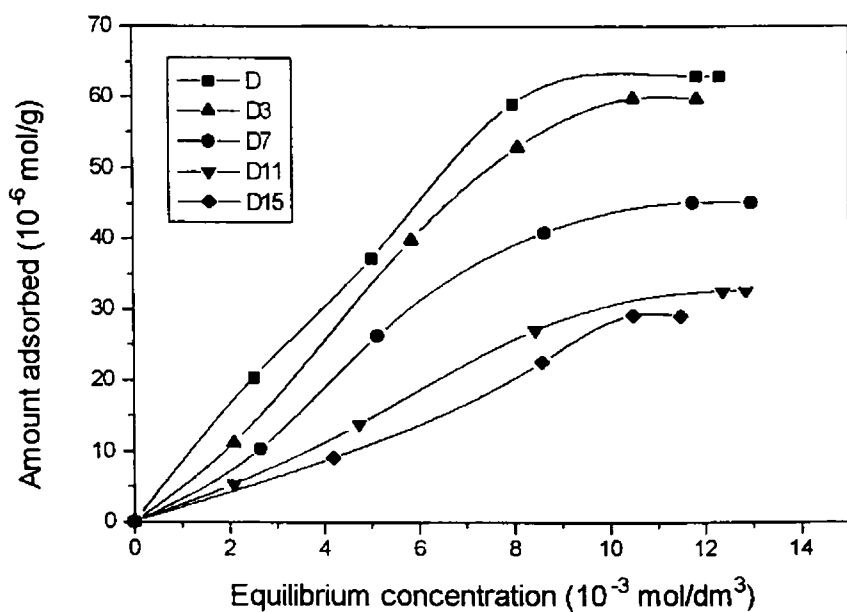


Fig. 3.16 Adsorption isotherms of chloranil in acetonitrile over Dy / V system

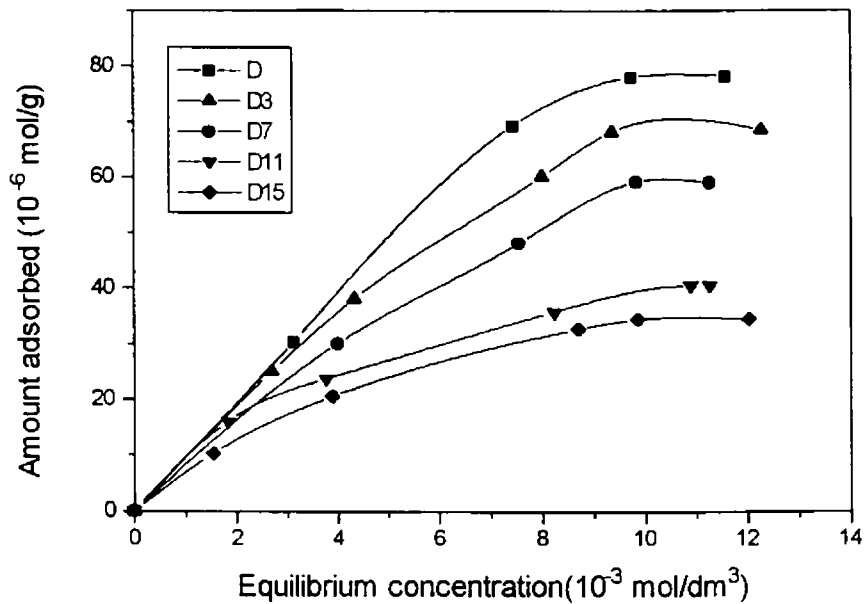


Fig. 3.17 Adsorption isotherms of TCNQ in acetonitrile over Dy / V system

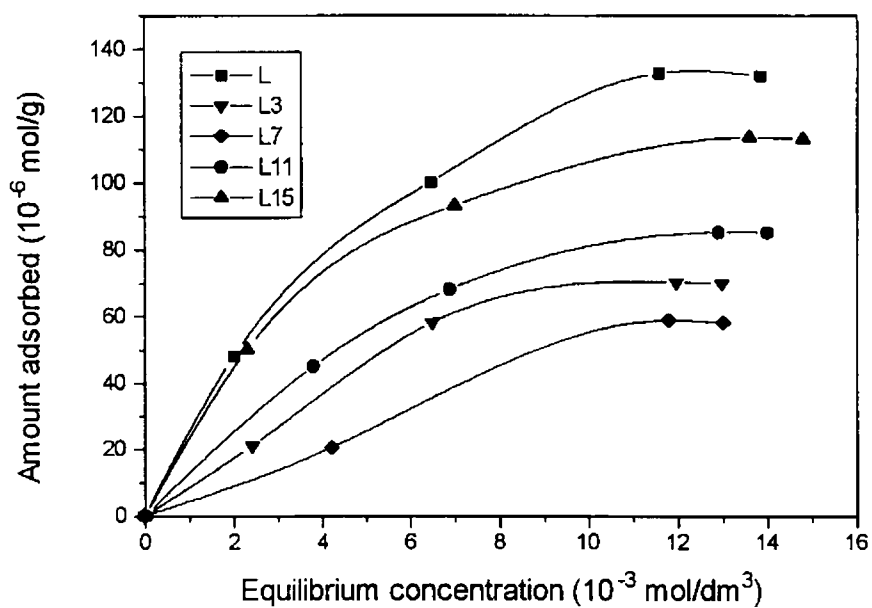


Fig. 3.18 Adsorption isotherms of chloranil in acetonitrile over La / V system

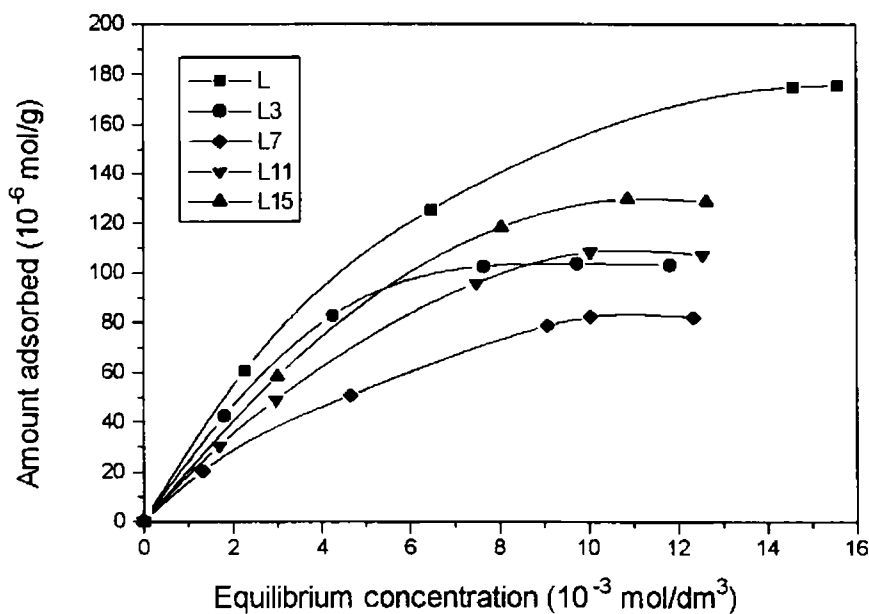


Fig. 3.19 Adsorption isotherms of TCNQ in acetonitrile over on La / V system

stronger basic sites. So the limiting amount of electron acceptor adsorbed in this case is lower. By comparing these results with electron affinity values, the limiting value of the electron affinity of the EA for electron transfer on samples under study ranges from 2.40 and 1.77. Limit of electron transfer in terms of electron affinity value of the EA is not altered by vanadia impregnation. It is concluded that electron donor sites of all the supported series are similar. No stronger basic sites are created on rare earth oxides by the incorporation of vanadia, which is in agreement with basicity determined by Hammett indicator method.

Table 3.7. Limiting amount of electron acceptors adsorbed

Catalyst	Limiting amount adsorbed (10^{-6} mol/m ²)	
	TCNQ	Chloranil
Sm ₂ O ₃	5.50	4.37
S3	5.26	4.26
S7	3.84	3.32
S11	2.28	1.91
S15	2.25	1.87
Dy ₂ O ₃	3.55	2.86
D3	2.69	2.09
D7	2.53	1.93
D11	2.15	1.73
D15	1.90	1.61
La ₂ O ₃	3.88	2.93
L3	2.95	2.00
L7	2.56	1.83
L11	2.67	2.11
L15	2.87	2.51

The difference between the adsorbed amounts of the two electron acceptors gives a measure of weaker basic sites, while amount of chloranil adsorbed gives a measure of strong basic sites. The amount of both strong and weak basic sites is reduced by incorporation of vanadia. (Table 3.8). By comparing the amount of these two types of donor sites on corresponding rare earth oxide and supported analogues, it can be inferred that consumption of strong basic sites are predominant while adding vanadia.

Table 3. 8 Amount of strong and weak basic sites on the system

Catalyst	Amount of donor sites (10^{-6} mol/m ²)	
	Weak	Strong
Sm ₂ O ₃	1.13	4.37
S3	1.00	4.26
S7	0.52	3.32
S11	0.37	1.91
S15	0.38	1.87
Dy ₂ O ₃	1.69	2.86
D3	0.60	2.29
D7	0.60	1.93
D11	0.42	1.73
D15	0.29	1.61
La ₂ O ₃	0.95	2.93
L3	0.96	2
L7	0.56	1.83
L11	0.56	2.11
L15	0.66	2.51

An idea about the distribution of the donor sites can be achieved from the radical ion concentration on the surface of the samples [15]. The radical concentration / m² should decrease with decrease in electron affinity of the electron

acceptors. There exists a linear relationship between \log (radical ion concentration / m^2) and electron affinity value of the electron acceptor, equation of the line being, \log (radical anion concentration) = $AX + B$, where A is the slope and X is the electron affinity value. Thus the distribution of electron donor sites having different strength can be evaluated by the slope of the straight line. The slope of the line becomes larger with increase of active donor sites. It has been proved that the limiting amount of electron acceptor adsorbed is proportional to the radical anion formed on the surface of the catalyst. So a plot of limiting amount adsorbed against the electron affinity of the EA should exhibit the same behaviour. From figure 3.20, it can be seen that, slopes of pure supports are high, indicating the distribution of donor sites having different strength to be larger for pure rare earth oxides. Distribution of electron donor sites is reduced by vanadia incorporation. From Table 3.7, it is clear that, for S and D systems, the limiting amount of electron acceptor adsorbed is in the order $0 > 3 > 7 > 11 > 15$ in terms of the wt % of vanadia in the supports. Since this trend is a measure of electron transfer, it is assumed that vanadia incorporation decreases the lewis basicity of the support. This is in accordance with

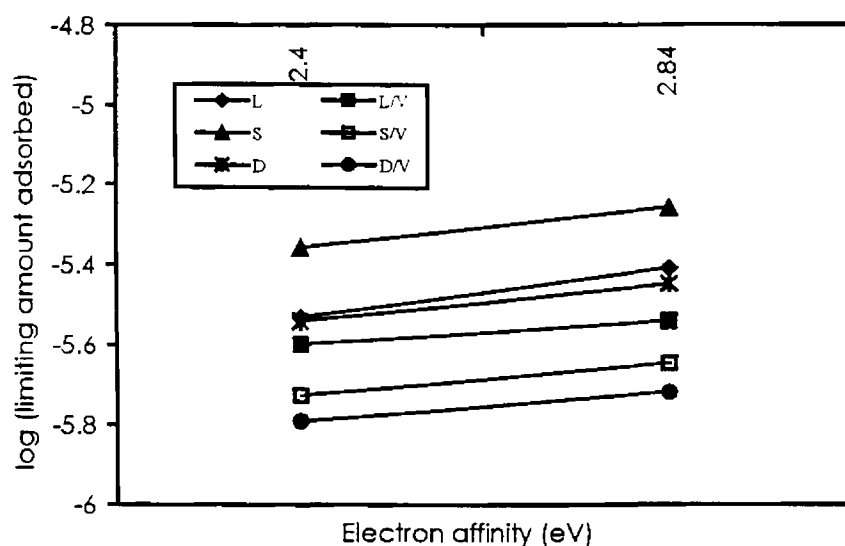


Fig. 3.20 Distribution of donor sites on pure supports and supported systems

Le Bars and coworkers' observation [16]. The factors that are responsible for the electron donating capacity are surface hydroxyl ions and surface O^{2-} centers. At higher activation temperatures, trapped electron centers also perform the role of electron donor sites [15,17]. However, it has been reported that, electron defect centers are created at an activation temperature above $500^{\circ}C$ [18]. So major contribution towards basic sites arises from surface hydroxyl ions. The decreasing amount of electron acceptor adsorbed may be due to decrease of surface hydroxyl ions as a result of vanadia addition. Supporting evidence for this conclusion is obtained from FTIR spectra of the supported systems.

Here also, La_2O_3 supported system shows a deviation from others as in the case of basicity determined by indicator method. The trend in electron transfer is the same as the results obtained from the Hammett indicator method. Basicity decreases to a minimum at a vanadia percentage = 7 and then increases. Enhancement of basicity generated by vanadia incorporation on TiO_2 has been reported by Mamoru Ai [19]. Incorporation of vanadia into La_2O_3 in minor amounts decreases the basicity of the system, while addition of vanadia > 7 wt%, enhances the basicity. This trend is opposite to that reported on SnO_2 , where a small % of vanadia enhances basicity, which decreases upon further addition of vanadia [20]. The basicity determined by indicator method is found to be higher than that obtained by electron donor adsorption.

3.6. 3 Temperature Programmed Desorption studies

Temperature programmed desorption of probe molecule is a well-established technique for measuring the acidity of supported catalysts. As this method is involved mainly in gas solid interaction, site titration by means of gas phase probe molecules appears to be one of the most reliable method to describe their surface behaviour. This procedure can be considered as a standardisation method because it allows the determination of both protonic and cationic acidities.

In general, surface OH groups and exposed cations are responsible for the acidity generation in the case of a solid surface. Ammonia being a small molecule, get adsorbed on most of the acidic sites independent of the size since it has comparatively less steric hindrance, which prevent the adsorption on smaller acid sites. Various modes of adsorption of ammonia on the catalyst surface are shown in Fig. 3.21. These include adsorption at Bronsted and Lewis acidic sites. Among these, the first two modes (a and b in Fig. 3.21) are weak adsorptions. The strongest interaction occurs when ammonia is coordinately bonded on Lewis site.

Temperature programmed desorption curves obtained for the catalysts are given in figures 3.22 to 3.24. Ammonia introduction is followed by evacuation for 15 minutes to eliminate weakly adsorbed hydrogen bonded ammonia. Measurements are taken starting from 100°C, in order to avoid the weak interaction due to physisorption. Below 100°C, the amount of ammonia desorbed was too high indicating the capacity of the samples to physisorb a large quantity of ammonia. Auroux *et al.* reported the same behaviour with La_2O_3 catalyst [21]. Two major

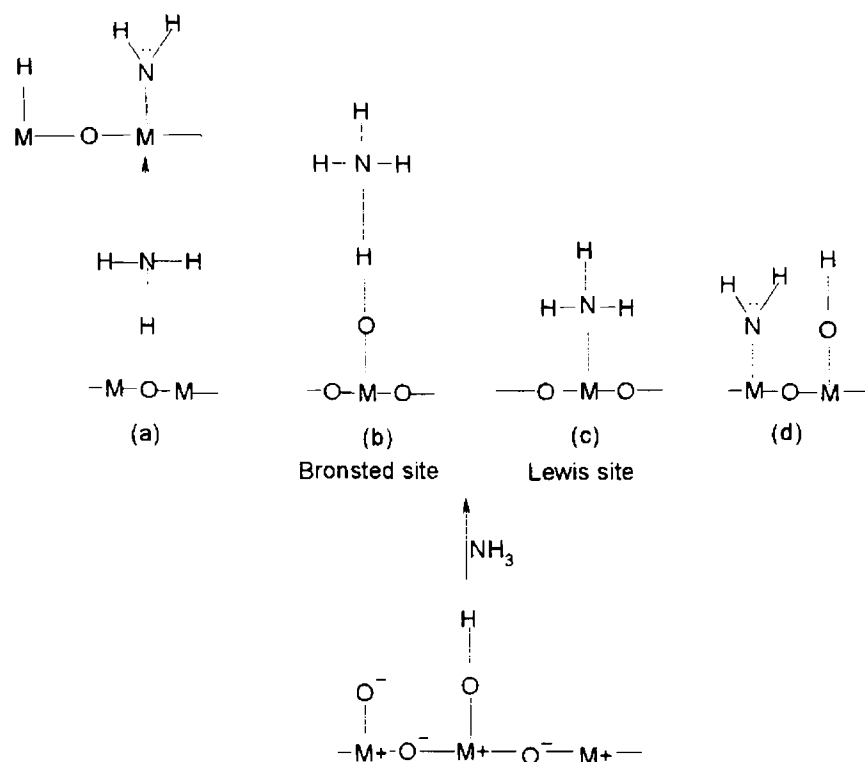


Fig. 3.21 Various modes of adsorption of ammonia on oxide surface

peaks are observed for all the systems. Peak maximum for the first region appears around 200°C and then the second at 500°C region. The area of the peaks corresponds to the acid amount in that particular temperature range. Surface will possess both Bronsted and Lewis sites. Identification of these two sites separately is possible only with the aid of an *insitu* IR spectra. NH₃ adsorbed on a Bronsted acid will give a band corresponding to NH₄⁺ species in the IR spectra and NH₃ adsorbed on the cation site (Lewis acid site) exhibit the band due to coordinatively bonded ammonia. The temperature of desorptions can be different depending upon the nature of the solid surface. However, weak sites are supposed to be Bronsted acid sites in the case of metal oxide catalysts. It is generally accepted that, evacuation of ammonia adsorbed surface at 400°C removes most of the Bronsted acid sites [21]. This is supported by the observation that the band due to pyridine adsorbed on Bronsted sites was practically nil at an evacuation > 200°C on V/Ti system [22]. In the present case, it is assumed that the amount of ammonia desorbed up to 300°C can be taken as a measure of Bronsted acidity. This is assumed on the basis that coordinately bound ammonia, which has strong interaction with the surface site, can be desorbed only at higher temperatures. So heating below 300°C bring about all the weakly bound ammonia; hence a measure of Bronsted acid sites. Amount of ammonia desorbed at higher temperatures is considered to be due to ammonia bound on Lewis acid sites. The 300 – 400°C region may be taken as a measure of medium strong acid sites. Shifting of peak maximum towards right indicates presence of stronger sites.

Figures 3.22 to 3.24 reveal that pure rare earth oxide supports possess a small amount of Bronsted acid sites and appreciable amount of Lewis acid sites. Upon vanadia addition, amount of ammonia desorbed at lower temperature region is increased and that at higher temperature region is decreased considerably for Sm/V and Dy/V systems. As per the explanations given above, there is an enhancement in Bronsted acid sites and reduction of Lewis acid sites.

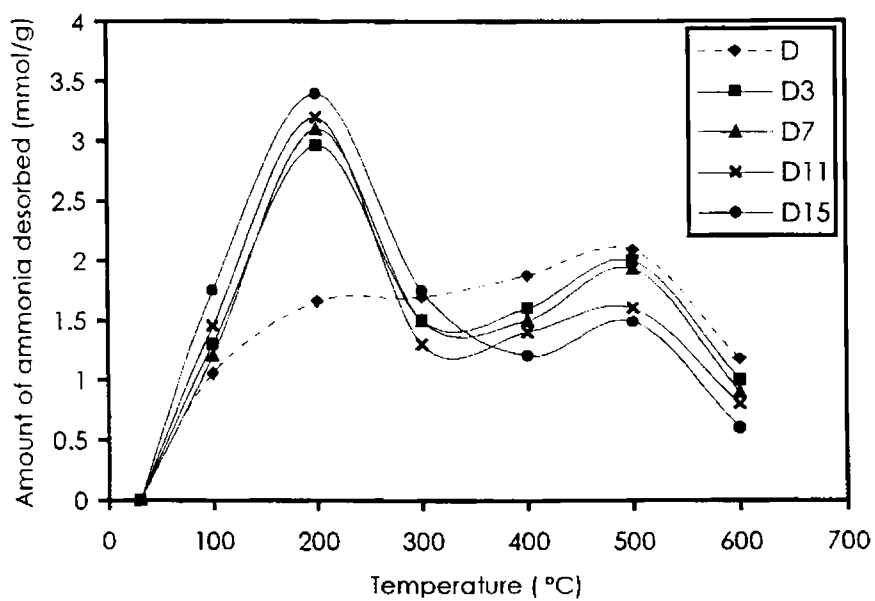


Fig. 3.22 TPD curves of ammonia over Dy / V system

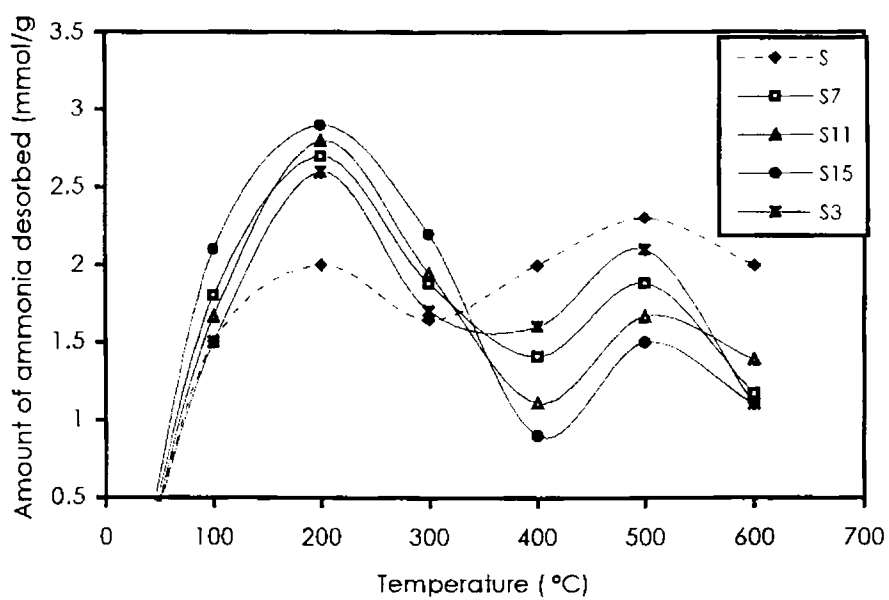


Fig. 3.23 TPD curves of ammonia over Sm / V system

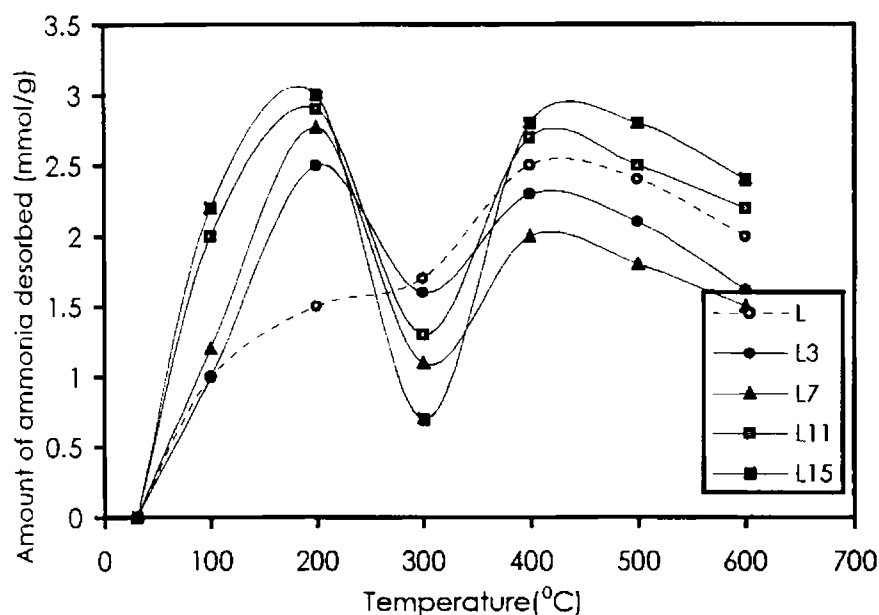


Fig. 3. 24 TPD curves of ammonia over La / V system

Sites responsible for Lewis type acidity are supposed to be coordinately unsaturated lanthanide ions. Kantcheva *et al.* attributed Lewis acidity to cations of the support [23]. They proposed that active acidic sites on the supported vanadia systems were due to surface OH groups that generates Bronsted acidity and strong Lewis acid sites due to exposed cations from support. Vanadia supporting is characterized by the consumption of strong Lewis acid site of the support while weak acid sites of the support remains unaffected. So it can be inferred that Lewis acid sites resulting from exposed cations of the rare earth oxides are being consumed upon vanadia addition. Evidences exist for the participation of Lewis acid sites of the support in the bond formation with vanadium species [24]. In the case of La/V system, vanadia content greater than 7 creates more Lewis sites than expected. The vanadium sites may also be acting as Lewis acid sites. Spectroscopic evidences are also in favour of this. *In situ* IR studies of NH₃ adsorption revealed the presence of NH₃ coordinated to V⁵⁺ ions [23].

Incorporation of V_2O_5 increases the concentration of Bronsted acid sites remarkably. Reports are there which show that Bronsted acidity is created even when the support lacks any such sites [25]. This is in accordance with views of Wachs that at higher percentage of supported oxide, Bronsted sites are developed [2]. Figures 3.22 to 3.24 show that no considerable change in the amount of Bronsted acid sites is found as the weight percentage of vanadia is increased from 3 to 15. It is well established that surface OH groups is one factor that contributes to acidity [26]. But in the case of supported systems, this is applicable at low vanadia loadings, where Bronsted acidity doesn't appear. It is reported by Turek *et al.* that a crowding effect is necessary to generate Bronsted acid sites, which is observed at higher loadings of the supported oxides [27]. They attributed Bronsted acid sites at high vanadia loadings to increase of surface density of molecularly dispersed species. In the case of rare earth supported vanadia, 3-wt percentage vanadia itself increases the Bronsted sites to a higher extent. This means that the crowding effect might have reached by the addition of 3% vanadia itself. Molecular dispersion would have been completed before 3% vanadia. It is assumed that contribution towards surface vanadia would be less by vanadia addition at higher percentages. Further vanadia loading initiate orthovanadate formation. This is confirmed by the fact that orthovanadate formation was not observed in XRD and IR data for vanadia % < 3. Further addition makes no remarkable change in Bronsted acid sites. Turek proposed that the simplest conceivable model of Bronsted acid site that can be proposed here consists of two surface species sharing a common proton located between two oxygens belonging to two different V – O – Support fragments [27]. Bronsted acidity is created independent of the structures of the proton connected surface metal oxide units if they are in the privileged configuration to each other.

3.6.4 Cyclohexanol decomposition reaction

Cyclohexanol decomposition is usually adopted to check the acid base property of the catalyst system. The amphoteric character of the alcohols permits their interaction with acidic and basic sites. As a result of this, dehydration and

dehydrogenation are catalysed by the oxide system resulting in the formation of cyclohexanol and cyclohexanone (Fig. 3.25). Dehydrogenation takes place with the intervention of both

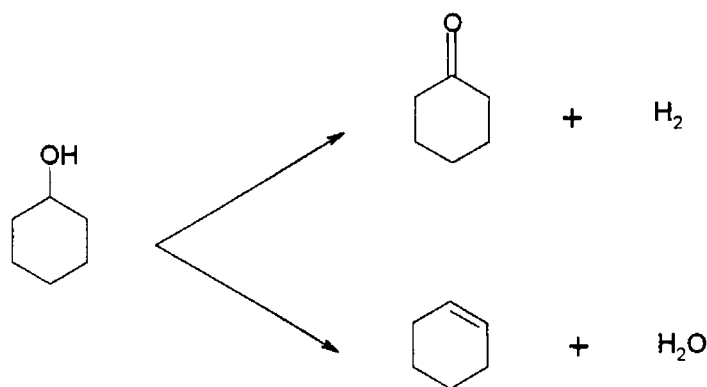


Fig. 3.25 Decomposition of cyclohexanol

acidic and basic sites and dehydration takes place with the participation of acidic sites (Fig. 3.26). So dehydrogenation rate is proportional to both acidity and basicity whereas dehydration is found to be proportional to acidity [28]. Bezouhanava *et al.* proposed a mechanism for the decomposition of cyclohexanol [29].

The reaction was performed in gas phase and the products were analysed by GC fitted with a 6' x 1/8" stainless steel column packed with 5 % NPQSB + H₃PO₄ on anachrom A 80 / 100 mesh.

Data of cyclohexanol decomposition are given in Tables 3.9 to 3.11. Pure Sm₂O₃ exhibited higher selectivity for dehydrogenated product. High selectivity of cyclohexanone on Sm₂O₃ indicates the presence of strong basic sites on rare earth oxide. Besides, rare earth oxides are found to possess a large amount of Lewis acid sites, which take part in dehydrogenation. From tables 3.9 to 3.11 it is clear that, vanadia addition bring about a dramatic enhancement in the selectivity of dehydration products. Figures 3.27 to 3.29 present the variation of rates of dehydration and dehydrogenation with vanadia content. Bronsted acid sites are found to be active for

catalyzing dehydration of cyclohexanol [29]. Enhancement of Bronsted acidity by vanadia incorporation is apparent from these data. This agrees well with the results obtained from measurement of acidity by TPD method. Methyl cyclopentene formation was not observed on pure samaria, which indicates the absence of strong

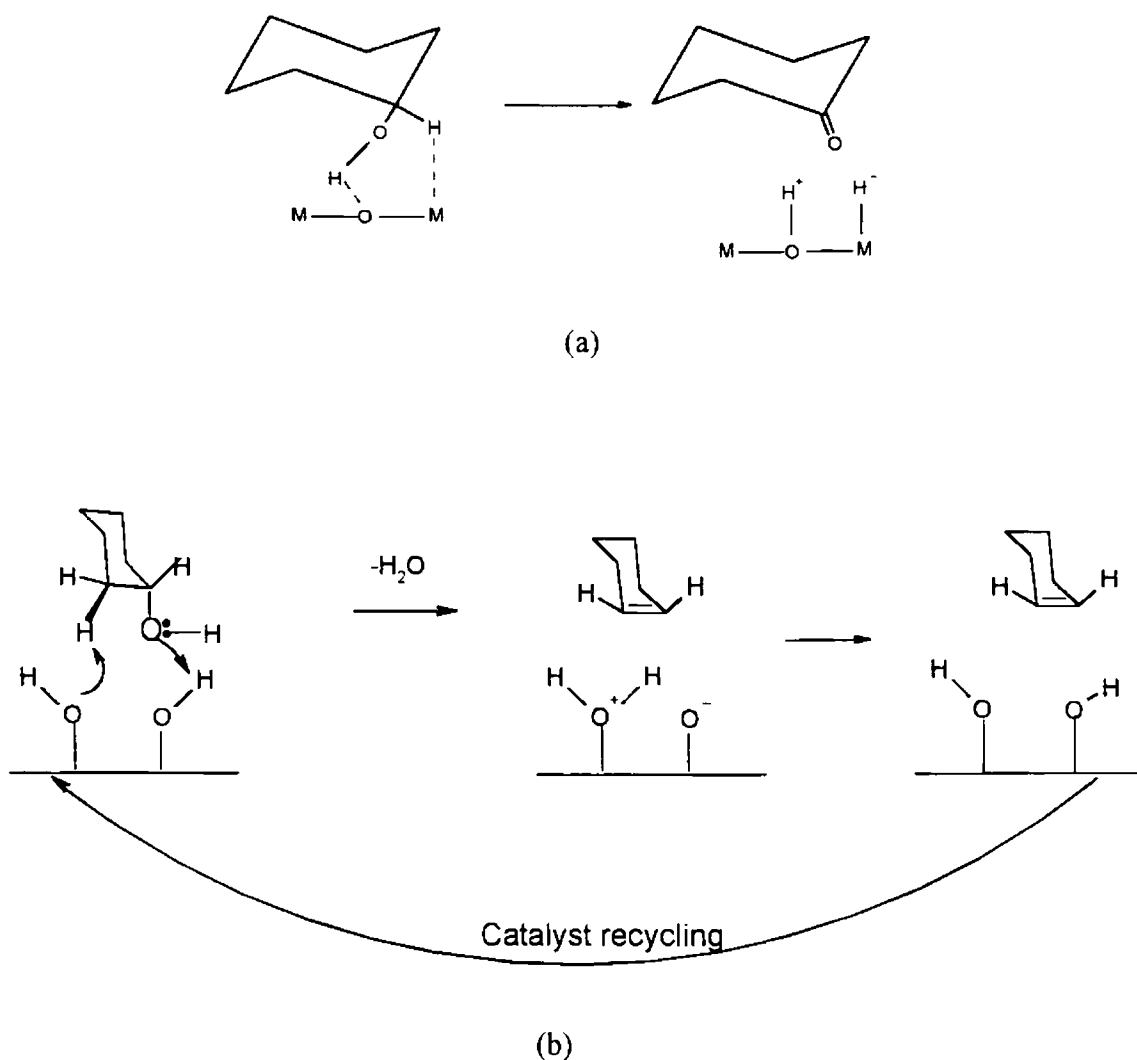


Fig. 3.26 Mechanism of (a) dehydrogenation and (b) dehydration of cyclohexanol on oxide surface.

acid sites. Pines *et al.* pointed out to the formation of methyl cyclopentene on stronger acidic sites, which is formed by the isomerisation of cyclohexene over highly acidic alumina [30].

Reduction of Lewis acid site is the reason of low selectivity of cyclohexanone on the supported vanadia system. It is apparent that the selectivity of dehydration products doesn't vary significantly as the composition of vanadia varies from 3 to 15 wt%. There is no commendable change in the selectivity of dehydration products. The addition of vanadia greater than 3% might not be increasing the Bronsted acidity significantly. So it is concluded from TPD data and the data on cyclohexanol decomposition reaction that further addition of vanadia is mainly utilized for the formation of orthovanadates.

$\text{La}_2\text{O}_3\text{-V}_2\text{O}_5$ systems exhibited a decrease of dehydration rate when vanadia percentage exceeds 7, while Bronsted acid sites still increased (Fig. 3. 29). This is supposed to be due to the reduction of protonic sites strong enough to catalyse dehydration at 11 and 15 % vanadia. This is confirmed from the TPD curves, which show a shift of peak maximum to the left in the region of lower temperature range, indicating major contribution from weak protonic sites. Selectivity of cyclohexanone exhibits an enhancement at higher vanadia content. Since the cyclohexanone formation is taking place by the participation of both acid and base sites, increased amount of Lewis sites may be the deciding factor here. Cationic sites are increasing, as seen by the increase of Lewis sites from TPD measurements, along with basicity shown by basicity measurements. These two factors combine to give higher selectivity for dehydrogenation products.

Table 3. 9. Cyclohexanol decomposition data over Sm / V catalyst system

Catalyst	Conversion (%)	Product distribution (%)			Selectivity (%)	
		MCP	Cyclohexene	Cyclohexanone	C=C	C=O
Sm ₂ O ₃	40.85	-	10.95	29.90	26.81	73.19
S3	38.61	1.19	33.73	3.69	90.44	9.56
S7	39.59	2.12	34.09	3.38	91.46	8.54
S11	42.40	3.43	35.76	3.21	92.42	7.58
S15	43.07	3.63	36.34	3.10	92.80	7.20

Reaction conditions : catalyst = 2.5 g; reaction temp. = 350°C; feed rate = 6 ml / h, TOS = 1 h

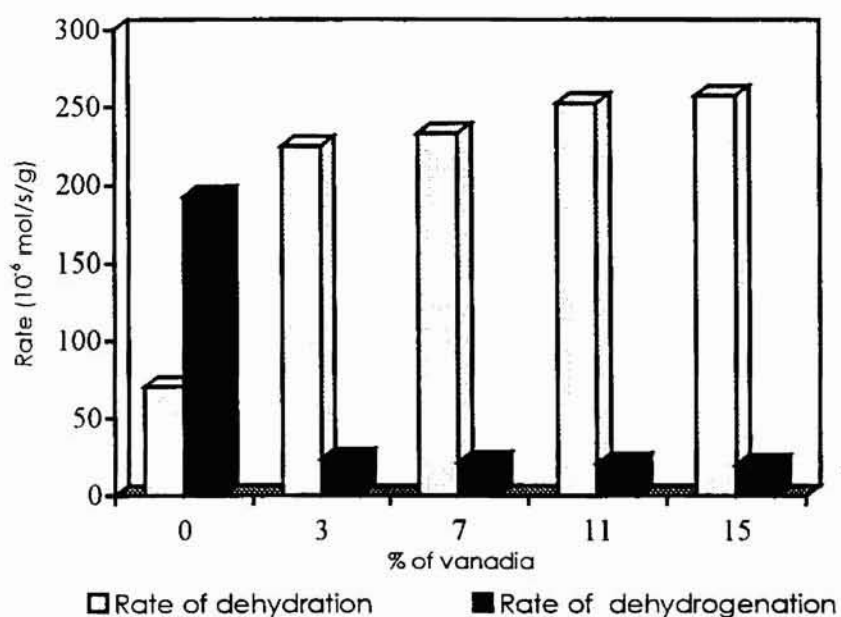


Fig. 3.27 Rate of reactions for Sm₂O₃ / V₂O₅ systems with different vanadia loadings.

Table 3. 10. Cyclohexanol decomposition data over Dy/V system

Catalyst	Conversion (%)	Product distribution (%)			Selectivity (%)	
		MCP	Cyclohexene	Cyclohexanone	C=C	C=O
D3	31.36	7.37	79.92	12.71	87.29	12.71
D7	33.04	9.77	77.69	12.54	87.46	12.54
D11	34.25	9.91	77.75	12.52	87.48	12.52
D15	44.02	12.21	75.94	11.86	80.14	11.86

Reaction conditions : catalyst = 2.5 g; reaction temp. = 350°C ; feed rate = 6 ml / h, TOS = 1 h

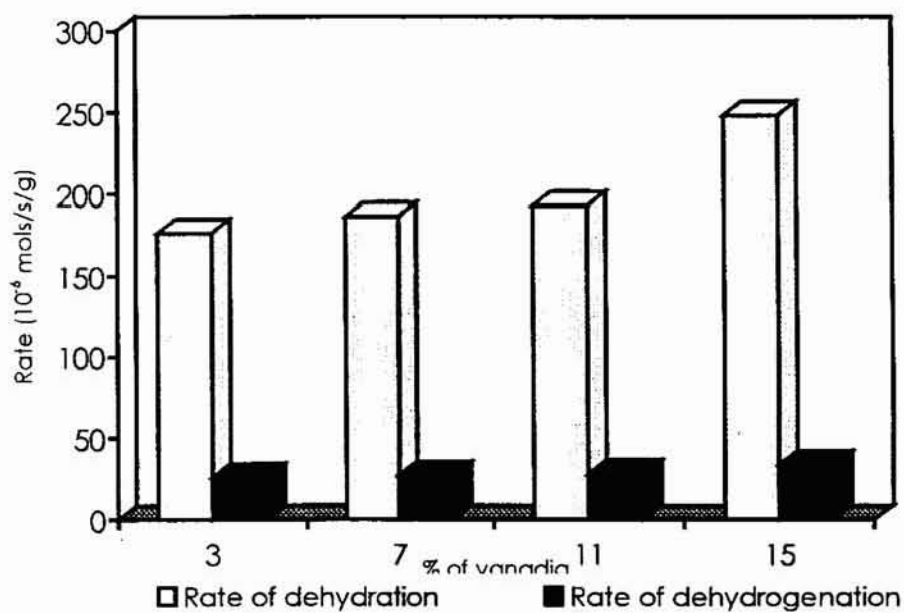


Fig. 3.28 Rate of reactions for Dy₂O₃ / V₂O₅ systems with different vanadia loadings.

Table 3.11. Cyclohexanol decomposition data over La/V system

Catalyst	Conversion (%)	Product distribution (%)			Selectivity %	
		MCP	Cyclohexene	Cyclohexanone	C=C	C=O
L3	34.37	0.88	28.56	3.90	87.74	12.26
L7	36.38	1.10	29.56	4.00	88.37	11.63
L11	37.39	1.22	22.33	4.47	86.48	13.52
L15	45.49	1.24	39.44	4.37	82.27	18.73

Reaction conditions : catalyst = 2.5 g; reaction temp. = 350°C; feed rate = 6 ml / h.
TOS = 1 h.

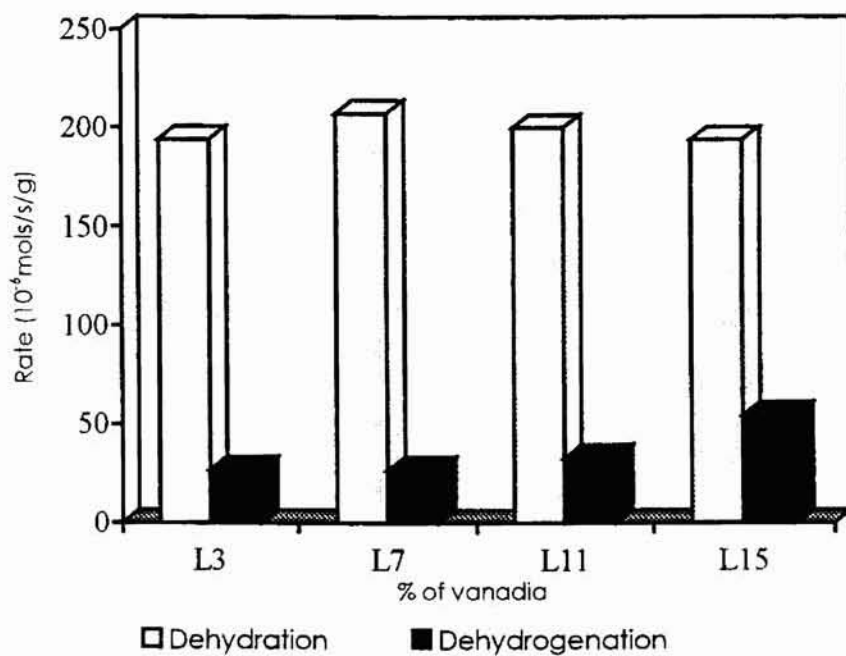


Fig. 3.29. Rate of reactions for La₂O₃ / V₂O₅ systems with different vanadia loadings.

References

1. A. Corma, J. M. Lopez-Neito, N. Paredes, M. Perez, Y. Shen, H. Cao and S. L. Suib, *Studies in Surface Science and Catalysis*, Vol. 72, (1992) pp. 213.
2. I. E. Wachs, *Catal. Today*, 27 (1996) 437.
3. L. D. Frederickson Jr. and D. M. Hausen, *Anal. Chem.*, 35 (1963) 818.
4. J. A. Gadsden, *IR spectra of minerals and related compounds*, 1975.
5. H. P. Boehm and H. Knozinger, J. R. Anderson & M. Moudart (Eds.), *Catalysis*, Vol. 4, Springer, Berlin, 1983, Chapter 2.
6. H. Eckert and I. W. Wachs, *J. Phys. Chem.*, 93 (1989) 6796
7. Xingtao Gao, J. L. G Fierro and I.E.Wachs, *Langmuir*, 15 (1999) 3169.
8. T. Blasco, J.M. Lopez Nieto, *Appl. Catal. A: Gen.*, 157(1997)117.
9. M. P. Rosynek, D. T. Magnuson, *J. Catal.*, 46 (1977) 402
10. M. N. Ambrozhi, L. M. Dvornikova, *Zh. Neorg. Khim.*, 11 (1966) 86
11. M. P. Rosynek, D. T. Magnuson, *J. Catal.*, 48 (1977) 417.
12. H. P. Oliveira, F. J. Anaissi and H. E. Toma, *Material Research Bulletin*, Vol. 33, No. 12, pp. 1783 – 1792 (1998)
13. M. M. Dubinin, *Chem. Rev.* 60 (1960) 235 .
14. B. D. Flockhart, I. R. Leith and R. C. Pink, *Trans. Faraday Soc.*, 65 (1969) 542.
15. K. Esumi, K. Meguro, *J. Colloid Interface Sci.*, Vol. 66, No. 1 (August 1978).
16. J. Le Bars, J. C. Vedrine, A. Auroux, S. Trautman, M. Baerns, *Appl. Catal. A: Gen.*, 119 (1994) 341.
17. K. Meguro, K. Esumi, *J. Colloid Interface Sci.*, Vol. 59, No. 1 (1977).
18. B. D. Flockhart, I. R. Leith and R. C. Pink, *Trans. Faraday Soc.*, 65 (1969) 542.

19. Mamoru Ai, *Bull. Chem. Soc. Jpn.*, Vol. 49 (5) 1328 (1976).
20. Mamoru Ai, *J. Catal.*, 40 (1975) 318.
21. A. Auroux and A. Gervasini, *J. Phys. Chem.*, 94 (1990) 6371.
22. F. Hatayama, T. Ohno, T. Maruoka, T. Ono and H. Miyata, *J. Chem. Soc., Faraday Trans.*, 87 (16) (1991) 2629.
23. M. M. Kantcheva, K. I. Hadjiivanov and D. G. Klissurski, *J. Catal.*, 134 (1992) 299.
24. N. Das, H. Eckert, H. Hu, I. E. Wachs, J. Walcer and F. Feber, *J. Phys. Chem.*, 97 (1993) 8240.
25. J. R. Sohn, S. G. Cho, Y. I. Pae and S. Hayashi, *J. Catal.*, 159 (1996) 170.
26. J. Bernholc, J. A. Horseley, L. L. Murrell, L. G. Sherman, S. J. Soled, *J. Phys. Chem.*, 91 (1987) 1526.
27. A. M. Turek, I. E. Wachs and E. De Canio, *J. Phys. Chem.*, 96 (1992) 5000.
28. Mamoru Ai, *Bull. Chem. Soc. Jpn.*, 50 (10) (1997) 2579.
29. C. P. Bezouhanava, M. A. Al – Zihari, *Catal. Lett.*, 11 (1991) 245.
30. H. Pines and C. N. Pillai, *J. Am. Chem. Soc.*, 82 (1960) 2401.

CHAPTER IV

CATALYTIC ACTIVITY

Introduction

It is concluded from the characterisation methods that the physical and chemical properties of the rare earth oxides are significantly influenced by vanadia incorporation. Amorphous and crystalline tetrahedral vanadium species are present in the system. Since the acid base properties of the systems are modified due to impregnation of vanadia, it is plain that the catalytic activity of the supported system would be greatly affected. The different catalytic properties of bulk and supported vanadia are usually related to the modification in the coordination and environment of the vanadium species, which can modify its redox properties. V_2O_5 based systems are renowned for their catalytic activity towards oxidation reactions. Vanadium ions in different oxidation states, the presence of which is characteristic of vanadia catalysts facilitate the electron transfer between the reactants and the catalyst.

It was reported that systems active and selective in the formation of acidic products contain usually the elements forming oxides of more acidic character than vanadium (Mo, P etc.) whereas ODH reactions, which produce basic substances proceed well on systems of basic oxides [1]. For investigating the catalytic activity of rare earth oxide supported vanadia system, we have selected oxidative dehydrogenation of ethyl benzene and ethanol. Phenol methylation reactions using methanol is also carried out which is found to depend on the acid base property of the system. Behaviour of the supported system towards the aforementioned reactions is discussed in the following sections.

4.1 Oxidative dehydrogenation of Ethyl benzene

Oxidative dehydrogenation of ethyl benzene yields styrene (Fig. 4. 1). It is a highly significant reaction from the industrial point of view due to the commercial importance of styrene. Industrially, styrene is prepared by alkylation of benzene

using ethylene. Generally used catalyst systems for the preparation of styrene from ethyl benzene include $\text{SiO}_2\cdot\text{Al}_2\text{O}_3$ [2,3] V-Mg-O [4], $\text{SnO}_2\text{-P}_2\text{O}_5$ system [5] etc.

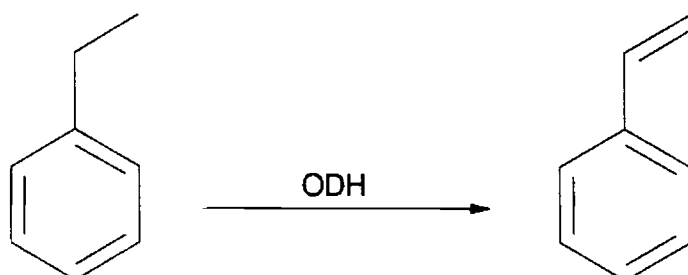


Fig. 4.1. 1 Oxidative dehydrogenation of ethyl benzene to styrene

The reaction was performed in a vapour phase down flow silica reactor. The products were analysed using a Shimadzu GC-15 A gas chromatograph fitted with a xylene master capillary column and FID. Influence of rare earth oxide supports, role of oxygen, influence of reaction temperature and flow rate etc. are analysed in detail.

Data on ODH of ethyl benzene for the three rare earth oxide supported vanadia systems are given in Tables 4.1.1 to 4.1.3. Pure vanadia and rare earth oxide support are also used as catalysts to study the effect of supporting vanadia on the catalytic properties. Along with styrene, small amount of benzene and toluene are also detected among the products. Carbon oxides are the other products, which are formed by the complete oxidation of the organics.

Calculations are done in the following manner.

$$\begin{aligned}\text{EB conversion} &= \text{mol EB converted} / \text{mol EB fed} \\ \text{Selectivity to ST, B or T} &= \text{mol product formed} / \text{mol EB converted} \\ \text{Selectivity to CO or CO}_2 &= \text{mol product formed} / (8 \times \text{mol EB converted})\end{aligned}$$

where, EB = Ethyl benzene; ST = Styrene; B = Benzene; T = Toluene

Table 4. 1. 1 Oxidative dehydrogenation of ethyl benzene over La / V system

Catalyst	Conversion	Selectivity (%)			
	(%)	Styrene	Toluene	Benzene	C-oxides
V ₂ O ₅	35.8	5.2	1.6	3.0	90.2
La ₂ O ₃	18.5	42.1	5.9	2.2	49.8
L3	16.5	65.1	4.1	2.0	28.8
L7	15.6	71.8	2.7	0.7	25.3
L11	16.0	70.3	2.3	1.6	24.8
L15	17.4	71.9	2.3	3.8	21.7

Reaction conditions: Reaction temperature: 475 °C; Feed rate: 6 ml/h; Catalyst: 2 g; Time on stream: 1 h.; Air flow rate: 20 ml/min.

Selective oxidation activity of pure vanadia was too poor, which catalysed almost complete oxidation of ethyl benzene, leading to more oxygenated products as evidenced by the higher percentage of carbon oxides formed. Carbon oxide selectivity of pure La₂O₃ was also high. From the ODH data, it is obvious that, selective oxidation activity of ethyl benzene to styrene is greatly influenced by V₂O₅

Table 4.1.2. Oxidative dehydrogenation of ethyl benzene over Sm / V system

Catalyst	Conversion	Selectivity (%)			
	(%)	Styrene	(%)	Benzene	C-oxides
S3	8.1	77.0	3.9	3.1	16.0
S7	13.8	84.7	1.7	3.0	10.6
S11	14.9	87.3	1.3	1.3	10.1
S15	16.6	86.6	1.2	0.9	10.4

Reaction conditions: Reaction temperature: 475°C; Feed rate: 6 ml/h; Catalyst : 2 g; Time on stream : 1 h.; Air flow rate : 20 ml/min.

Table 4.1.3. Oxidative dehydrogenation of ethyl benzene over Dy / V system

Catalyst	Conversion (%)	Selectivity (%)			
		Styrene	(%)	Benzene	C-oxides
D3	15.5	85.0	2.3	1.7	11.0
D7	22.1	90.2	2.0	1.5	6.3
D11	23.2	91.2	1.4	0.9	6.5
D15	25.2	91.2	1.2	0.5	7.2

Reaction conditions: Reaction temperature: 475°C; Feed rate: 6 ml/h; Catalyst: 2 g; Time on stream: 1 h; Air flow rate: 20 ml/min.

incorporation. Addition of vanadia to La_2O_3 induces remarkable selective oxidation activity. Selectivity of styrene was almost doubled. Styrene selectivity was found to be independent of percentage conversion of ethyl benzene. Styrene selectivity was found to be maximum for Dy / V systems. Almost constant selectivity was detected for the three systems at higher vanadia loadings

4.1.1 Selective oxidation activity of the supported system

The selectivity enhancement observed in the supported systems is explained as follows. V_2O_5 is having layer structure and all the layers take part in the oxidation reaction because diffusion of oxygen from other layers of the lattice is much faster in V_2O_5 [6]. This will lead to complete oxidation preferentially. According to Sachtler *et al.* [7,8], the selectivity in oxidation reaction is determined by two factors; 1) by the intrinsic activity of lattice oxygen 2) by their availability. If only a limited number of lattice oxygen is available, oxidation stops at a particular level to result partial oxidation products. Abstraction of too many hydrogen will lead to breaking of C - C bond resulting total oxidation products. In the supported systems, there is no large reservoir of bulk oxygen that is available to abstract so many oxygen. Thus the locally limited amount of reactive lattice oxygen might be the explanation for

selective oxidation activity. Pure rare earth oxides also catalyse complete oxidation of the organics. Lanthanide oxides possess low binding energy that in turn makes the lattice oxygen highly mobile [9]. So oxygen insertion takes place in the partial oxidation products resulting carbon oxides.

Of the transition metal oxides, V-Mg-O system was found to be the most active and selective catalyst in the ODH of ethyl benzene to styrene [4]. Almost constant styrene selectivity independent of reaction temperature and ethyl benzene conversion was reported for V-Mg-O systems, especially for magnesium orthovanadate ($\text{Mg}_3\text{V}_2\text{O}_8$). The selectivity of styrene reported by us using Ln/V systems is comparable to that obtained for magnesium orthovanadates. Maximum selectivity of styrene was achieved when vanadia was supported on Dy_2O_3 . The styrene selectivity order was $\text{Dy/V} > \text{Sm/V} > \text{La/V}$.

According to Tagawa *et al.*, the acid sites of Hammett H_0 values between 1.5 and -5.6 are found to be the active site for ethyl benzene conversion which adsorb ethyl benzene reversibly. Oxidation of the same occurs on the basic sites of pK_a lying between 17.2 and 26.5 [3]. The tendency to have maximum activity suggests the cooperative effect of the acid base properties of the catalyst. However, in the rare earth oxide supported vanadia systems, no such sites were detected by Hammett indicator method. So the influence of acid base properties on the selective oxidation activity will be negligible here. According to Blasco *et al.*, the catalytic behaviour of vanadium based systems in selective oxidation strongly depend on the redox property of the vanadium species as well as on the acid base character of support and catalyst [10,11]. So apart from the acido basic properties, the redox property plays an important role in ODH reaction of ethyl benzene.

The role of vanadia in developing selective oxidation activity to styrene on rare earth supports is apparent from the data in Tables 4.1.1 to 4.1.3. The activity for partial oxidation of the supported system is due to the coordination environment of

vanadium ion in the catalysts. Two types of vanadia species were detected in Ln / V systems. Surface vanadia species and lanthanide orthovanadates. The absence of polyvanadates and the existence of vanadia as vanadia tetrahedra are concluded from the IR data. The IR band observed in the region $\sim 1060 \text{ cm}^{-1}$ indicates the presence of monooxo species on the surface. It is generally accepted that at very low vanadia loadings, tetrahedral isolated vanadium species are present on the surface of the support [12]. Monomeric tetrahedral systems of the type $(\text{M-O})_3 - \text{V} = \text{O}$ are reported on the surface of the catalyst systems at low loadings for a number of supported systems [13,14]. Corma et al [15] and Patel *et al.* [16] also confirmed the existence of vanadium species as isolated tetrahedra on the surface of the support.

Grzybowska *et al.* have shown that V^{5+} exists in isolated VO_4 tetrahedra and orthovanadates [1]. Isolated tetrahedral V^{5+} species are proven to be active and selective centers for oxidative dehydrogenation reactions. It is accepted that vanadia in a tetrahedral coordination is most active in oxidative dehydrogenation [17,18,19]. This is in agreement with the report that in the case of alkanes, orthovanadates were observed to be selective in ODH reactions [16]. Further evidence is provided by Corma *et al.* who reported high selectivity for orthovanadates including LaVO_4 and SmVO_4 in which vanadium is in tetrahedral coordination [15]. For the present system, both the species being in tetrahedral geometry, this condition is satisfied, which indicate the active species to be vanadia in tetrahedral coordination both in amorphous and crystalline form.

Both the species have a common feature that they have isolated vanadate units, where every oxygen ion links one vanadium and one lanthanide ion. The environment of vanadyl units, ie., the existence of bond $\text{V} - \text{O} - \text{M}$ in the catalyst affect the distribution of electron cloud around vanadium and oxygen atoms which will reflect in the degree of ionicity of $\text{V} - \text{O}$ bond; ie., nucleophilicity of vanadium ions and electrophilicity of vanadium ions. In oxidation reactions, surface oxygen is proposed as a site capable of abstracting H atoms as H ions to form an OH group

[20]. So the activity depends on the nucleophilicity of the oxygen of the catalyst. Oxygen attached to a V^{5+} in tetrahedral coordination is found to be highly nucleophilic [1].

Among the three systems, Dy / V series showed higher activity. The lowest activity was found for La / V systems. Conversion of ethyl benzene increased with vanadia loading in the case of Sm/V and Dy/V systems. In the case of La/V series, conversion decreases with vanadia loading and then increased (This will be explained later, while discussing the reaction path). The difference in activity among the three supported systems can be correlated with their redox properties of the ion in Ln – O – V bond. Deo *et al.* have showed that the strength of the V – O – M (M = metal ion of the support) bond primarily determines the catalytic activity in the case of supported vanadia systems [21]. Reducibility plays an important role in deciding the activity of the supported system [6]. Higher the reducibility of the metal ion in the support metal oxide, higher the activity towards oxidation reactions. Among the three lanthanide ions, Dy is most reducible and it exhibits higher activity.

Above 3 % vanadia, styrene selectivity was almost constant. Here this behaviour is supposed to be due to the formation of lanthanide orthovanadate, which may be forming predominantly after 3 % vanadia. Up to 3 %, V_2O_5 surface species may be contributing to styrene selectivity. At higher vanadia concentration, vanadates have a prominent role, which exhibits a constant selectivity towards styrene. This is a characteristic behaviour of magnesium orthovanadate, which exhibits constant styrene selectivity even when the reaction parameters are changed [4.].

Enhancement of selectivity by tetrahedral vanadium is connected with the availability of the lattice oxygen at the reaction site apart from the nucleophilicity of lattice oxygen. This oxygen availability is expressed as the average number of oxygen molecule that reacts with each hydrocarbon molecule, otherwise known as

average oxygen stoichiometry (AOS) [17]. The number of vanadyl units that can effectively interact with the adsorbed hydrocarbon unit determines the AOS in the case of a particular system. The effective size of such a unit is governed both by the size of the reactant and the rate of reoxidation of the active center. In the case of rare earth supported vanadia, VO_4 units are isolated (sufficiently apart), which supplies only a limited number of oxygen atoms to react with hydrocarbon molecule, improving selectivity. Higher AOS will lead to low selectivity. Apart from this, the rate of creation of oxygen vacancies, and the rate of replenishing of oxygen by migration of lattice oxygen decide the activity.

Superiority of supported catalyst over crystalline vanadia is established as follows. In crystalline vanadia V-O-V bonding is present. In supported system, V-O-Ln bond is present. The oxygen of the V – O – Ln bond is richer in electron density than in V-O-V, since lanthanide ion has lower electronegativity than vanadium ion. This renders the oxygen in Ln-O-V bond comparatively nucleophilic than the one in V_2O_5 . For selective oxidation to occur, the oxygen should attack the hydrogen of the side chain, which is more probable by nucleophilic oxygen. So comparatively nucleophilic oxygen in orthovanadate prefer to attack high electrophilic hydrogen in the side chain of ethyl benzene. For complete oxidation to occur, bonding between carbon and oxygen has to occur. The carbon atom is sandwiched between π electrons. So the 'H' in this carbon would be attacked preferentially by an electrophilic oxygen over a nucleophilic one. In the case of V-O-V, the oxygen is more electrophilic and interacts with the ring hydrogen. This leads to rupture of C-C bond offering complete oxidation products [4].

In retrospect, the bonding in M-O-V was suggested to be the primary factor that determines the selectivity in ODH reaction [22,23]. Reducibility of the lanthanide ion affect the ease of removal of oxygen ions, i.e., the oxidizing ability of the system. The reducibility of an oxide is thought to be an important property affecting its catalytic performance and selectivity. A catalyst that is too difficult to

be reduced is too inactive with high selectivity, while that is too easily reduced is active but non selective. So if the vanadate unit is composed of a more reducible ion, the selectivity of ODH product will be low with high activity [16]. Here, the reducibility of the rare earth ions is in the order, $\text{La} < \text{Sm} < \text{Dy}$. La is least reducible. In other words, oxygen in La-O-V is more nucleophilic to attack the H of the ethyl benzene. So maximum selectivity is anticipated for L series of catalysts. In this study, results obtained are contradictory. Styrene selectivity was found to be high for Dy / V system. La / V system has the lowest styrene selectivity among the series. This is highlighted in Fig. 4.1.2.

The unexpected behaviour of La/V systems can be explained as follows. After 'H' abstraction, the partial oxidation product can desorb to gas phase or undergo further reaction with insertion of oxygen to form carbon oxides. The fate of the adsorbed product depends on a) the number of available lattice oxygen in the vicinity and the mobility of oxygen. i.e., mobility of oxygen which help to replenish the oxygen vacancies formed on oxidation. It leads to products with higher number of oxygen and eventually result in more percentage of carbon oxides; b) desorption rate of styrene. i.e., rate of diffusion of the oxygen in the lattice relative to the residence time of organic species on the catalyst surface. It affects the selectivity. Residence time of the product on the surface before desorption is an important factor which controls the selectivity of the products. The residence time will depend on the ease of desorption of styrene from the catalyst surface, which in turn depends on the acido-basic properties of the catalyst. This is dependent on the nature of adsorbate; an acidic product formed will be easily desorbed from an acidic catalyst, and a basic one get easily detached from a basic surface. Styrene being basic is less strongly bound and thus more easily desorbed from a catalyst, which shows higher basicity. As far as this factor is considered, the selectivity of styrene is expected to be high for the La/V series. Higher basicity of La/V series is confirmed through acid base property studies. But here, the first factor, that is the replenishment of lattice oxygen or the mobility may be the significant contributing factor. Rare earths possess low

binding energy for lattice oxygen and among La, Sm and Dy, O¹⁸ binding energy is low for La [9]. More mobile lattice oxygen leads to higher degree of oxidation leading to complete combustion products on La / V samples. So the selectivity follows the order Dy / V > Sm/V > La / V.

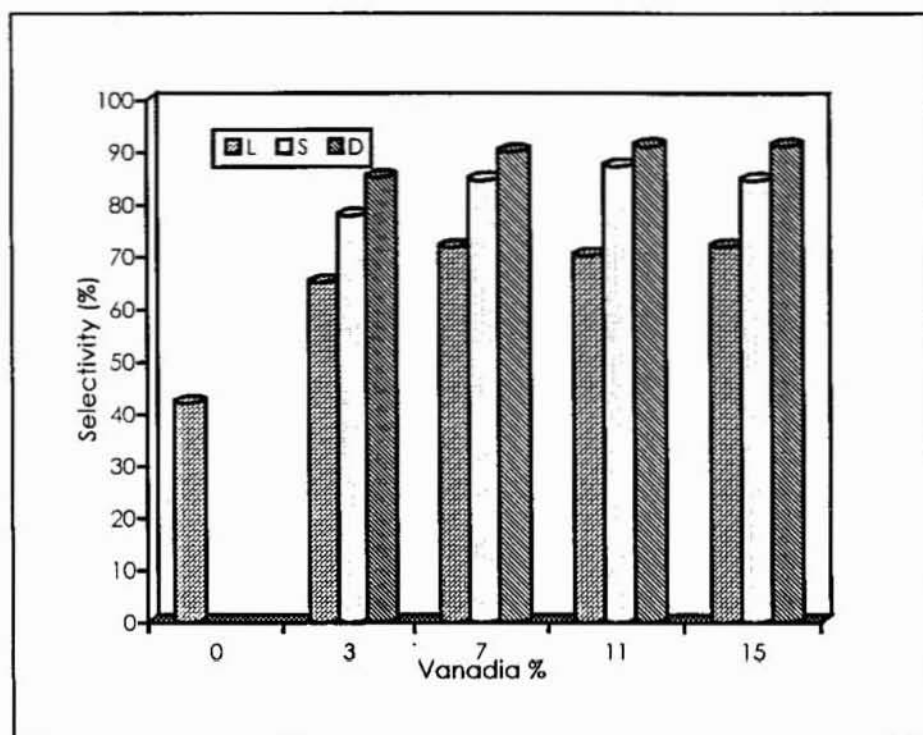


Fig. 4.1.2. Selectivity of styrene for the different supported systems

The formation of toluene and benzene is caused by the interaction of ethyl benzene with acidic and basic centres of the catalyst surface. Wang *et al.* suggested that strong acidic sites could abstract alpha hydrogen of ethyl benzene facilitating the formation of benzene [24]. From ammonia desorption studies it was concluded that Lewis acid sites are decreasing with vanadia addition. Lewis acid sites are the strong acid sites on the catalysts surface. The decrease of benzene selectivity as vanadia content increases is explained by the reduction of Lewis sites. Similar observation was made with La/V systems also. An increased Lewis acidity was observed by vanadia addition at higher vanadia loadings, which leads to an increased

selectivity for benzene for L11 and L15. Strong basic sites on the catalyst preferably abstract beta hydrogen leading to cleavage of C-C bond of side chain resulting high yield of toluene. Krause proposed the role of strong basic sites for toluene formation [25]. Thus the decrease of toluene formation observed at higher vanadia percentage is explained since basic sites are reduced at higher vanadia loadings. From adsorption measurements using electron acceptors, strong basic sites are found to be consumed as the vanadia composition increases. The toluene selectivity order for La / V series also follows the order of basicity of the oxides.

4.1.2 Reaction in absence of air

To understand the reaction mechanism, the dehydrogenation of ethyl benzene is carried out in the absence of air. Data on dehydrogenation reaction of ethyl benzene is given are Tables 4.1.4 – 4.1.6.

The reaction proceeds considerably in the absence of air. In the absence of external oxygen, ethyl benzene conversion was almost halved. Reason for the reduced conversion may be the reduction of the catalyst. The formation of styrene reduces the catalyst system and the possibility of reoxidation is limited. In ODH, conversion is higher because external supply of air maintains the conversion by supplying O₂ needed for hydrogen abstraction by reoxidising the catalyst. Besides, deposition of carbonaceous materials is also another factor, which leads to poisoning of active sites.

The selectivity towards styrene formation is increased under nonoxidative reaction conditions. High styrene selectivity in absence of air must be due to absence of gaseous oxygen. A reduction of styrene selectivity in presence of gaseous oxygen is reported by Chang *et al.* [4]. This is in agreement with the conclusion of a kinetic

Table 4.1.4. Dehydrogenation of ethyl benzene over La / V system

Catalyst	Conversion (%)	Selectivity (%)			
		Styrene	Toluene	Benzene	C-oxides
La ₂ O ₃	6.2	78.3	10.4	2.5	8.8
L3	6.5	82.3	8.8	2.3	6.6
L7	7.3	86.6	6.4	2.3	5.3
L11	7.2	85.3	5.6	2.7	6.4
L15	7.8	87.2	5.8	2.6	4.4

Reaction conditions: Reaction temperature: 475 °C; Feed rate: 6 ml/h; Catalyst: 2 g; Time on stream: 1 h.

Table 4.1.5 Dehydrogenation of ethyl benzene over Sm / V system

Catalyst	Conversion	Selectivity (%)			
		Styrene	Toluene	Benzene	C-oxides
S3	6.4	82.9	9.8	2.8	4.6
S7	6.8	90.8	4.0	1.4	3.7
S11	7.2	90.0	4.0	1.5	3.4
S15	7.5	87.9	4.0	1.8	3.2

Reaction conditions: Reaction temperature: 475 °C; Feed rate: 6 ml/h; Catalyst: 2 g; Time on stream: 1 h.

study on ethyl benzene conversion over a V-Mg-O catalyst that surface adsorbed oxygen is active in the combustion of hydrocarbon [26]. A similar degradation by gaseous oxygen of the dehydrogenation product of butene has been reported on iron oxide [27].

Table 4.1.6. Dehydrogenation of ethyl benzene over Dy / V system

Catalyst	Conversion	Selectivity (%)			
		Styrene	Toluene	Benzene	C-oxides
D3	6.5	85.0	5.0	4.0	6.0
D7	5.5	90.9	4.5	2.7	1.9
D11	5.7	91.2	4.3	2.2	2.1
D15	6.8	91.7	2.2	2.6	3.3

Reaction conditions: Reaction temperature: 475 °C; Feed rate: 6 ml/h; Catalyst: 2 g; Time on stream: 1 h.

The comparatively low activity observed for vanadia based systems for the oxidative dehydrogenation can be explained by the structure of vanadia species in the system. The activity depends on the availability of the active sites. Since the lattice oxygen is taking part in dehydrogenation, the reactivity and selectivity towards ODH product is decided by the AOS (average number of oxygen molecules that react with each hydrocarbon). The number of vanadia species, which constitutes the surface active sites that can effectively interact with adsorbed alkyl species determines the availability of AOS. Orthovanadates and surface vanadia species constitute the active phase, where the VO₄ units are isolated from each other. So hydrocarbon interacts with a limited number of VO₄ units leading to low conversion with high selectivity [17].

Effect of reaction temperature, contact time and time on stream for the reaction were studied over the supported vanadia systems. Since all the three series exhibited more or less the same behaviour, S7 is taken as a representative of the supported systems.

4.1.3 Effect of reaction temperature

ODH of Ethyl benzene was performed at different temperatures (475, 500 and 525°C) to understand the effect of reaction temperature on the system. Activity and selectivity of the system at different temperatures are given in Table 4.1.7. The conversion was increased with temperature, while the selectivity exhibited no considerable variation, as depicted in Fig. 4.1.3. Among various catalysts employed for ODH of ethyl benzene, $Mg_3V_2O_8$ exhibited a similar behaviour [4]. Styrene selectivity was constant independent of reaction temperature and ethyl benzene conversion. This is a unique property of magnesium orthovanadate. Other magnesium vanadates do not exhibit such an activity.

Table 4.1. 7. Influence of reaction temperature on conversion and selectivity

Temperature (°C)	Conversion (%)	Selectivity (%)			
		Styrene	Toluene	Benzene	C-oxides
475	13.1	84.6	2.7	3.0	9.7
500	18.0	85.0	2.0	3.0	10.0
525	24.0	83.3	1.2	3.5	12.0

Reaction conditions: Catalyst : 2 g; Flow rate : 6 ml/h; TOS : 1h.; Air flow rate : 20 ml/min.

4.1.4 Effect of flow rate

The reaction was performed under different flow rates, 2, 6 and 8 ml / h. Higher feed rate decreases the contact time of the reactants with the catalyst surface. The results are shown in Figure 4.1.4. It is plain that a small feed rate will increase the residence time of the reactant on the catalyst surface. The higher the residence time, higher is the probability of reactive adsorption leading to higher conversion. So the increase of activity is expected. The possibility of product readsorption and the

production of more oxygenated products is probable at low flow rates, which leads to less selectivity. This is of prime importance while explaining the lower selectivity of styrene at low flow rates, because the mobile lattice oxygen produces more carbon oxides at higher contact times.

4.1.5 Deactivation study

Time on stream studies conducted on S7 revealed that these systems showed little change in activity and selectivity Fig.4.1.5. The conversion was more or less the same, although a slight deactivation was observed after 6 hours. Hence the stability of the catalyst system upon reduction was elucidated. Selectivity also remained a constant. The catalyst turned dark grey after continuous use, probably due to carbon deposits and reduction of the catalyst. The original colour could be regained by treating the catalyst in flowing air at 400°C for 2 h.

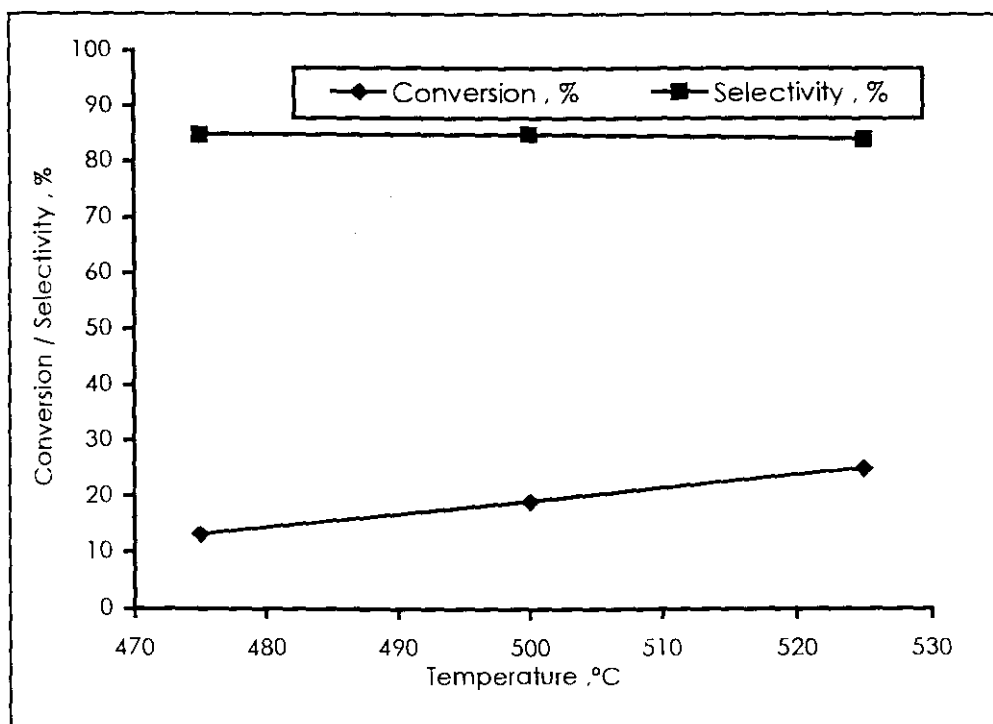


Fig. 4.1.3 Effect of temperature on ethyl benzene conversion and styrene selectivity

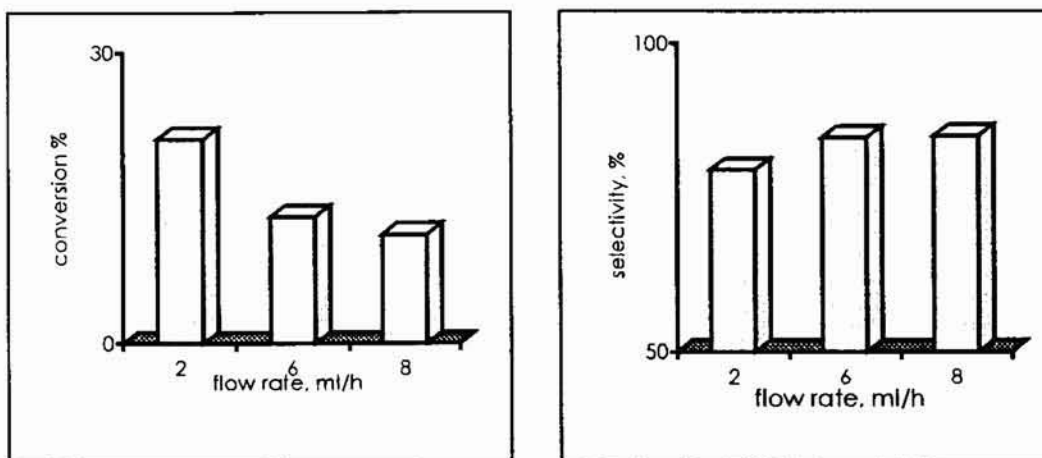


Fig. 4.1.4 Effect of feed rate on conversion of ethyl benzene and selectivity of styrene

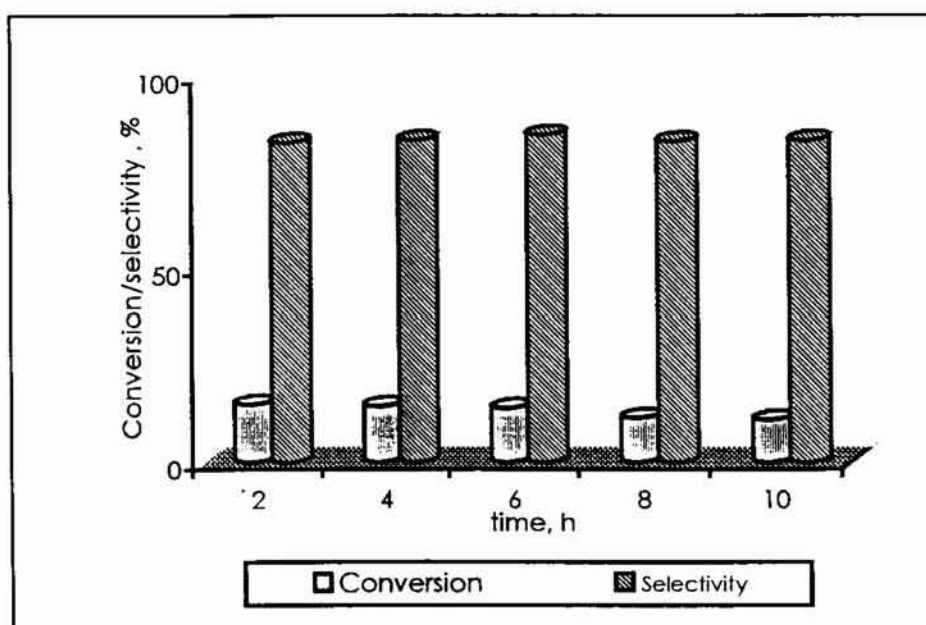


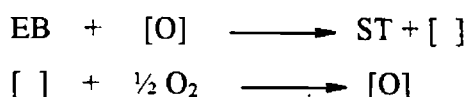
Fig. 4.1.5. Deactivation studies of ODH of ethyl benzene on S7

Mechanism

The fact that the catalytic activity and percentage conversion were significantly reduced when the experiment was conducted in absence of air, pointed out to the role of gaseous oxygen in the reaction. In ODH of ethyl benzene, one of

the most probable mechanism consists of the abstraction of H from ethyl benzene by the lattice oxygen to form styrene and the reoxidation of the catalyst by gas phase oxygen [28]. This mechanism is known as Mars and van Krevelen mechanism. On rare earth supported systems, oxidative dehydrogenation is supposed to occur through the above mechanism, where reoxidation of the reduced vanadia based catalyst comprise chemisorption of an oxygen molecule from gas phase. In non-oxidative dehydrogenation, the absence of gaseous O₂ may be reducing the activity. This type of mechanism is shown by Tagawa *et al.* on Si-Al system [3].

This can be represented as,



where [O] is the lattice oxygen and [] is the vacancy site in the lattice.

In the ODH of ethyl benzene, the activation of a C-H bond should be considered first, which is often regarded as the rate determining step [3]. The dissociative adsorption is not taking place on the catalyst surface. In the activation of hydrocarbons containing π electrons, abstraction of H atom on an oxide centre is facilitated by the donation of π electrons to a Lewis site, which leads to the weakening of the C-H bond (allylic type oxidation). The oxygen in the catalyst abstracts the H in ethyl benzene. Hydrocarbon activation centre is then considered to be a couple of $\text{M}^{n+} - \text{O}$ which is regarded as an acid base pair. In the stationary state of all oxidation products, catalysts contain both oxidised and reduced vanadium ions, the ratio depending on the reaction conditions and the nature of hydrocarbon being oxidised. Reduced vanadium ions chemisorb gaseous oxygen reversibly and are converted to lattice O²⁻. Stoichiometric vanadium never chemisorb oxygen. Dissociation of molecular oxygen with electron transfer according to overall reaction is shown below [29, 30].



The electrons will be supplied by the reduced vanadium ions (V^{5+} or V^{4+}) in the lattice. The oxygen supplying entity in the case of ODH reaction of ethyl benzene is a matter of dispute even now. The role of $V=O$ of the terminal group in hydrogen abstraction was suggested. But studies on molybdina supported vanadia revealed that such an active species is not necessary to create the active site [1]. It was shown by quantum chemical calculations that stronger OH bonds are formed for bridging oxygen. The oxygen of $M-O-V$ bond was proposed as the 'H' abstracting unit, since it was found to form strong H bonding by abstracting 'H' from the hydrocarbon [1]. In some other cases, the Bronsted acid sites were also suggested to be the active 'H' abstracting site [1]. But according to the reports, higher nucleophilic character of bridging oxygen leads to selectivity in orthovanadate systems. Thus a tentative suggestion can be given that the bridging oxygen may be active species that abstract the hydrogen from ethyl benzene. But the probability of Bronsted sites as the active site cannot be ruled out here since it was observed that vanadia addition enhances Bronsted acidity from TPD studies by ammonia.

Oxidation reactions on vanadia based systems follow the process mechanism involving parallel and consecutive reactions. The oxygenated products are formed in a series of successive steps (with or without the desorption of intermediate products to gas phase.) Carbon oxides are formed both in parallel route directly from a substrate and through consecutive route by the oxidation of final oxygenated products.

The role of vanadia species in creating active sites for selective oxidation clearly explains the improved conversion as the addition of V_2O_5 is increased for Sm/V and Dy/V series. Styrene selectivity was almost independent of conversion indicating that acid base property has no significant influence and the redox property governs the activity and selectivity. So the activity increase is entirely attributed to increase in percentage of vanadia in tetrahedral coordination. In the case of Sm/V and Dy/V systems this is true. But in La/V series activity for ODH was not proportional to vanadia content pointing to the fact that some other factor decides the

activity. Effect of vanadia loading on the activity in terms of conversion for the three systems is revealed in Fig 4.1.6.

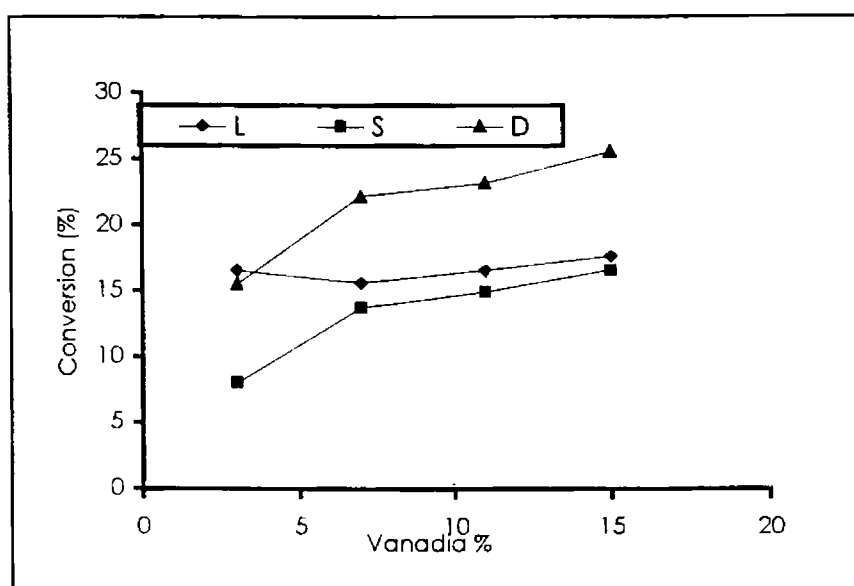


Fig. 4.1.6 Effect of V_2O_5 % on activity

The activity of La/V systems first decreases and then increases at higher vanadia percentages; the order being $L3 > L7 < L11 < L15$. So the deciding factor for activity may not be the vanadate units exclusively. Acid base properties also may be involved [10,11]. The role of basic surface OH groups and Lewis acid sites are also suggested as sources of activity for some systems [3]. But such active acid and base sites were found to be absent in the rare earth supported vanadia systems. However, a tentative mechanism according to the above reference can be cited. The various steps are 1) coordination of ethyl benzene to the Lewis acid sites of the support, enhancing the acidic nature of alpha hydrogen. 2) basic group adjacent to the acid group abstract α H from the ethyl benzene to give a relatively stable adsorbed species. 3) elimination of water after the abstraction of α H creating anion vacancy. 4) reversibly adsorbed surface oxygen is converted to O^- species. 5) the abstraction of β H of ethyl benzene by this oxygen to regenerate the catalyst. The reaction pathway according to the above reference is shown in figure (Fig.4.1.7).

This mechanism suits well with the data on acidity and basicity measurements. The temperature programmed desorption studies using ammonia revealed that after 7 wt % vanadia, there was an increase of Lewis sites, which was peculiar for the La/V catalysts. Again, from the adsorption studies using electron acceptors and indicator method, basic OH groups are increasing for 11 and 15 wt % vanadia. The basic OH may be either from La or V. Taking these two aspects into consideration, the trend in activity exhibited by La / V catalysts can be justified. But the type of active sites observed on Si-Al system is not seen in La / V systems. Participation of acid base properties for the reaction is obvious from the results. But this type of influence is not prominent in Sm/V and Dy/V systems, where the redox property of the Ln-O-V bond decides the activity.

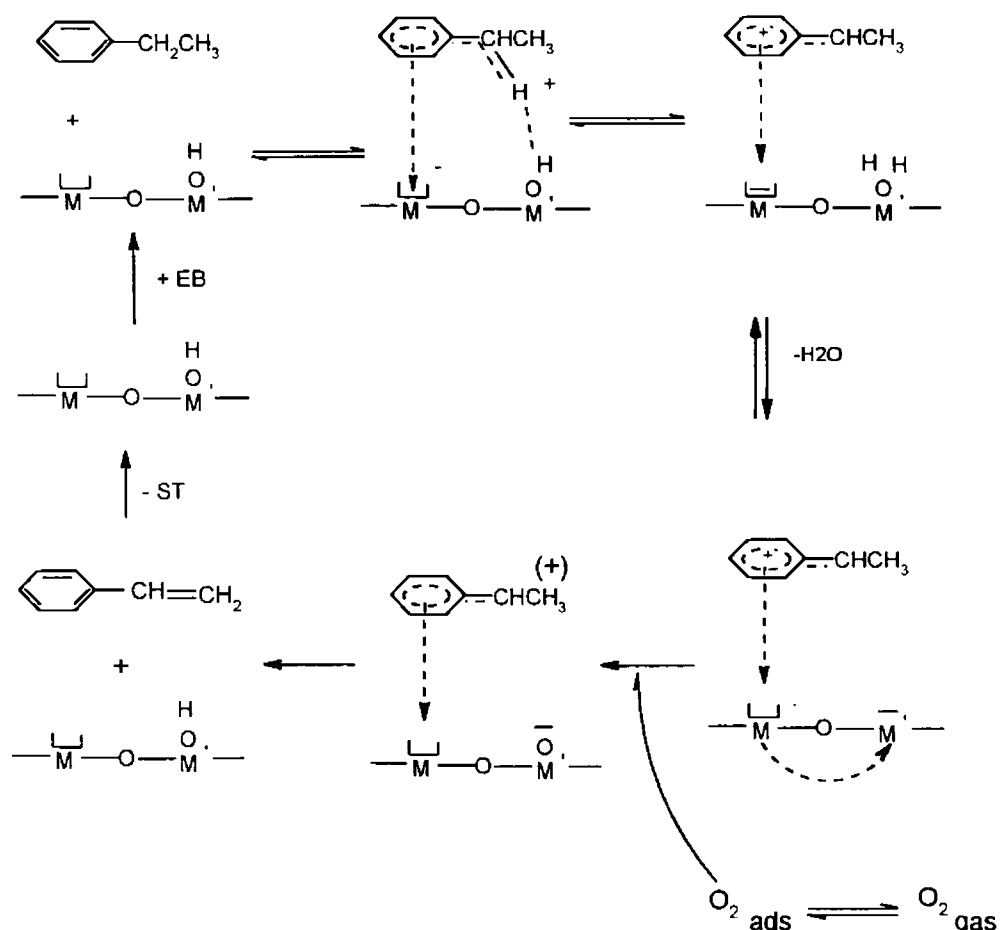


Fig. 4.1.7. Reaction mechanism for ODH of ethyl benzene

4. 2 Oxidative dehydrogenation of ethanol

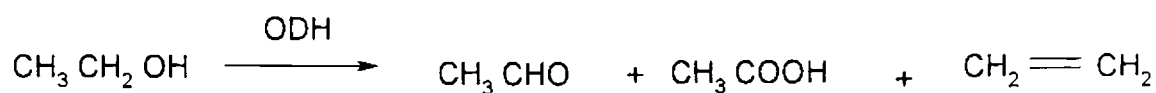
Introduction

Decomposition of ethanol is an important reaction in connection with the utilization of biomass as a chemical source. The reaction was performed in a vapour phase down flow silica reactor. An infusion pump on the top of the reactor introduced ethanol. The products were collected and analysed by gas chromatograph using a Porapak N column fitted with TCD.

Table 4.2.1. Data of ethanol decomposition on La₂O₃/V₂O₅ system

Catalyst	Conversion (%)	Selectivity (%)			
		CH ₃ CHO	CH ₃ COOH	Ethylene	C-oxides
La ₂ O ₃	80.0	14.5	-	60.0	25.5
L3	77.9	28.0	12.8	49.2	10.0
L7	80.2	34.4	14.3	41.0	10.1
L11	81.4	41.5	16.4	32.0	9.5
L15	90.1	45.6	15.6	31.8	7.0
V ₂ O ₅	95.0	5.0	-	2.0	93.0

Reaction conditions: Reaction temperature: 300°C; Flow rate: 8 ml/h; air flow rate: 30 ml/min; TOS: 1h; Catalyst : 2.5 g



4.2.1 *Effect of vanadia*

Oxidative dehydrogenation of ethanol yield acetaldehyde and ethylene as the major products (Table 4.2.1). Further oxidation of acetaldehyde formed acetic acid on the rare earth oxide. Complete oxidation of the organics gave carbon oxides. Pure vanadia gave more than 80 % carbon oxides. Acetaldehyde selectivity was about 5 %. This is not surprising while we consider the higher mobility of oxygen in vanadia system [6]. Oxygen from other layers of the lattice also migrates to the reaction site. Hence the activity is very high. The consecutive oxidation leads to almost complete oxidation of ethanol on the active sites. Lanthanide oxide also catalysed complete oxidation due to mobility of oxygen in the lattice along with dehydration [9]. Supported oxides exhibited high selectivity indicating the participation of vanadia in the active species. Partial oxidation activity in terms of the total amount of acetaldehyde and acetic acid formation increased with vanadia content.

While comparing the ODH activity of the system for ethyl benzene and ethanol it is noticed that the activity is comparatively high in the case of ethanol. Though the activity was less, the selectivity of partial oxidation products was high for ethyl benzene oxidation. It was reported that alcohols get dissociatively adsorbed on vanadia catalysts as alkoxy groups [21]. These alkoxy groups can undergo various reaction pathways to yield different products. The types of reaction pathways adopted depend on the nature of active sites present on the catalyst surface (redox and acid base sites). Redox sites favour selective oxidation of alcohol while acid/base sites catalyse dehydration. Strong basic sites interact with the reactants so as to produce C-oxides ultimately. Comparison of the activity and selectivity of La_2O_3 and supported analogues shows that the amount of partial oxidation products (acetaldehyde and acetic acid) increases as the vanadium oxide is deposited on La_2O_3 . It is clear from the results that the selectivity of partial oxidation products doesn't follow any particular trend with acid base properties. So it is confirmed that redox properties are predominating in determining the selectivity. The formation of higher

amount of partial oxidation products on the catalysts indicates that surface vanadia forms redox sites.

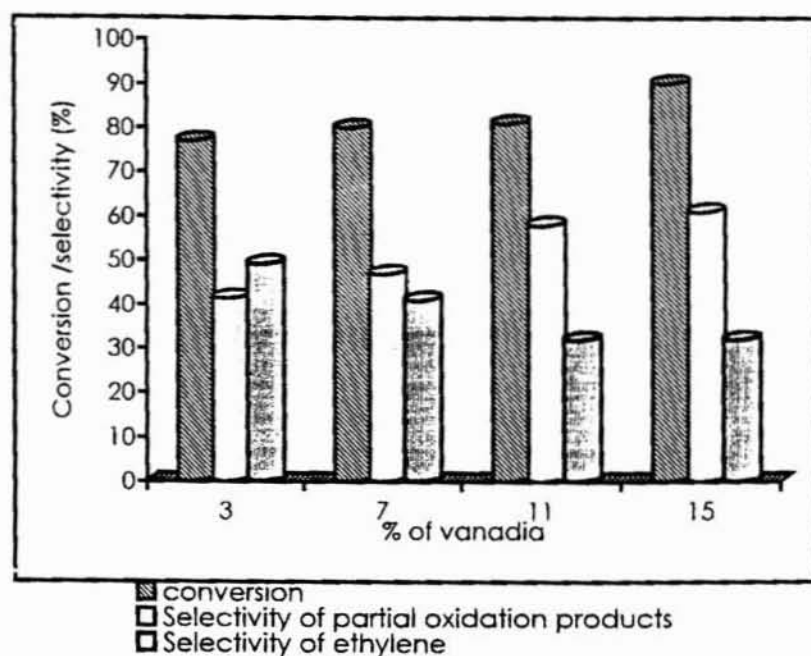


Fig. 4.2.1. Activity and selectivity of La/V system for the oxidative dehydrogenation of ethanol.

Table 4.2.2. Ethanol decomposition data on La / V catalysts.

Catalyst	Conversion (%)	Selectivity (%)			
		CH ₃ CHO	CH ₃ COOH	Ethylene	C-Oxides
L15	90.1	45.6	15.6	31.8	7.0
S15	80.1	40.3	16.6	38.4	4.7
D15	78.2	38.6	15.8	39.6	6.0

Reaction conditions: Reaction temperature: 300°C; Flow rate : 8 ml/h; air flow rate : 30 ml/min; TOS 1h.; Catalyst: 2.5 g

Three types of sites on the surface were proposed to be active in the case of supported systems for the ODH of ethanol [31]. i.e., M-O -V, V-O-V and V=O bonds, where 'M' is the metal ion in the support. The V-O-V bridges are found to be active in certain catalysts [32]. But the characterisation techniques have revealed that there are no such bonds in rare earth oxide supported vanadia, since crystalline vanadia is absent in the supported catalysts. Only terminal V=O and M-O-V bonds are present, which originate either from the surface vanadia or from lanthanide orthovanadate. Hence only the other two factors are important.

The knowledge of V-O-M bond strength and hence the number of active sites is one of the fundamental criteria that determines the oxidation activity of supported metal oxides. According to Deo *et al.*, the activity of the catalyst is related to the number of participating surface vanadia groups and depends on the reducibility of M-O-V bond (M is the metal ion in the support), where bridging oxygen controls the activity [21]. The reducibility of the metal ion in the V-O-M bond becomes the deciding factor. Accordingly, if the metal ion is more reducible, the activity of oxygen for hydrogen abstraction will be high, which leads to high conversion. In the present case, Dy ion is more reducible and is expected to show maximum activity while La/V, which is least reducible should exhibit low activity. The data on catalytic activity shown in Table 4.2.2. is contradictory. Activity (in terms of conversion) is high for the La/V system. So the possibility of V-O-S bond as the active site is ruled out.

The participation of V=O in determining the activity of ODH of ethanol has been emphasised by several authors [33,34]. This is in accordance with the result of methanol oxidation reported by Trifiro *et al.* [35]. According to them, the activity is directly connected to M=O terminal bonds, which opens with the addition of a hydrogen atom from alcohol which in turn leaves a free valence for the metal used for bonding with the dehydrogenated molecule (oxy reduction mechanism). Hence the active sites are concluded to be V=O species in the catalyst. This may be

originating from both surface species and orthovanadates. Studies on ethanol oxidation in which amorphous vanadia i.e., the extra lattice vanadia, act as the active sites are reported in literature [33]. V=O in orthovanadates may also be participating in catalysing the oxidative dehydrogenation. This is supported by the views of Ramis *et al.* that magnesium orthovanadates are active and selective for the decomposition of alcohols that get adsorbed in a dissociative manner [36]. Extension of this observation can be applied to rare earth supported systems also, where orthovanadates occur as isolated tetrahedra similar to magnesium orthovanadates. Here a striking similarity is noticed between magnesium orthovanadate and LnVO_4 that they are more active in ethanol ODH when compared to alkanes. Active two dimensional vanadates for ethanol oxidative dehydrogenation are reported by Nakagawa *et al.* [34]. It was presumed that oxygen in the V=O act as strong basic sites which abstract hydrogen from alcohols. The selectivity towards partial oxidation products can be explained on the basis of basicity of the supported vanadia systems. Basic catalyst could activate oxygen but it may not be sufficient to activate a basic product like acetaldehyde or ethylene that is essential for total oxidation activity. So the complete oxidation activity is found to be low for the supported analogues.

It was found that as vanadium content is increased ethylene selectivity also exhibited a corresponding reduction. Pure La_2O_3 was found to be very active for dehydration. This may be due to decrease of Lewis acid sites on the surface. It is accepted that Lewis acid sites on the supports play an important role in the dehydration of ethanol on supported catalysts [32]. As vanadia was deposited the number of active sites was diminished. It is not surprising since surface vanadium oxide is known to titrate surface lewis acid sites as evident from acid base properties studies. Vanadia species was getting anchored through the Lewis acid sites on the surface. This was confirmed earlier by the ammonia desorption studies. Through TPD studies it was observed that Lewis acidity is decreasing as the vanadia concentration in the catalyst increased. Involvement of acid base properties apart from the redox properties was evident from these results. In this context, it is relevant

to consider the selectivity of the supported system towards dehydration in cyclohexanol decomposition. Decomposition of cyclohexanol carried out on the supported vanadia yielded a higher percentage of cyclohexene as vanadia content was increased indicating that dehydration was prominent. This is because, cyclohexanol dehydration is known to take place on weakly acidic sites [37]. The generation of weak acid sites (Bronsted) by vanadia addition explains the higher selectivity of cyclohexene formation. But dehydration of ethanol was not so prominent because ethylene formation needs much stronger sites. It is also confirmed that vanadia incorporation reduces the number of strong acid sites.

4.2.2 Effect of support

Oxidative dehydrogenation of ethanol was carried out using different supported systems to study the effect of support on the activity of the active species. In the case of methanol oxidation, it was observed that the reactivity depends on the nature of the oxide support [21]. Comparison of the three supported vanadia analogues shows that La/V catalyst is more active and selective among the three systems under study (Table 4.2.2.). The higher activity of La/V is explained on the basis of strength of terminal V=O species.

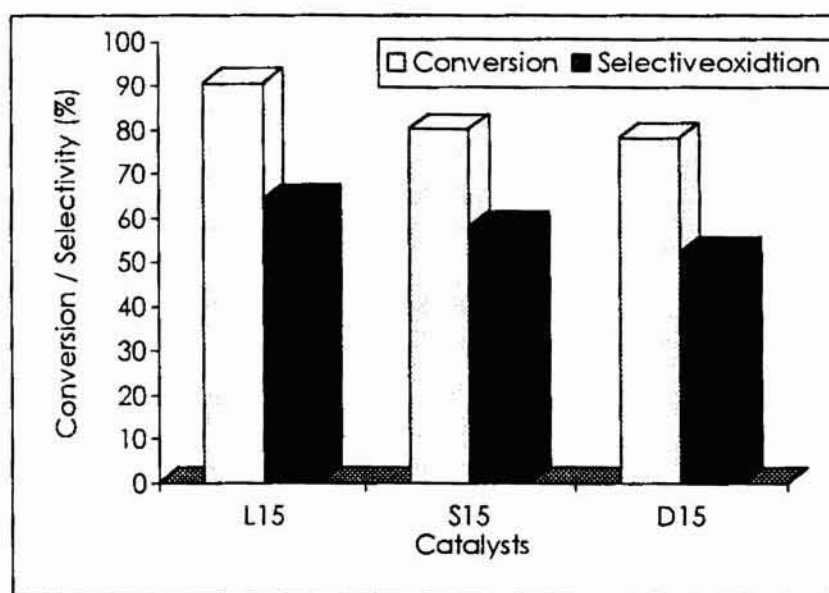


Fig. 4.2.2 Activity and selectivity of different supported systems

The strength of V=O bond was related with the position of Raman band in the case of alcohol decomposition by Deo *et al.* on various supported vanadia systems [21]. In the present study, IR band position was correlated to the V=O strength. The position of IR band of terminal V=O bond was directly related to the V=O bond strength and a stronger V=O bond gave a higher IR band position. As explained in the previous chapter, among the three supported systems, La/V showed lowest terminal V=O bond strength (both for surface species and orthovanadates) indicating weak terminal bonds while comparing among the systems. The V=O band position was related to the electronegativity of the metal ion in the oxide support. La being less electronegative, showed lowest value for V=O frequency in the IR spectrum. So the oxygen in V=O will be more basic to enable the easy abstraction of hydrogen from alcohol species. This results in higher activity towards ethanol ODH (Fig. 4.2.2.).

Mechanism

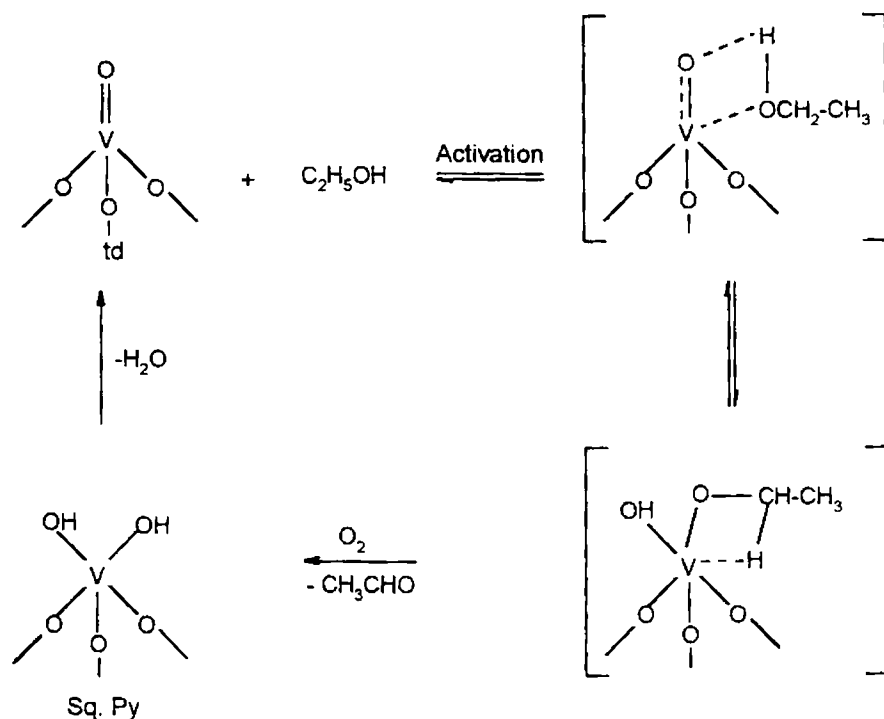


Fig. 4.2.3 Reaction mechanism for selective oxidation of ethanol over supported vanadia system.

The selective oxidation of ethanol over supported metal oxides was studied extensively and a general pathway for the reaction was established. Different steps in the reaction are a) adsorption and activation of ethanol on active metal site b) decomposition and desorption of the ethoxide species and c) reoxidation of the catalyst [32,33]. Following this route, Kannan *et al.* suggested a mechanism for the reaction on vanadia species [Fig. 4.2.3]. A dissociative adsorption of ethanol was proposed and the V=O groups are found to be responsible for the aldehyde formation [33]. As per this mechanism, the selectivity depends on the V=O bond strength.

4.3 Methylation of Phenol

Introduction

Influence of vanadia addition on the acid base property of the supported system is well established through different analytical procedures in the previous chapter. These catalysts should be screened for various acid and base catalysed reactions. Vapour phase methylation of phenol was selected as the test reaction. Reaction of methanol with phenol is an acid base reaction, catalysed by both acid and basic sites. Both O- and C- alkylated products are derived from the reaction, which include anisole, methyl anisole, o-cresol, different isomers of xylenol, trimethyl phenols etc.

Alkyl phenols are industrially important intermediates in the manufacture of plastics, pesticides, pharmaceuticals etc [38,39]. Most important ones among this category are o-cresol and 2,6-xylenol. They are used widely in the production of resins, insecticides and antioxidants. Ortho cresol is used in the manufacture of epoxy cresol novolak resins. 2,6-xylenol is a monomer of a good heat resisting poly-(2,6-dimethyl) phenylene oxide resin, which is a component in the alloys used in electronic industry [40].

The reaction was carried out in vapour phase with 3 g catalysts in a silica reactor. Prior to reaction, the catalysts were activated at 500 °C for 2 h in flowing air. The products were analysed by a GC 15 A gas chromatograph fitted with FID and a FAP – S- 10 % on 60/80 Chromosorb W (AW) column. Phenol conversion and selectivities are expressed in wt %. The selectivity of products are obtained in the following manner.

$$\text{Selectivity(\%)} = \frac{\text{Yield}}{\text{Total conversion of phenol}} \times 100$$

Both O- and C- alkylated products are obtained for the catalyst systems. Anisole, ortho cresol, 2,6-xyleneol and trimethyl phenol (TMP) were the main products. Traces of methyl anisole were also detected in some systems. The reaction can be expressed as shown in Figure 4.3.1.

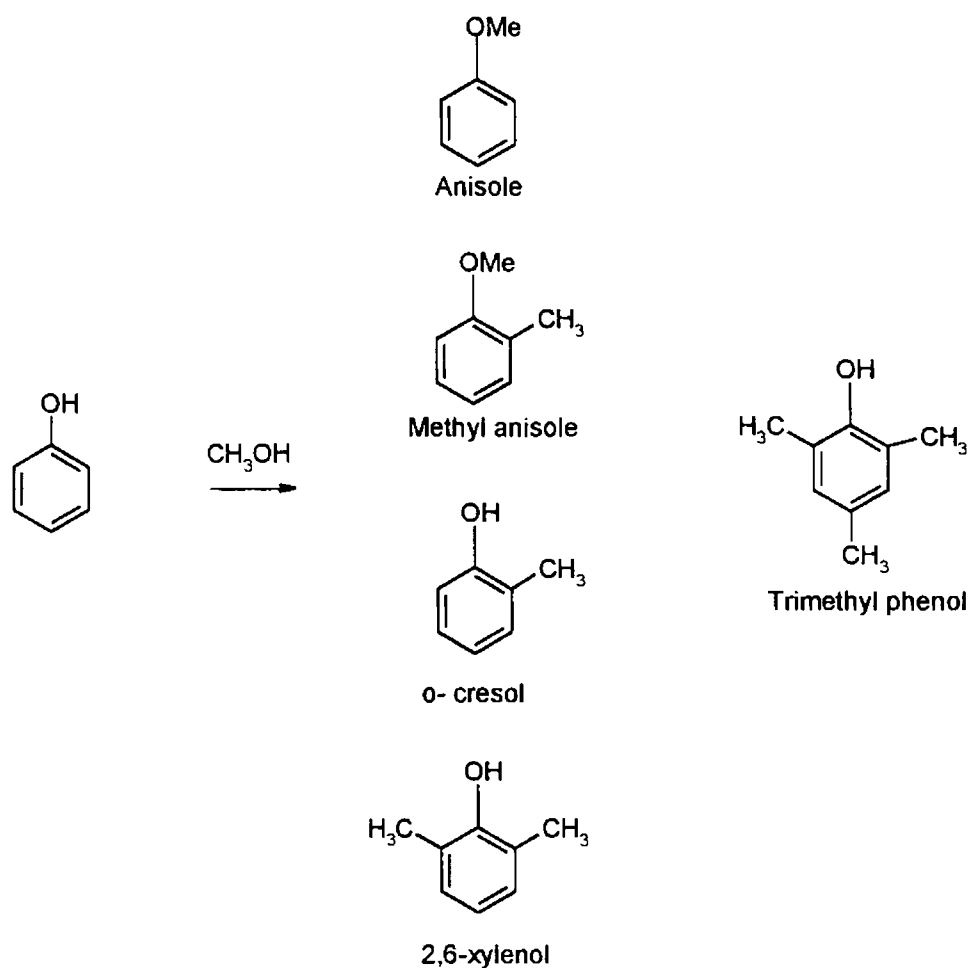


Fig. 4. 3. 1 Products of methylation of phenol.

The catalytic activity and selectivity of the supported systems towards methylation of phenol is given in Tables 4.3.1 to 4.3.3.

Table 4.3. 1 Conversion and selectivity of products in the methylation of phenol on Dy/V system

Catalyst	Conversion (%)	Selectivity (%)				
		Anisole	Me anisole	o-cresol	2,6-xylenol	TMP
D3	29.5	4.1	-	72.1	21.2	2.6
D7	47.1	2.1	-	55.3	35.1	7.5
D11	68.1	2.6	-	42.6	36.5	8.3
D15	73.5	5.1	13.3	25.5	44.9	11.1

Reaction conditions : Reaction temperature : 350 °C; Phenol : methanol ratio : 1 : 7;
Flow rate : 4 ml/h; TOS : 1.5 h.

Table 4. 3. 2. Conversion and selectivity of products in the methylation of phenol on Sm/V system

Catalyst	Conversion (%)	Selectivity (%)				
		Anisole	Me anisole	o-cresol	2,6-xylenol	TMP
S	20.0	5.6	3.2	68.4	20.9	1.9
S3	21.8	3.5	-	65.7	26.9	3.9
S7	43.3	3.2	-	47.9	37.6	11.5
S11	74.5	5.5	10.6	31.4	23.5	28.8
S15	78.3	4.4	9.3	22.3	26.1	37.9

Reaction conditions : Reaction temperature : 350 °C; Phenol : methanol ratio : 1 : 7;
Flow rate : 4 ml/h; TOS : 1.5 h.

Table 4.3.3 Conversion and selectivity of products in the methylation of phenol on La/V

system		Selectivity (%)				
Catalyst	Conversion (%)	Anisole	Me anisole	o-cresol	2,6-xyleneol	TMP
L3	13.7	26.7	-	69.3	4.0	-
L7	26.3	29.2	-	57.2	12.1	1.5
L11	23.3	24.8	-	67.1	6.7	1.4
L15	22.4	22.7	-	68.7	7.2	1.4

Reaction conditions: Reaction temperature: 350 °C; Phenol: methanol ratio: 1: 7; Flow rate : 4 ml/h; TOS : 1.5 h.

Major fraction of the products includes ring-alkylated phenols, which indicate catalysis of C- alkylation by rare earth oxide supported vanadia. Ring alkylated products include o-cresol, 2,6-xyleneol and trimethyl phenol (TMP). O-alkylated products include anisole derivatives. C-alkylated product selectivity was more than 70% for all the systems. La / V series showed lowest conversion of phenol among the three supported system. Order of catalytic activity in terms of phenol conversion was Dy / V > Sm / V > La/V. Anisole formation was high for the La/V series of catalysts. Sm/V and Dy/V series exhibited poor selectivity towards O-alkylation. Anisole (O-methylation) first formed undergoes further methylation on Sm/V and Dy/V catalysts. No methyl anisole is detected in the case of vanadia supported on La₂O₃. It was found that as the vanadia percentage increased, concentration of higher alkylated phenol also increased with a corresponding decrease of o-cresol.

4.3.1 Influence of acid base properties on selectivity

In general, basicity was found to have an adverse effect on the catalytic activity towards phenol alkylation. Higher concentration of ring-alkylated products indicates that weak acidic/strong basic sites are present in the supported system. Earlier workers have reported that weak acid/strong basic sites favour C-alkylation.[41,42] In the present case, it was confirmed through adsorption of electron acceptors that supported vanadia system possesses strong basic sites. Moreover, for all the three systems there was an enhancement in weak acidic sites as evident from the ammonia adsorption studies. Enhancement of C-alkylation by weak acidic sites was confirmed through further studies [43,44].

Anisole formation was comparatively higher for La / V systems. Only traces of anisole were observed for S and D series. Anisole formation over systems of L series can be explained by the higher acidity of the samples. This is in accordance with the studies by Benzouhanava *et al.* [42] that strong acidic sites favour O-alkylation. Amount of ammonia desorbed at higher temperature was large for vanadia supported on La₂O₃, indicating the presence of strong acid sites.

Several mechanisms were suggested for the alkylation of phenol [45]. Alkylation over acidic catalysts was supposed to proceed through anisole formation, which rearranges intramolecularly to give o-cresol. Stronger acidic sites favour meta and para cresols. Xylenol formation occurs via consecutive methylation of cresol. Basic and bifunctional catalysts adopt direct ring alkylation route. Ortho product selectivity is found to be high on basic systems by direct ring alkylation. Conversion of phenol decreases with decrease in basicity if the reaction proceeds through the rearrangement of an anisole intermediate. In contrast increase in basicity decreases the activity if direct C-alkylation takes place to give o-cresol selectively. Here it is found that conversion of phenol is increasing with decrease in basicity of the catalyst. Hence direct ring alkylation is expected to take place on the supported system without the formation of anisole intermediate. From the data in Tables 4.3.1 to 4.3.3, it is

clear that ortho cresol selectivity decreases with vanadia addition. 2, 6-Xylenol selectivity first increases followed by a decrease as the vanadia content increased, whereas TMP selectivity goes on increasing. Hence it can be inferred that ortho cresol formed undergoes consecutive methylation to give higher alkylated phenols. So the reaction pathway can be considered as shown in the figure.

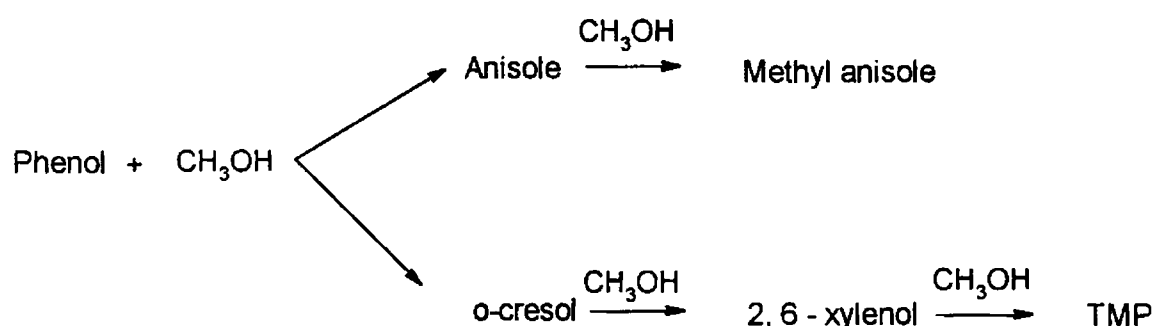


Fig. 4. 3. 2 Reaction pathway of methylation of phenol on rare earth oxide supported vanadia.

4.3.2 Ortho selectivity

Ortho selectivity of the supported systems are shown in Fig. 4. 3. 3. For Sm/V and Dy/V systems, ortho selectivity (o-cresol, 2,6-xylenol and methyl anisole) decreased with vanadia addition. It can be understood in terms of decrease of basicity as confirmed by Hammett indicator and adsorption studies. Selectivity for the formation of ortho products is in the order of basicity. For Sm/V and Dy/V series basicity order was 3 > 7 > 11 > 15 % vanadia. For La/V systems, the order is 3 > 7 < 11 < 15. These orders were maintained in the ortho product selectivity. This agrees well with Tanabe [46] that basic catalysts alkylate selectively at ortho position. Accordingly, the o-selectivity should be proportional to basic strength. This is in agreement with our data (Tables 4.3.1- 4.3.3). However, there are reports that acidic catalysts predominantly alkylate at ortho position [47].

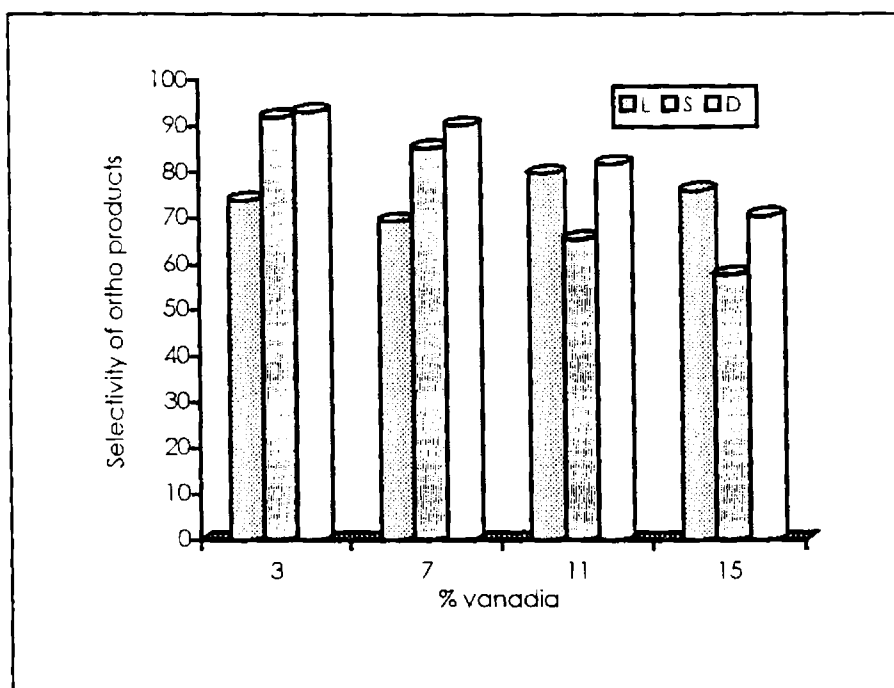


Fig. 4.3.3 Ortho selectivity of different supported vanadia system

According to Tanabe *et al.* [48] Bronsted sites interact with the electron cloud of benzene ring. So ring will be parallel to the surface giving access to positions other than ortho for attack by alkylating group. So strong Bronsted acid sites reduces the ortho product selectivity. The interaction can be shown as follows.

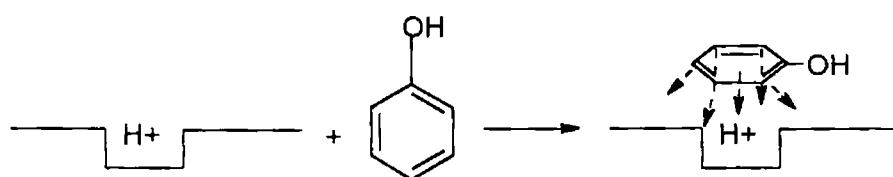


Fig. 4.3.4 Interaction of phenol with Bronsted sites

It was found that ortho selectivity is decreasing by vanadia addition, which is achieved through adsorption of phenol on Lewis acid sites as reported by Klemm *et al.* (shown in Fig. 4.3.5) [49]. Such an orientation prevents the interaction of the catalyst with the π electron cloud of the benzene ring. Phenol interacts with Lewis

acid base centers giving phenolate ion (on Lewis acid site) and H^+ (on basic site). This proton induces formation of carbonium ion from methanol, which interact with the adsorbed phenolate ion at ortho positions

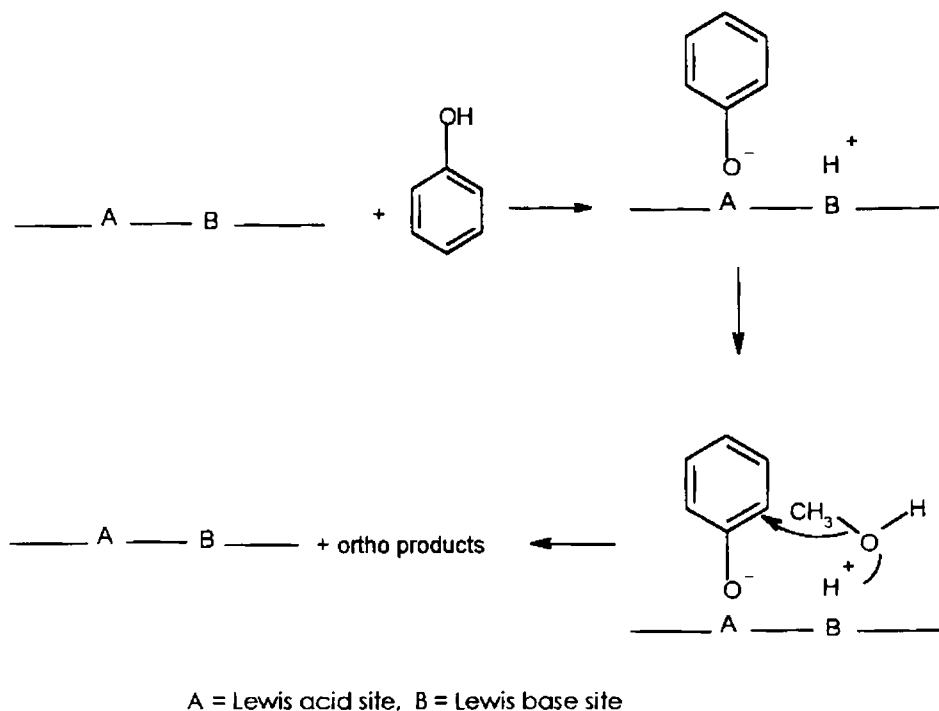


Fig. 4. 3. 5 Adsorption of phenol on Lewis site

Lewis acid base sites are necessary for adsorption of phenol to yield ortho methylated products. It was confirmed through acid base studies that both Lewis acidity and Lewis basicity are decreasing with increase of vanadia loading since vanadia species get adsorbed by the titration of basic OH groups and Lewis acid sites on the surface of the support. From the TPD of ammonia, it is confirmed that Bronsted acid sites are increasing with a concomitant decrease of Lewis sites. The ortho selectivity at low vanadia loadings can be understood from these observations. At higher vanadia loadings, Bronsted acid sites increase yielding higher methylated phenols. For La/V systems, number of strong Bronsted sites is decreasing and Lewis acidity is increasing at higher vanadia percentage, favouring the formation of ortho products for L11 and L15.

As a generalization, Tanabe *et al.* proposed a model for adsorption of phenolate ion on acidic and basic systems. The selectivity of the products during alkylation can be explained by the adsorption mode of phenolate ion on the surface of the catalyst. IR study of phenol adsorbed on Si-Al and MgO revealed that o-selectivity is strongly controlled by the adsorbed states of phenol [50]. The different modes of adsorption of phenolate ion on basic and acidic catalyst are shown in figure 4.3.6.

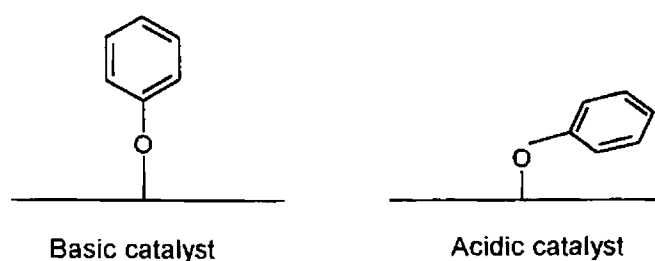


Fig. 4. 3. 6 Different adsorption modes of phenolate ion on basic and acidic catalysts

On basic catalyst, the electron cloud of the benzene ring will be repelled by the catalyst surface, rendering the adsorbed phenolate ion in an almost vertical position. So the ortho position will be easily susceptible for attack by an adsorbed methyl group. This type of repulsion will be comparatively low in case of an acidic catalyst. So the alkyl group will have access to other positions as well, yielding higher alkyl phenols.

References

1. B. Grzybowska-Swierkosz, *Appl. Catal. A: Gen.*, 157 (1997) 409.
2. T. Tagawa, T. Hattori and Y. Murakami, *J. Catal.*, 75 (1982) 56.
3. T. Tagawa, T. Hattori and Y. Murakami, *J. Catal.*, 75 (1982) 66.
4. W. S. Chang, Y. Z. Chen and B. L. Yang, *Appl. Catal. A: Gen.*, 124 (1995) 221.
5. Y. Murakami, K. Iwayama, H. Uchida, T. Hattori and T. Tagawa, *J. Catal.*, 71 (1981) 257.
6. C. Doornkamp, M. Clement, X. Gao, G. Deo, I. E. Wachs and V. Ponc, *J. Catal.*, 185 (1999) 415.
7. W. M. H. Sachtler and N. H. De Boer, "Proceedings 3rd International Congress on Catalysis, Amsterdam, 1964" p. 240, Wiley, New York, 1965.
8. W. M. H. Sachtler, G. J. H. Dorgelo, J. Fahrenfort and R. J. H. Voorhoev, "Proceedings 4th International Congress on Catalysis, Moscow, 1968" (B. A. Kazanski, Ed.) p. 454, Adler, New York, 1968.
9. M. P. Rosynek, *Catal. Rev. – Sci. Eng.* 16 (1) (1977) 111.
10. T. Blasco, J. M. Lopez Nieto, *Appl. Catal. A: Gen.*, 157 (1997) 117.
11. E. A. Mamedov and V. Cortes - Corberan, *Appl. Catal. A: Gen.*, 127 (1995) 1.
12. N. Das, H. Eckert, H. Hu, I. E. Wachs, J. Walcer and F. Fehre, *J. Phys. Chem.*, 97 (1993) 8240 .
13. H. Eckert and I. W. Wachs, *J. Phys. Chem.*, 93 (1989) 6796
14. Xingtao Gao, J. L.G. Fierro and I. E. wachs, *Langmuir*, 1999, 15, 3169.
15. A. Corma, J. Lopez Nieto, N. Paredes, M. Perez, Y. Shen, H. Cao, S. L. Suib, *Stud. Surf. Sci. Catal.*, 72 (1992) 213.
16. D. Patel, P. J. Andersen and H. H. Kung, *J. Catal.*, 125 (1990) 132.
17. H. H. Kung and M. C. Kung, *Appl. Catal. A:Gen.*, 157 (1997) 105.
18. J. G. Eon, R. Olier and J. C. Volta, *J. Catal.*, 145 (1994) 318.

19. T. Blasco, A. Galli and J. M. Lopez Nieto and F. Trifiro, *J. Catal.*, 169 (1997) 203.
20. A. Bielanski, J. Haber, *Oxygen in Catalysis*, Marcel Dekker, New York, NY, 1991, and the references therein.
21. G. Deo and I. E. wachs, *J. Catal.*, 146 (1994) 323.
22. O. S. Owen and H. H. Kung, *J. Mol. Catal.*, 79 (1993) 265.
23. O. S. Owen, H. H. Kung and M. C. Kung, *Catal. Lett.*, 12 (1992) 45.
24. I. Wang, W. S. Chang, R. J. sheiu, J. C. Wu and C. S. Chang, *J. Catal.*, 83 (1983) 438.
25. A. Krause, *Sci. Pharm.*, 38 (1970) 266.
26. G. V. Shaknovich, I. P. Belomestnykh, N. V. Nekrasov, M. M. Kostyukovsky and S. L. Kiperman, *Appl. Catal.*, 12 (1984) 23.
27. B. L. Yang and H. H. Kung, *J. Catal.*, 77 (1982) 410
28. J. Hanuza and B. Jezowska-Trzebiatowska, *J. Mol. Catal.*, 4 (1978) 271.
29. J. H. Lunsford, *Catal. Rev.*, 8 (1973) 135.
30. A. Bielansky, J. Haber, *Catal. Rev.*, 19 (1979) 1.
31. G. Deo, I. E. Wachs, *J. Catal.*, 129 (1991) 307.
32. K. Imumaru, M. Misonova and T. Okuhara, *Appl. Catal. A: Gen.*, 149 (1997) 133.
33. S. Kannan, T. Sen, S. Sivasankar, *J. Catal.*, 170 (1997) 304 .
34. Y. Nakagawa, T. Ono, H. Miyata and Y. Kubokawa, *J. Chem. Soc. Faraday Trans.*, 1, 79 (1983) 2929.
35. F. Trifiro, I. Pasquon, *J. Catal.*, 12 (1968) 412].
36. G. Ramis, G. Busca and V. Lorenzelli, *J. Chem. Soc. Faraday Trans.*, 90 (9) (1994) 1293

37. C. P. Bezouhanava, M. A. Al-Zihari, *Catal. Lett.*, 11 (1991) 245.
38. H. Fiege, in B. Elvers, S. Hawkins and G. Schultz (Editors), *Ullmann's Encyclopedia of Industrial Chemistry*, 5th ed., VCH Verlag, 1991, Vol. A19, p.313.
39. S. Narayanan, *Res. Ind.*, 34 (1989) 296.
40. R. Dowbenko, in J. I. Kroschwitz and Mary Houl-Grant (Editors), *Kirk Othmer Encyclopedia of Chemical Technology*, 4th ed., Vol. 2, 1992, p.106.
41. V.V. Rao, K.V.R.Chari, V. DurgaKumari and S.Narayanan, *Appl.Catal.*,6 (1990) 89.
42. C. Benzouhanava and M.A. Al-Zihari, *Appl.Catal.*,8 (1992) 45 .
43. M. Marczewski, J.P. Bodibo, G.Perof and M.Guisnel, *J. Mol.Catal.*,50 (1989) 211
44. R.T. Tliemat-Manzalji, D.B.Bianchi and G.M. Pajonk, *Appl. Catal* 101(1993) 339
45. E. Santhaceasia, D. Galosa and S. Carra, *Appl. Catal.*, 64 (1990) 83.
46. K.Tanabe in B.Imelik, C.Naccahe, G.Coudurier, Y.B.Taarit and J.C.Vedrine (Eds), *Catalysis by acids and bases (Stud. Surf. Sci. Catal.,Vol.20)*, Elsevier, Amsterdam,1985 p-1
47. V.V. Rao, V. DurgaKumari and S.Narayanan, *Appl.Catal.*,49 (1989) 165 .
48. K. Tanabe, K. Nishizaki, in F. C. Tompkins (Ed), *Proc. 6th Int. Congress on Catalysis*, The Chemical Society, London (1977).
49. L. H. Klemm, C. E. Klopfenstein and J. Shabtai, *J. Org. Chem.*, 35 (1970) 1069.
50. K. Tanabe & T. Nishizaki, *Proc. 6th Intern. Congr. Catalysis*, 2, (1977) 863.

CHAPTER V

SUMMARY AND CONCLUSIONS

Summary of the work

Incorporation of vanadia on suitable supports generates active and selective oxidation catalysts. The influence of vanadia on the physico chemical and catalytic properties of rare earth oxides are analysed in the present investigation. Different compositions of vanadia supported lanthanide oxides are prepared, characterised and the catalytic activity of the systems towards reactions of industrial importance is studied.

Supported vanadia catalysts were found to be effective catalysts for a variety of oxidation reactions from literature. A general introduction on the supported vanadia system including methods of preparation and earlier work in the area are reviewed in Chapter I.

Chapter II gives a brief account of various reagents and materials used for the present study. The techniques employed for the preparation, physico chemical characterisation and catalytic studies of the supported system are described. Different techniques implemented for the characterisation include: a) EDX analysis; b) XRD studies, FTIR spectral studies; c) Surface area and pore volume measurements; d) Thermal studies and e) Acid base property studies.

Physical and chemical characterisation of the prepared rare earth oxide supported vanadia catalysts are presented in Chapter III. From EDX analysis data, the composition of the supported system is obtained. Both amorphous and crystalline vanadate units are detected through XRD patterns and IR spectral studies. The crystalline phase of vanadia is found to be that of orthovanadates. Amorphous vanadia exists as isolated tetrahedra. It was found that vanadia addition generally reduces macropores in the support. Surface areas are not much affected. The supported system was found to be stable up to 800°C from thermal studies. Basicity measurements adopting Hammett indicator method revealed that basicity is reduced

by incorporation of vanadia into rare earth oxides. Adsorption of electron acceptors was used to probe the electron donating property. A reduction of basic OH groups on the surface of the support is observed by vanadia loading. The number of strong basic sites was diminished to a large amount compared to weaker ones. Ammonia adsorption at various temperatures showed that Bronsted acid sites are enhanced upon vanadia addition. Increase of Bronsted acidity was confirmed through cyclohexanol decomposition reaction also. Cyclohexene was favourably formed on the supported system compared to pure support. The number of Lewis acid sites of the support is reduced by incorporation of vanadia. Surface studies using different experimental methods indicated the participation of basic OH groups and Lewis acid sites of the support in the bond formation with vanadia species.

Acid base properties are significantly influenced by vanadia incorporation. The influence of vanadia addition on the catalytic activity and selectivity of the supported system is summarized in Chapter IV. Since vanadia supported on basic substances are known for their catalytic activity and selectivity in oxidative dehydrogenation reactions, these types of reactions were performed with ethyl benzene and ethanol over the catalysts. Vanadia creates redox sites on the rare earth oxide support. Activity for partial oxidation is enhanced through supporting vanadia on rare earth oxides. It was observed that vanadium should be well dispersed and stabilized in a low coordination number in order to limit the consecutive reaction of formed ODH products. The supported systems were found to be more active in ODH of alcohol where the reactant is adsorbed in a dissociative manner. The selectivity was high in the case of ODH of ethyl benzene. This is attributed to the locally limited active oxygen, which is low in the case of tetrahedral vanadia. In the case of ethanol ODH, the oxygen in the V=O species is deciding whose basicity plays an important role. Phenol methylation reaction carried using the supported systems indicated that C-alkylation is favoured over O-alkylation. Weak acid sites were generated in general, which lead to formation of higher alkylated phenols. Ortho product selectivity was found to be proportional to basicity of the catalysts.

Conclusions

General conclusions drawn from the studies are

- ⇒ Isolated tetrahedral V^{5+} species both in amorphous (surface species) and crystalline (lanthanide orthovanadates) forms are present on the supported system.
- ⇒ The vanadia incorporation significantly affect the physico-chemical characteristics of the supports.
- ⇒ Surface Bronsted sites were increased by incorporating vanadia in rare earth oxides, while a reduction was noticed in Lewis acidic sites.
- ⇒ Modification of rare earth oxide by vanadia decreased the basicity of rare earth oxides.
- ⇒ Vanadia species are formed by titrating basic surface OH groups and Lewis acid sites of the supports.
- ⇒ Rare earth oxide supported vanadia are found to be highly selective for oxidative dehydrogenation of ethyl benzene.
- ⇒ The activity of the supported system for ODH of ethanol was high in comparison with ethyl benzene.
- ⇒ The supported system catalysed C-alkylation in the methylation of phenol.

Further scope of the work



It is concluded from the studies that rare earth supported vanada catalysts are selective for the oxidative dehydrogenation of ethyl benzene to styrene. The active sites were found to be the rare earth orthovanadates. The V^{5+} ion in the tetrahedral coordination decides the high selectivity to styrene due to its special property of locally limited active oxygen. Hence further scope of work is to utilize rare earth orthovanadates as the catalyst for ODH reactions. It is expected to get high activity and selectivity on pure orthovanadates. The selecti^{on}_λ of the metal for the orthovanadate can be decided by an understanding of the reducibility of the metal ion.